THE UNIVERSITY OF CHICAGO

T CELL-INTRINSIC 4-1BB SIGNALING REGULATES TUMOR-INFILTRATING CD8$^+$ T CELL ACCUMULATION AND RESPONSE TO IMMUNOTHERAPY

A DISSERTATION SUBMITTED TO
THE FACULTY OF THE DIVISION OF THE BIOLOGICAL SCIENCES
AND THE PRITZKER SCHOOL OF MEDICINE
IN CANDIDACY FOR THE DEGREE OF
DOCTOR OF PHILOSOPHY

COMMITTEE ON CANCER BIOLOGY

BY
BRENDAN LEIGH HORTON

CHICAGO, ILLINOIS
DECEMBER 2017

Zeus has led us on to know,
the Helmsman lays it down as law
that we must suffer, suffer into truth.
We cannot sleep, and drop by drop at the heart
the pain of pain remembered comes again,
and we resist, but ripeness comes as well.
From the gods enthroned on the awesome rowing-bench
there comes a violent love.

-Aeschylus, *The Oresteia*

Translated by Robert Fagles

TABLE OF CONTENTS

LIST OF FIGURES

ACKNOWLEDGMENTS

There are many people who have given me opportunities to work in their laboratories over the years. Paul Rawson at the University of Maine let me spend a summer in his laboratory learning PCR. This gave me the first glimpse of what the laboratory is like and who a caring mentor is. Rosemary Smith and Scott Collins, also at the University of Maine, hosted me for one summer during college for a Research Experience for Undergraduates (REU). Spending time with them and their graduate students gave me valuable insights into academic research. I also got to work with lobsters, which was pretty cool. Suzie Pun at the University of Washington hosted me for another REU program I participated in over a summer in college. I will always remember her intensity, success, and rigor. Ester Kwon was the graduate student that put up with me that summer, and I am more thankful for that, now having been in her shoes. Thomas Gilmore at Boston University allowed me to work in his lab for a year and a half. I greatly appreciated the amount of experiments he allowed undergraduates to do. I couldnt have done anything in that lab without Melanie Herscovitch, who was a graduate student at the time. She was instrumental in helping me do experiments, for talking about science, life in science, and graduate school. I learned a lot in lab from her, and a lot about lab from her as well. Cynthia Bradham was my undergraduate faculty advisor. She always told me the truth, whether I wanted to hear it or not. Her developmental biology class was one of my favorites, and really got me interested in cellular processes. Her discussion section was extremely well taught, and particularly helpful in teaching me to analyze papers. She let me into her graduate grant writing class, where I read and wrote grant applications for the first time. It would not be the last. Dorothy Sipkins laboratory at the University of Chicago allowed me to experience great contrast during my time in graduate school. I am ever thankful that Tom Gajewski took a chance and welcomed me into his lab. He gave me a second chance at graduate school when he didnt have to. I have learned a huge amount from him about logical thinking, designing experiments, and generally how to be successful. The lab environment he fosters has always

been welcoming. I met so many great scientists and people during my time in his lab. Without them, I wouldnt be here. Leticia Corrales and Seng-Ryong Woo were excellent post-docs who helped me to learn how to do science. Jason Williams is the heart of the lab. He led the way for the other graduate students that joined after him. Ayelet Sivan was always there for interesting discussions of all types. Stefani Spranger was a great mentor who also became a great friend. Watching her success always gave me hope. Blake Flood was always eager for in depth science conversations. Kyle Cron always kept us informed about politics. Vyara Matson was full of kind encouragement. I'm sure Jess Fessler will do great things, and she has already become a good friend. I also couldnt have done this without my thesis committee: Marisa Alegre, Anita Chong, and Justin Kline. They have provided very insightful comments throughout my thesis work. Especially important were the friends I made; they got me through good times and bad: Noel and Laurie Pauli, Steve Kregel, Joanna Wroblewska, Alan Chang, Sahar Mozaffari, Kevin Lei, Theresa Leung, Dan and Jackie Leventhal, and Dennis Zimmermann. Last but not least Dana Gilmore, your love and support are beyond words.

ABSTRACT

Subsets of human tumors are infiltrated with tumor antigen-specific $CD8^+$ T cells (TIL), yet despite this infiltration, tumors progress. TIL are thought to be inactivated by the immunosuppressive tumor microenvironment, especially through the engagement of inhibitory receptors such as CTLA-4 and PD-1. Antibodies that block CTLA-4, PD-1, or PD-L1 can enhance the ability of $CD8^+$ TIL to control tumors, and have had great success in leading to durable responses in cancer patients. However, not all patients respond to these therapies, even when TIL are present. Combination immunotherapy is one strategy being tested to improve immunotherapy response rates. We have recently found that the co-stimulatory receptor 4-1BB is expressed on a subset of antigen-specific $CD8^+$ TIL. Agonist antibodies that stimulate 4-1BB have led to tumor regression in pre-clinical studies. Therefore, we set out to test whether agonist 4-1BB could synergize with blockade of PD-L1 or CTLA-4, and to study the mechanisms of synergy. Unexpectedly, we found that $CD8^+$ TIL actively proliferate and undergo apoptosis, leading to a cycle of $CD8^+$ TIL activation and death. Agonist 4-1BB synergized with blockade of PD-L1 or CTLA-4 not through increasing TIL proliferation, but through decreasing $CD8^+$ TIL apoptosis, which led to a remarkable accumulation of antigen-specific $CD8^+$ TIL. Gene expression profiling and experiments with transgenic mice suggest that increased NF-κB signaling in $CD8^+$ TIL was responsible for many effects of anti-4-1BB immunotherapy. Additionally, we found that endogenous 4-1BB signals promoted accumulation of $CD8^+$ TIL during the endogenous anti-tumor immune response. 4-1BB signaling in T cells was required for the efficacy of anti-PD-L1 antibodies, and the deletion of dendritic cells led to failure of anti-PD-L1 immunotherapy. Our data suggest that co-stimulation through 4-1BB is critical to counter antigen-driven apoptosis of $CD8^+$ TIL, and for the effectiveness of anti-PD-L1 immunotherapy. Strategies to maximize co-stimulation in the tumor microenvironment and inhibit TIL apoptosis should be considered in the development of cancer immunotherapies.

CHAPTER 1

INTRODUCTION

1.1 Overview

Cancer and the immune system are linked in many different ways. From the early observation of immune cell infiltrates into tumor lesions by Paul Ehrlich, to Peyton Rous discovery that viruses could transform cells, to the success of checkpoint blockade immunotherapy, the fields of cancer biology and immunology have been intertwined for as long as they have existed. However, only in the wake of the recent success of immunotherapy of cancer in humans has it been widely appreciated that the immune system can mount an endogenous response against growing cancers. Interestingly, somatic mutations in the genome, which are necessary for the development of cancer, also allow for the immune system to differentiate malignant cells from normal cells, providing the host with a mechanism to mount an immune response against tumors. Augmenting this spontaneous immune response has long been the goal of tumor immunologists, in the hope that the immune system could provide the magic bullet to cure cancer that has been so elusive. While current immunotherapy continues to be incredibly successful and offers cures to some patients that would have seemed magical only a few years ago, immunotherapys success has also served to highlight its current limitations. Low response rates hamper todays immunotherapies, as scientists discover new ways in which cancer eludes detection and destruction by the immune system. New strategies to widen to the applicability of anti-cancer immunotherapy and to better understand its mechanisms of action are the focus of many studies, including the experiments contained within this thesis.

1.2 Somatic mutations drive cancer

Cancer is driven by mutations to the genome that endow tumor cells with the so-called "Hallmarks of Cancer" which include unlimited replicative potential, resistance to cell death,

and the ability to metastasize to distant locations throughout the body (Hanahan, 2000). That cancer was driven by abnormalities in hereditary material was first hypothesized over 100 years ago by Theodor Boveri, a German biologist who studied chromosomes and their link to cellular behavior and heredity. Building on observations made by David von Hansemann, a pathologist who correlated aneuploidy and neoplasia, Boveri proposed a causal relationship between aberrant chromosomes and malignancy in 1914, in what would become a startlingly prescient prediction for its time (Boveri, 2008; Weinberg, 2008). It took many more years, however, for researchers to provide definitive proof that changes to the genome were indeed the causal elements of human cancer.

Studies performed by Peyton Rous using a sarcoma virus, now known as the Rous sarcoma virus or RSV, were critical to demonstrating that genetic material was the cause of cancer. Rous showed in 1911 that cell-free tumor filtrates could transmit cancers from one chicken to another (Rous, 1911). The vector for this transmission was RSV. In 1970 it was identified that a specific RNA subunit of RSV was responsible for its transforming ability (Duesberg, 1970). This work, performed by Peter Duesberg and Peter Vogt, was the first identification of a specific gene that leads to cancer, named src for sarcoma. It was still unclear, however, that cancer-causing genetic material could originate from changes to a cells own genome without viral infection. Shortly after the identification of src came studies from Michael Bishop and Harold Varmus identifying that the src gene was in fact present in normal, non-transformed cells, and that an activated version of cellular src had been incorporated into RSV (Stehelin, 1976). This 1976 work demonstrated that the causal genetic agent of a cancer virus was itself derived from normal cellular material, and led to the idea that mutation or activation of specific genes could lead to cancer without viral involvement. This work was truly groundbreaking at the time, fundamentally changing what was the current understanding of cancer causality (Bister, 2015).

Direct evidence that changes to the normal genome cause cancer came from two other lines of research. The first, similar to the work with RSV, utilized the rodent tumor viruses

Harvey murine sarcoma virus and Kirsten murine sarcoma virus. Analogous to RSV and src, the Harvey and Kirsten viruses contained isoforms of the ras protein, named either H-ras or K-ras depending on which virus the ras protein came from (Cox, 2010). In the late 1970s and early 1980s, Scolnick and colleagues identified that ras was also a cellular protein, like src (Scolnick, 1974). In 1979, another group lead by Robert Weinberg, utilized what was then new technology in molecular biology and transfected NIH/3T3 murine fibroblasts with DNA from chemically transformed cells (Shih, 1979). This transfection transferred malignant properties to NIH/3T3 cells, demonstrating that cellular DNA from non-virally transformed cells could lead to cancer. The data from Scolnick and Weinberg was brought together in 1982 when three groups, including Weinbergs, determined that the transforming gene in the NIH/3T3 transfection experiments was, in fact, a mutated version of cellular ras (Santos, 1982; Der, 1982; Parada, 1982). This led to the identification of mutated ras in multiple cancer types, and eventually the general acceptance of mutations to cellular genes as the causative agents in cancer initiation.

The second line of evidence linking mutations to cancer utilized a completely different technique. Like Boveri many years before her, Janet Rowley performed studies on chromosomes from human cancer cells to make discoveries of specific genetic alterations that led to cancer. In 1973 she published two papers demonstrating that specific chromosomal translocations were found in specific types of leukemias (Rowley, 1973a; Rowley, 1973b). This included the identification of two translocations: t(15;17) resulting in the fusion of the promyelocytic leukemia gene to that encoding the retinoic acid receptor (PML-RARA) that is present in acute promyelocytic leukemia (APL), and t(9;22) that results in the fusion of the breakpoint cluster region gene to the abelson proto-oncogene (BCR-ABL), which is present in almost all cases of chronic myeloid leukemia (CML). Extremely adept at staining chromosomes, Rowley discovered many specific chromosomal translocations found in specific types of blood cancer, raising the idea that specific genetic lesions gave rise to specific types of cancers (Druker, 2014). Rowleys work would lead to several therapeutic strategies

that targeted the specific mutations she had discovered. All trans retinoic acid binds to both the retinoic acid receptor and PML-RARA fusion protein, and is used in combination with anthracyclines or arsenic to treat APL, with overall 5 year survival rates near 90% (Cooms, 2015). Even more famously, her discovery of the translocation t(9;22) that results in the BCR-ABL fusion led to the development of the first FDA approved kinase inhibitor, imatinib, which won FDA approval in 2001 (Woondong, 2013). Treatment of BCR-ABL$^+$ CML with imatinib leads to overall survival rates also near 90% (Sacha, 2014). Together these drugs led the way into a period of designing therapeutics against specific mutations in cancer. The immune system can also target mutations present in cancer cells, and therefore, in an indirect sense, immunotherapy does as well. Tumor cells are not only driven by somatic mutations to the genome, but also continue to accumulate additional mutations to their genomes as a cancer progresses. These additional mutations can lead to therapeutic resistance, or simply be passenger mutations with little functional consequence. With every mutation, however, is an additional chance of generating a new T cell epitope that can lead to a strong anti-tumor T cell response. Therefore mutations are a kind of Achilles heel for cancer they endow tumor cells with their invulnerabilities, but also have the potential to sensitize them to the arrows of the immune system.

1.3 Tumors contain T cell epitopes

It was for many years unclear if T cells could mount an endogenous response against tumors. There were doubts about whether tumors could activate the innate immune system to properly stimulate T cells. It was also unclear what antigens tumors might be able to present to T cells that could lead to their activation. Also, due to peripheral tolerance mechanisms that lead to the hypofunctionality of self-reactive T cells, it was unclear as to whether there would be functional T cells that could recognize antigens on tumor cells. However, we know now that tumor cells can activate dendritic cells (DCs) that infiltrate the tumor microenvironment. Evidence suggests this occurs when tumor-derived DNA activates DCs

in a STING-dependent manner (Woo, 2014; Woo, 2015). It has also been clearly demonstrated that antigens in tumors can be recognized by T cells. Many types of antigens can be recognized by $CD8^+$ T cells and lead to their activation: overexpressed self-antigens, such as Her2 in breast cancer, otherwise germ cell-specific antigens, or so-called cancer testis antigens such as the MAGE family of proteins, antigens restricted to specific cell lineages such as those involved in the pigmentation of melanocytes, and antigens that are the result of mutations (Coulie, 2014; Gubin, 2015). Recently, neoantigens that arise from somatic mutations in tumor cells have received increased attention, as they are believed to give rise to the strongest anti-tumor T cell responses, similar to foreign antigens. Advances in high throughput peptide screening techniques have made detection of neoantigens feasible, and allowed for the rapid identification of neoantigens and $CD8^+$ T cells that are reactive to them (Cohen, 2015; Gros, 2016). Studies have clearly demonstrated that neoantigens are relevant for the anti-tumor immune response, and for immunotherapy of cancer. Increased prevalence of neoantigens, and tumor mutational load, correlates with improved outcomes to immunotherapy in some cancers, indicating that neoantigens play a crucial role in anti-tumor immunity (Snyder, 2014; Lu, 2014; Rizvi, 2015; Le, 2015). However, it does not appear that simply having an increased number of antigens is sufficient to increase the strength of the anti-tumor immune response. The correlation between increased immunotherapy efficacy and mutational load or number of neoantigens is likely stochastic, in that having more neoantigens increases the possibility of generating a strongly stimulating T cell epitope. In one lung cancer study, the presence of a neoantigen in the majority of cancer cells was correlated with positive outcomes to immunotherapy, whereas increased mutations and sub-clonal neoantigens were correlated with worse response to immunotherapy (McGranahan, 2016). Therefore, the quality of neoantigen, as well as its relative abundance in the cancer cell population, are critical; the simple presence of tumor-specific mutations or neoantigens does not guarantee a positive response to immunotherapy.

Interestingly, the density of neoantigens does not predict whether tumors are T cell-

inflamed or not (Spranger, 2016), indicating that the adjuvanticity and antigenicity of tumors are separate. A functional anti-tumor immune response therefore requires two key conditions: tumors must sufficiently recruit and activate innate immune cells, and sufficient numbers of tumor-associated antigens must be present for T cell priming, expansion, and a continued T cell response within the tumor microenvironment.

1.4 Innate immune activation

The immune system consists broadly of two compartments: innate immune cells that sense conserved, pattern-associated signals, and adaptive immune cells that utilize somatically recombined receptors to recognize specific peptide epitopes. Certain innate immune cells, like macrophages and DCs, are specialized to present peptide antigens to T cells in the context of MHC class I or II molecules (Sprent, 1995). This is achieved by engulfing extracellular material through phagocytosis or pinocytosis, and processing engulfed proteins in types of multi vesicular bodies where peptide fragments are loaded onto MHC. These loaded MHC molecules are then transported to the surface of the APC for presentation to T cells (Roche, 2015). While macrophages are more phagocytic, DCs are superior at antigen presentation, and are essential for the activation of anti-tumor T cell responses (Steinman, 1973; Steinman, 1978; Diamond, 2011; Fuertes, 2011). Antigen presentation can occur in the context of MHC-II to $CD4^+$ T cells, or MHC-I to $CD8^+$ T cells (Roche, 2015). Because they are able to mediate direct cell killing and interact with non-APC cell types through MHC-I, $CD8^+$ T cells are regarded as the most dominant effectors of the anti-tumor immune response. While MHC-I usually is loaded with intracellular peptides, the Batf3-lineage of DCs that express either CD8 or CD103 are adept at presenting peptides derived from extracellular material on MHC-I a phenomenon known as cross-presentation (Hildner, 2008). Through cross-presentation, $CD8^+$ T cells are activated against antigens that originate from outside APCs, including those derived from tumor cells.

A T cell response is initiated when APCs are activated by a pathogen associated molecular

pattern (PAMP) or damage associated molecular pattern (DAMP) (Janeway, 2002; Kono, 2008). These PAMPs and DAMPs are conserved molecules that mediate the sensing of pathogens or cellular damage by APCs. For example, one prominent PAMP is lipopolysaccharide, a component of bacterial cells walls (Poltorak, 1998). PAMPs and DAMPs are sensed by pattern recognition receptors (PRR), of which there are many. While some sensors have evolved to detect bacteria, others have evolved to detect viruses through the sensing of cytosolic DNA or RNA (Wu, 2014). Other PRRs detect cellular damage, and mostly sense the release of intracellular contents into the extracellular space, such as ATP, or molecules like HMGB1 (Takeuchi, 2010). Sterile inflammation is a product of PRRs sensing these cellular components, and allows the immune system to respond to injury where wound healing and tissue remodeling is required, but where there are no pathogens present (Chen, 2010).

After encountering PAMPs or DAMPs, DCs undergo rapid changes that allow them to activate a T cell response (Reis e Sousa, 2004). DC activation leads to increased MHC expression, increased antigen processing, increased expression of co-stimulatory molecules and cytokines, and DC migration to T cell-rich areas of lymph nodes (Yanagihara, 1998). In the lymph nodes, activated DCs present antigens to T cells, which themselves become activated after encountering their cognate antigens.

1.5 T cell activation

In contrast to sensing broad categories of molecular patterns, the adaptive immune system, comprised of B cells and T cells, utilize somatic recombination of their DNA to generate unique receptors capable of recognizing antigens in a highly specific manner (de Villartay, 2003). Each T cell expresses a unique TCR that can optimally recognize a unique peptide-MHC complex, allowing for tremendous specificity and diversity in the immune response. T cells develop in the thymus, where their TCRs are screened for optimal recognition of peptides in host MHC molecules, with T cells that bind too weakly or too strongly removed from the developmental process through cell death, or divergence to alternative T cell lineages

(Daley, 2013; Stritesky, 2013; McDonald, 2015; McDonald, 2014; Malchow, 2016). Self-reactive T cells that enter the periphery are thought to be tolerized. When T cells receive TCR stimulation in the absence of co-stimulation, or from quiescent DCs, they can enter a hyporesponsive state called anergy (Hawiger, 2001). Anergic T cells have dampened functions and are no longer able to respond robustly to antigenic stimulation (Schwarz, 1990). Therefore only T cells that generate receptors within a certain range of affinity for self can successfully develop in the thymus and remain fully functional T cells that are not tolerized in the periphery.

Nave T cells in the periphery become properly activated only after antigen presentation by fully activated APCs (Reis e Souza, 2006). APCs present peptide-MHC complexes on the APC surface that bind to the T cells TCR, leading to TCR signaling (Huppa, 2003). When T cells receive TCR signaling along with the proper co-stimulatory signals and cytokines, they become activated, leading to their proliferation and differentiation (Reis e Souza, 2006). Generation of a cytotoxic $CD8^+$ T cell response is thought to be especially important for an anti-tumor response, as they are able to directly recognize tumor cells through MHC-I and mediate direct cell killing through delivery of cytotoxic granules and FasL (Garrido, 2016; Kline, 2012).

After activation in lymph nodes, each activated $CD8^+$ T cell proliferates rapidly to generate large clonal populations. To exit the lymph node and reenter circulation, $CD8^+$ T cells use the sphingosine-1-phosphate (S1P) receptor 1 (Matloubian, 2004; Shiow, 2006). The blood contains high levels of S1P, which functions as a chemokine gradient to guide T cells into circulation (Maceyka, 2014). Once in the circulation, $CD8^+$ T cells use other chemokines, CXCL9 and CXCL10, to sense where to enter the tumor microenvironment (Spranger, 2015). Once at the tumor site, $CD8^+$ T cells can carry out their effector functions, including production of IFN-γ and cytolysis.

1.6 Role of co-stimulation in T cell activation and cancer

T cells require multiple signals from DCs to become properly activated effector cells. These signals include engagement of the TCR, the provision of co-stimulatory ligands, and cytokine signaling such as IL-12 or IFN-α/β (June, 1994; Curtsinger, 2010). APCs present peptides in the context of MHC-I that activate the TCR of $CD8^+$ T cells. Activation through the TCR is required for the activation of nave cells into effectors, but alone it is not sufficient to generate a successful T cell response. Co-stimulation through other cell surface receptors is also required during the priming of $CD8^+$ T cells. Co-stimulation can be delivered through a variety of ligands on APCs that bind receptors on T cells. CD28, an immunoglobulin superfamily member, is perhaps the best characterized co-stimulatory receptor that T cells express. CD28 receives signals through the B7 molecules, CD80 and CD86, which become upregulated on APCs after APC activation (Reis e Sousa, 2006). In the context of TCR signaling that takes place during cognate antigen presentation to T cells, the additional ligation of CD28 by CD80 or CD86 results in the T cell upregulating IL-2 and the high affinity IL-2 receptor subunit, CD25. IL-2 CD25 interactions then provide the additional signals necessary for T cell survival and for the high rates of T cell proliferation that generate large numbers of effector T cells (Acuto, 2003).

While CD28 is the classical co-stimulatory receptor associated with T cell co-stimulation, there are others that also provide co-stimulatory signals to T cells. Several of these co-stimulatory receptors belong to the TNF receptor superfamily, including CD27, OX-40, GITR, and 4-1BB (Ward-Kavanagh, 2016). The ligands for these molecules, CD70, OX-40L, GITRL, and 4-1BBL, respectively, can be expressed on APCs during their maturation (Ward-Kavanagh, 2016). Engagement of 4-1BB has been shown to strongly affect $CD8^+$ T cells in particular, and in some situations can even replace CD28 signaling (Saoulli, 1998). 4-1BB is upregulated upon T cell activation, and binds to 4-1BBL, which can be expressed on DCs as well as B cells and macrophages (Kwon, 1989; Ward-Kavanagh, 2016). Ligation of 4-1BB has been found to affect T cells in a variety of ways. Co-stimulation through 4-1BB

can extend T cell proliferation during priming to augment the primary immune response (Shuford, 1997; Habib-Agahi, 2007). Ligation of 4-1BB can also enhance T cell survival through the upregulation of Bcl-x_L (Lee, 2002). 4-1BB signaling may also play a role in supporting memory T cell maintenance and secondary expansion (Pulle, 2006; Bertram, 2004).

It was once thought that after successful priming, effector $CD8^+$ T cell function was independent of further co-stimulation. This had been demonstrated experimentally in vitro and in vivo (Flynn, 1996; Kim, 1999), and made sense for $CD8^+$ T cells that would have to kill non-APCs that might not express co-stimulatory molecules. However, the discovery of the co-stimulatory molecule ICOS on T cells, and its ligand, ICOS-L, which can be expressed on cells other than APCs, raised the question of whether T cells could receive co-stimulation in non-lymphoid tissues (Hutloff, 1999; Mueller, 2000). Additionally, primed T cells at effector sites can express multiple co-stimulatory molecules, including 4-1BB, and many studies have indicated that engagement of different co-stimulatory receptors can alter effector cell function (Chen, 2013). Interestingly, we have recently found that 4-1BB is upregulated in vivo in the tumor microenvironment on tumor antigen-specific $CD8^+$ T cells (Williams, 2017). The agonist engagement of 4-1BB can induce tumor regression in multiple mouse models (Melero, 1997; Williams, 2017). The expression of 4-1BB on $CD8^+$ tumor-infiltrating T cells (TIL) raises the question of whether the anti-tumor efficacy of agonist 4-1BB antibody is due to enhancing $CD8^+$ T cell priming or the effector phase of the anti-tumor $CD8^+$ T cell response. Little is known about the requirements of activated effector cells for co-stimulatory signals. A recent study suggests that interactions with APCs in the tumor microenvironment promotes the effector responses of $CD8^+$ TIL (Broz, 2014). It remains unknown why these APCs are beneficial to the anti-tumor immune response, but providing co-stimulation to $CD8^+$ TIL remains a possibility.

Interestingly, forced expression of co-stimulatory molecules, including CD80, CD86, or 4-1BBL by tumor cells leads to their spontaneous immune-mediated control, suggesting that

co-stimulation in the tumor microenvironment could directly enhance T cell function to control tumors (Chen, 1992; Townsend, 1993; Yang, 1995; Mogi, 2000). It is still unknown, however, to what extent endogenous co-stimulation augments $CD8^+$ TIL function within the tumor microenvironment. The expression of co-stimulatory molecules on tumor-infiltrating APCs has not been well studied. It is also not clear how the temporal or spatial separation between T cell interactions with antigen-MHC complexes expressed on tumor cells and co-stimulatory receptors potentially expressed on tumor-infiltrating APCs would allow for co-stimulation to lead to enhanced tumor cell killing. However, tumor regression can be induced by treating tumor-bearing mice with agonist antibodies against many co-stimulatory receptors, including CD27, OX-40, GITR, and 4-1BB, indicating clearly that there is some role for co-stimulation in immune mediated tumor control (French, 2007; Gough, 2008; Boczkowski, 2009; Melero, 1997). However, how increased co-stimulation functions to enhance tumor control remains unknown. Interestingly, in multiple syngeneic murine tumor models, we find 4-1BB expression on $CD8^+$ TIL that also express PD-1 and LAG-3 (Williams, 2017). The combination of 4-1BB agonist antibodies with blockade of CTLA-4 or LAG-3 can cause potent tumor regression of syngeneic tumors (Curran, 2011; Williams, 2017), raising the question of whether engaging 4-1BB directly on dysfunctional $CD8^+$ TIL is necessary or sufficient to mediate tumor control during combination immunotherapy.

1.7 T cell inflammation of tumors

The observation that immune cells can infiltrate tumors goes back to 1891 when Paul Ehrlich observed accumulation of mast cells in human tumors (Westphal, 1891). Ehrlich went on to propose in 1909 that the immune system could play a protective role against cancer (Ehrlich, 1909). Today it is recognized that the infiltration of immune cells into tumors can have prognostic value in cancer diagnosis (Jass, 1987; Pages, 2005). Importantly, $CD8^+$ T cell infiltration into tumors correlates with responsiveness to immunotherapy (Tumeh, 2014). Subsets of multiple types of human tumors are inflamed by $CD8^+$ T cells (Spranger, 2016).

Studies from our laboratory and others have demonstrated that this is a process that begins when DCs infiltrate the tumor microenvironment in response to chemokines made by tumor cells (Spranger, 2015; Diamond, 2011; Fuertes, 2011).

When DCs are successfully recruited to the tumor microenvironment, they become activated in a STING-dependent manner, potentially by tumor cell-derived DNA, and produce type I interferons (Woo, 2014). Especially important are the Batf3-lineage of DCs, identified by their expression of either CD8α or CD103 (Hildner, 2008). These DCs are specialized to process extracellular proteins and present the subsequent peptides on MHC-I where they can activate $CD8^+$ T cells. Deletion of these DCs leads to failed $CD8^+$ T cell priming and an inability to mount an effective immune response against tumors (Hildner, 2008). Type I interferon signaling on Batf3 lineage DCs is crucial for their ability to activate $CD8^+$ T cells specific for tumor antigens (Fuertes, 2011; Diamond, 2011). Activated $CD103^+$ DCs migrate from the tumor site to lymph nodes in a CCR7-dependent manner, where $CD103^+$ DCs cross-present tumor antigens to activate $CD8^+$ T cells (Roberts, 2016). $CD8^+$ T cells proliferate in the lymph node and circulate back to the tumor to carry out effector functions. DCs are therefore important in multiple temporal and anatomic locations to activate the anti-tumor T cell response. Still underexplored is the potential role of co-stimulation that DCs might provide to effector T cells in the tumor microenvironment, and how they contribute to the maintenance of an ongoing effector T cell response.

1.8 Regulation of T cell infiltration into tumors

Only a fraction of tumors analyzed from patients appear to be inflamed with infiltrating T cells (Harlin, 2009), and many factors have been found to influence the ability of the immune system to sense and infiltrate tumors. Because infiltration of $CD8^+$ T cells into the tumor microenvironment is prognostic for whether a patient will respond to current immunotherapies (Tumeh, 2014), it has been of great interest to determine factors that regulate T cell recruitment to tumors. Some tumors avoid immune detection altogether by

the immune system. Using data from human tumors, our laboratory recently found that activated -catenin in tumor cells was able to repress the expression of chemokines necessary for DC recruitment (Spranger, 2015). Failed recruitment of DCs led to a lack of T cell priming against tumor associated antigens, and a lack of T cell infiltration into β-catenin-expressing tumors. Interestingly, DCs were not only required for priming of T cells, but their recruitment to the tumor microenvironment as well. T cells were recruited by chemokines produced by DCs. Even after therapeutic vaccination or adoptive T cell transfer, β-catenin$^+$ tumors did not attract T cells, highlighting the multiple important roles that DCs play in the tumor microenvironment (Spranger, 2017).

Other tumor cell intrinsic pathways can also contribute to limiting the amount of T cell infiltration after detection of tumors by the immune system. Loss of PTEN in tumor cells can lead to decreased T cell infiltration (Peng, 2016). PTEN deletion in tumor cells resulted in increased immune-suppressive cytokine production that was thought to reduce T cell infiltration into tumors, which led to decreased effectiveness of PD-1 and CTLA-4 blockade immunotherapy. MYC amplification can also limit the number of T cells recruited to a tumor site (Casey, 2016). MYC activation can lead to increased expression of PD-L1, which can dampen T cell responses, and upregulation of CD47, which is a "dont eat me signal to prevent cells from becoming phagocytosed by macrophages. MYC expression can therefore prevent both innate and adaptive immune mechanisms from acting on tumor cells. Inactivation of MYC led to the rejection of syngeneic tumors that grow progressively when MYC is activated, and the overexpression of PD-L1 or CD47 could prevent rejection of these tumors despite MYC inactivation, highlighting the importance of these molecules in inhibiting immune responses.

Host factors also contribute to the level of T cell inflammation that occurs after immune detection. One important such factor is the host microbiota. Our laboratory recently found that C57BL/6 mice from different vendors had different levels of tumor control of transplanted melanomas (Sivan, 2015). All mice were able to mount a response against these

tumors, indicating that it was not detection of the tumor cells that was changed between mice. Rather, the number of T cells primed against tumor antigens was different between vendors, and this resulted in different infiltration of T cells into the tumor microenvironment and different effectiveness of immunotherapy. While these mice were all similar genetically, their microbiota differed, and transfer of microbiota from the better protected mice could confer increased immune control of tumors to mice from the other vendor.

Multiple factors therefore contribute to the ability of the immune system to detect a growing tumor, and the number of T cells that infiltrate into tumors. Once T cells reach the tumor, there are additional regulatory mechanisms that serve to dampen their function and allow tumor progression.

1.9 T cell dysfunction in the tumor microenvironment

While T cells infiltrating the tumor microenvironment can have positive prognostic implications, the presence of activated TIL in progressing tumors also indicates that the endogenous T cell response is ultimately incapable of preventing tumor progression. It is currently thought that TIL are unable to prevent tumor progression because their functions are blunted within the tumor microenvironment, due to the multiple immune-inhibitory mechanisms present within tumors (Gajewski, 2013). Eventually, TIL enter a state of hyporesponsiveness, often referred to as exhaustion or dysfunction (Speiser, 2016). Exhaustion or dysfunction occurs in the face of a progressing tumor, and in other situations where a T cell antigen is chronically present, such as chronic viral infection (Kahan, 2015). Such models have been useful in defining the functions and transcriptional profile of exhausted $CD8^+$ T cells. Exhaustion from chronic antigen stimulation leads to a stepwise decline in T cell function, where the cytokines IL-2, TNF-α and finally IFN-γ are no longer expressed (Wherry, 2011). This coincides with a gradual loss of cytotoxic ability. Eventually, exhausted T cells are thought to enter senescence or undergo apoptosis. Exhaustion appears to be a type of terminal differentiation, with characteristic gene expression patterns, associated transcrip-

tion factors, and unique epigenetic landscapes (Paley, 2012; Doering, 2012; Pauken, 2016; Sen, 2016).

A $CD8^+$ T cell dysfunctional state is also present within the tumor microenvironment, and is a potential mechanism of tumor progression despite its infiltration with antigen-specific $CD8^+$ T cells (Speiser, 2016). The tumor microenvironment employs many immune suppressive mechanisms that act in concert to promote tumor immune escape. For example, tumors recruit suppressive cell populations, such as regulatory T cells and myeloid-derived suppressor cells. Many mechanisms have been described to explain how these cell populations downregulate effector T cell function. In particular, their secretion of anti-inflammatory molecules like IL-10 and arginase are thought to play a critical role in $CD8^+$ TIL functional suppression (Gajewski, 2013). Another important mechanism of T cell inhibition are inhibitory receptors expressed on effector T cells during and after their activation, like CTLA-4 and PD-1 (Fuertes Marraco, 2015). Ligation of these receptors blunt T cell function. Both CTLA-4 and PD-1 can send potent suppressive signals to effector T cells (Parry, 2005; Wei, 2013). CTLA-4 limits the activation of T cells during priming through the inhibition of co-stimulatory signaling through CD28. However, our laboratory has found that there are roles for CTLA-4 in the tumor microenvironment after T cell priming (Spranger, 2014). PD-1 is also thought to play a critical role in the tumor microenvironment. The ligand for PD-1, PD-L1, can be expressed by both tumor cell and myeloid cell populations (Latchman, 2004). PD-1 can act like a rheostat for T cell function it is upregulated when activated T cells encounter their antigen, and the engagement of PD-1 by PD-L1 serves to dampen T cell function (Honda, 2014). CTLA-4 and PD-1 serve to restrain immune responses in order to limit tissue damage during an immune response, and to prevent the development of autoimmunity (Tivol, 1995; Nishimura, 1999). However, in the tumor microenvironment, immune-mediated tissue destruction is desired. These immune inhibitory mechanisms are co-opted within the tumor microenvironment and eventually restrain TIL function. It is thought that immune suppression in the tumor microenvironment plays a critical role in

promoting T cell dysfunction and tumor progression.

It is still unclear if these immunosuppressive mechanisms in the tumor themselves lead to a state of dysfunction, or if the chronic exposure to tumor antigen that results from the failure of TIL to completely eliminate tumor cells is primarily responsible for the dysfunctional state. One study has shown that in the genetic absence of PD-1, exhausted cells still accumulate after chronic viral infections, indicating that exhaustion can occur without PD-1 signaling (Odorizzi, 2015). Additionally, other studies have found that chronic exposure to tumor antigens can lead to a permanent programmed state of tolerance or dysfunction (Schietinger, 2012; Schietinger, 2016). While some data suggests that the dysfunction of $CD8^+$ T cells in viral models and tumor models is similar, our laboratory oratorys recent data as well as data from other mouse and human studies have shown that $CD8^+$ TIL are not exhausted in the same way as in chronic viral infections (Williams, 2017; Boldajipour, 2016; Daud, 2016). $CD8^+$ TIL do not appear to be functionally inert. Although $CD8^+$ TIL phenotypically resemble exhausted T cells in hosts with chronic viral infections in their expression of multiple inhibitory receptors, (Williams, 2017) their functionality is distinct. TIL from both murine melanomas and from human cancer patients display only a partially exhausted phenotype (Williams, 2017; Daud, 2016), but retain the ability to produce high levels of IFN-, as well as the ability to lyse target cells ex vivo (Williams, 2017). These studies raise new questions about the nature of T cell dysfunction in the tumor microenvironment, including what function of $CD8^+$ T cells is restored by immunotherapy that is necessary for tumor control.

We have found in previous studies that after successful immunotherapy in mouse models, $CD8^+$ TIL are able to produce more IL-2 (Spranger, 2014; Williams, 2017). It is unclear if increased IL-2 is a necessary function of TIL for tumor regression after immunotherapy, or if increased IL-2 is simply a marker of a more functional T cell response that is able to lead to tumor regression. In an adoptive transfer study, production of IL-2 by transferred T cells was necessary for tumor regression, indicating a possible functional role for IL-2 after

immunotherapy (Kline, 2012). Another possibility is that it is not only T cell function, but also T cell number that is a critical factor in determining the ability of T cells to successfully control tumors after immunotherapy. It is possible that TIL retain the required functionality to reject progressing tumors, but are restricted in their accumulation by some mechanism present in the tumor microenvironment. In one study PD-1 immunotherapy led to increased numbers of T cells in patients tumors (Tumeh, 2014). There was also an increased number of Ki-67$^+$ CD8$^+$ TIL, suggesting that increased proliferation after immunotherapy might account for increased TIL number.

In chronic viral infection studies, it is known that exhausted CD8$^+$ T cells undergo apoptosis (Wherry, 2011). Blockade of PD-L1 decreases the fraction of apoptotic CD8$^+$ T cells (Blackburn, 2008), resulting in an increased number of antiviral CD8$^+$ T cells. Whether T cells in tumors are undergoing apoptosis has not been well explored. It has been hypothesized that FasL expression on tumor cells can kill TIL, leading to immune escape, however conclusive evidence to support this notion is lacking (Igney, 2005). In adoptive transfer experiments, overexpression of Bcl-2 in transferred antigen-specific T cells was sufficient for increased tumor control (Charo, 2005). However, this was in the setting of sublethal irradiation and concomitant IL-2 administration, so it is difficult to determine what the effect of increased T cell survival alone would be on tumor control. It is possible that increased survival of T cells could play a role in their accumulation within tumors and increased tumor control after immunotherapy.

1.10 Checkpoint blockade immunotherapy

Whatever the cause or nature of TIL dysfunction, in T cell-inflamed tumors, blocking the immune-dampening signals transmitted by CTLA-4, PD-1, or PD-L1 through the administration of monoclonal antibodies is sufficient in some cases to lead to tumor regression (Hodi, 2010; Topalian, 2012; Brahmer, 2012). Because CTLA-4 and PD-1 serve as checkpoints that modulate immune activation, immunotherapies that interrupt their signaling are

known as checkpoint blockade therapies. Blockade of CTLA-4 or PD-1/PD-L1 signaling has had a huge impact on cancer treatment, offering previously unheard of durable control of metastatic disease. However, durable benefit is limited to a minority of patients (Ji, 2012; Tumeh, 2014). As CTLA-4 and PD-1 are thought to regulate unique aspects of T cell activation, combined blockade was a logical next step for attempting to improve responses to checkpoint blockade immunotherapy. Combined CTLA-4 and PD-1 blockade immunotherapy has resulted in benefits in progression-free survival for the combination group compared to CTLA-4 alone (Larkin, 2015). The field remains optimistic, however, that combinations of different immunotherapies will increase the magnitude of responses and overall response rate to immunotherapy. Innumerable clinical trials are underway testing the efficacy of agonist antibodies against co-stimulatory molecules, including 4-1BB. It is possible that providing positive co-stimulatory signals to T cells will enhance their functions in different ways than removing inhibition through immune checkpoints.

In preclinical studies, combinations of agonist 4-1BB antibody plus either CTLA-4 or PD-1 blockade results in enhanced tumor control compared to single treatments (Curran, 2011; Chen, 2015). The expression of 4-1BB on dysfunctional $CD8^+$ TIL that also express PD-1 and CTLA-4 (Williams, 2017) raises the question of whether activation of 4-1BB on $CD8^+$ TIL is responsible for the synergy with blockade of CTLA-4 or PD-1. 4-1BB is expressed during T cell priming and also by effector T cells, and it is unknown if agonist 4-1BB antibodies improve tumor control by engaging 4-1BB during T cell priming or during the effector T cell response. Our laboratory and others have found that blockade of CTLA-4, PD-L1, or PD-1 enhances the function of T cells already within the tumor microenvironment at the time of treatment (Spranger, 2014; Tumeh, 2014). However, it is unknown if this will be the case with agonist 4-1BB antibodies.

It is also unknown whether endogenous co-stimulation in the tumor microenvironment is important for the outcome of immunotherapy. Recently published data suggest that inhibiting CD28 signaling is the primary mechanism of PD-1 that inhibits T cell function

(Hui, 2017), while another group found that co-stimulation through CD28 is critical for the efficacy of PD-L1 blockade in chronic viral infections and cancer (Kamphorst, 2017). This suggests that lack of co-stimulation might explain some patients who do not respond to checkpoint blockade immunotherapy, despite the presence of infiltrating $CD8^+$ T cells. If this is true, then providing exogenous co-stimulation through the delivery of agonist antibodies directed against co-stimulatory molecules may improve response rates to current checkpoint blockade. Because many $CD8^+$ TIL can express 4-1BB (Williams, 2017), it will be important to understand what role 4-1BB plays in $CD8^+$ TIL function and response to immunotherapy. Provision of exogenous co-stimulation through agonist 4-1BB antibodies may enhance the therapeutic effect of current checkpoint blockade immunotherapy, increasing the fraction of patients that derive benefit. In this thesis I will describe work which tests the hypothesis that tumor regression resulting from an agonistic anti-4-1BB antibody combined with blockade of CTLA-4 or PD-L1 is mediated by $CD8^+$ TIL present in the tumor microenvironment at the time of immunotherapy administration. I will also describe experiments assessing whether removal of 4-1BB signaling will impact the efficacy of blockade of PD-L1, as well as the mechanisms of these effects. These concepts have been explored through the completion of three Specific Aims:

1. Determine the cellular and molecular mechanisms necessary for tumor control after agonist 4-1BB antibody plus blockade of CTLA-4 or PD-L1.

2. Determine the biochemical signaling pathways that mediate an enhanced $CD8^+$ T cell response to agonist 4-1BB antibody plus blockade of CTLA-4 or PD-L1.

3. Determine the importance of endogenous 4-1BB signaling to mounting an anti-tumor T cell response and the efficacy of anti-PD-L1 immunotherapy.

CHAPTER 2

MATERIALS AND METHODS

2.1 Mice

C57BL/6 (B6NTac), Rag2$^{-/-}$ (RAGN12), and CD45.1 (B6.SJL) mice were purchased from Taconic. Thy1.1 (000406) mice were purchased from The Jackson Laboratory.

Autochthonous melanoma mice were bred in our facility. These mice contain a tyrosinase driven Cre-ER, two floxed alleles of PTEN, and a lox-stop-lox BRAFV600E cassette. Their genotype is referred to as Tyr:Cre-ER^{+}, LSL-Braf$^{V600E+/}$, Pten$^{fl/fl}$. Originally, the Tyr:Cre-ER mice were crossed onto LSL-Braf^{V600E} and subsequently crossed with the loxP-Pten mouse strain. Those mice were maintained as Tyr:Cre-ER+, LSL-Braf$^{V600E+/-}$, Pten$^{fl/fl}$ (Cheung, 2008; Suzuki, 1998; Dankort, 2007; Bosenberg, 2006). Mice expressing a transgene encoding the 2C TCR were bred in our facility. Lck^{pr}– Bcl-x$_L$ mice were a kind gift from Dr. Alegre (Zhou, 2005). 4-1BB$^{-/-}$ mice were a gift from Dr. Kwon and Dr. Croft (Kwon, 2002; Lee, 2006). All mice were housed at University of Chicago in specific pathogen-free conditions in accordance with the National Institute of Health animal care guidelines. All experiments were approved by the Institutional Animal Care and Use Committee at The University of Chicago and followed international guidelines.

2.2 Cell culture and inoculation

B16.F10 cells that were engineered to express the model antigen SIY (B16.SIY), MC57.SIY, 1969.SIY, and MC38 cells were cultured in DMEM supplemented with 10% FBS. To this medium 3-(N-Morpholino)propanesulfonic acid (MOPS), beta-mercaptoethanol, penicillin and streptomycin were added, as described (Williams, 2017). This is referred to as complete medium. For experiments, cells were released from culture flasks with 0.05% trypsin-EDTA (Thermo-Fisher catalogue number 25300054). Complete medium was added to quench the

trypsin, and cells were collected into 50 mL conical tubes. Cells were centrifuged at 500 x g for 3 minutes to collect cell pellets. Cells were washed with PBS once and counted on a hemocytometer with trypan blue staining. Cells were resuspended at a concentration of $20x10^6$ cells per mL in PBS. $2x10^6$ cells in a volume of 100 microliters were inoculated subcutaneously into the right flank of animals for experiments. For tumor measurements, tumors were measured with digital calipers. The lengths of the longest side and the side perpendicular to the longest side were measured. These lengths were multiplied to obtain the tumor area.

2.3 Antibody treatments

All therapeutic and depleting antibodies were purchased from Bio X Cell (West Lebanon, NH). 100 micrograms of α4-1BB (LOB.12.3), αCTLA-4 (UC10-4F10-11) and αPD-L1 (10F.9G2) were given intraperitoneally beginning seven days after tumor inoculation. For tumor outgrowth assays, antibodies were given on days 7, 10, 13 and 16 after tumor inoculation. To deplete CD4-, CD8- or NK1.1-expressing cells, 250 micrograms of either αCD4 (GK1.5) or αCD8 (2.43) or αNK1.1 (PK136) were given 24 hours before tumor inoculation, and then subsequently at seven day intervals throughout the experiment

2.4 FTY720 administration

FTY720 was purchased from Enzo Life Sciences. FTY720 was dissolved in DMSO and then diluted in PBS before administration. 5 micrograms per mouse was given daily by oral gavage in 100 microliters of total volume. Oral gavage of FTY720 began seven days after tumor inoculation, and continued for the duration of the experiment.

2.5 Flow cytometry

Fluorescently-labeled SIY-loaded pentamers were purchased from ProImmune. Fluorescently labeled antibodies recognizing the following molecules were used in analyses: BD Biosciences: CD45 (30-F11), CD3 (145-2C11), CD4 (RM4-5), CD8 (53-6.7), BrdU (Bu20a), Ki-67 (35/Ki-67), and active caspase-3 (C92-605); eBioscience: LAG-3 (C9B7W), 4-1BB (17B5) Biolegend: PD-1 (RMPI-30). Thermo-Fisher: γH2AX (CR55T33). Fixable viability dyes, including ef780, were used to gate out dead cells and were purchased from eBioscience. Tumors, lymph nodes and spleens were physically dissociated through a 70 μM cell strainer to generate cell suspensions. Tumor suspensions were centrifuged over a Ficoll-hypaque gradient to isolate live mononuclear cells. Cell suspensions were stained with SIY pentamer, viability dyes, and antibodies in PBS containing 1% FBS for 20 minutes at room temperature. Antibody were diluted 1:200 in buffer. Viability dyes were diluted 1:500 in buffer. SIY pentamer was diluted 1:50 in buffer. For intracellular antigens, cells were subsequently fixed and permeabilized in FoxP3 buffer (eBioscience) for 30 minutes at room temperature, washed, and then stained with antibodies against intracellular antigens for 30 minutes at room temperature. For annexin V staining, cells were first stained with extracellular antibodies and fixable viability dyes. Immediately before analysis, cells were stained with the annexin V staining kit (BD Biosciences, catalog number 559763). Data was acquired using an LSRII or an LSRFortessa instrument located in the Flow Cytometry Core at the University of Chicago. Flow cytometry data was analyzed using FlowJo Vx (Treestar).

2.6 BrdU

0.8 milligrams of BrdU (BD 555627) was given intraperitoneally 24 hours before sacrifice. After staining extracellular antigens, cells were fixed and permeabilized with FoxP3 buffer (eBioscience) for 30 minutes at room temperature. Cells were then resuspended in PBS with 300 micrograms per milliliter DNAse I (Roche) at 37 degrees Celsius for 1 hour. Cells were

subsequently stained with anti-BrdU antibody at room temperature for 30 minutes.

2.7 T cell activation for adoptive transfer

Splenocytes were isolated from 2C or 2C Bcl-x_L mice under sterile conditions. Single cell suspensions were generated by physically dissociating spleens through a 70 micron filter. Single cells were pelleted at 500 x g for 3 minutes. Red blood cells were lysed by resuspending the cell pellets with Geys solution for 2 minutes while shaking or vortexing at room temperature. The remaining cells were resuspended in complete medium and plated at 1.2 million cells per mL onto non-tissue-culture treated 96-well plates coated with 0.2 micrograms/mL anti-CD3 and 0.5 micrograms per mL anti-CD28 antibodies. For coating the plates: the anti-CD3 antibody (clone 145-2C11) and anti-CD28 antibody (clone 37.51) were diluted in PBS to blank 0.5 μg/mL and 0.2 μg/mL. This solution containing diluted antibodies was added to 96-well plates and incubated at room temperature for 2 hours. The antibody-containing solution was removed and 96-well plates were incubated with a sterile 2% BSA solution for 30 minutes at room temperature. The 2% BSA solution was removed just prior to the addition of splenocytes. Splenocytes were plated on these coated 96-well plates for 72 hours. Expanded T cells were then transferred to non-tissue-culture treated 6 well plates. Fresh complete medium was added and cells were incubated for another 72 hours, at which point they were activated effector cells. One million activated effector cells were then transferred intravenously to mice with 7-day established B16.SIY tumors.

2.8 ELISPOT

A MultiScreen-IP Filter Plate, 0.45 micron (Millipore MAIPS4510) was coated with anti-IFN-γ antibody (BD Biosciences 552569) diluted in sterile PBS at 4 degrees Celcius overnight. The next day, the coating solution was removed under sterile conditions and complete medium was used to block non-specific protein binding for at least 2 hours at room temper-

ature. Splenocytes from nave, tumor-challenged non-treated, or tumor-challenged, immunotherapy-treated mice were harvested 10 days after tumor inoculation under sterile conditions. Single cell suspensions were prepared by physical dissociation of spleens through a 70 micron filter. $1x10^6$ splenocytes were added per well into the coated 96 well plate. Cells were either left un-stimulated, stimulated with 160nM SIY-peptide (SIYRYYGL), or stimulated with PMA (100 ng/ml) and Ionomycin (1 μg/ml) as positive control. After a 24 hour culture period, IFN-γ production was assessed according to manufacturers instructions (BD Biosciences 552569).

2.9 Sorting $CD8^+$ TIL for RNA isolation, quantitation PCR, and gene expression profiling

Tumors were physically dissociated through a 70 micron cell strainer to generate a cell suspension which was washed several times and then centrifuged over a Ficoll gradient. The isolated mononuclear cells were magnetically separated and positively selecting those expressing CD8 (Miltenyi). After staining with fluorescently labeled antibodies against CD3, CD4 and CD8, the selected cells were sorted, with the $CD3^+$ $CD4^-$ $CD8^+$ cells being sorted directly into RLT buffer (Qiagen). RNA was isolated with RNeasy micro columns (Qiagen), reverse transcribed with the High Capacity cDNA Reverse Transcription kit (Applied Biosystems), and qPCR was performed using Taqman probes for 18s and IL-2 (Applied Biosystems). Polymerase chain reaction parameters were 1) 50C 2 min, 1 cycle, 2) 95° C 10 min, 1 cycle, 3) 95°C 15 seconds $\rightarrow$ 60°C 30 seconds $\rightarrow$ 72°C 30 seconds, 40 cycles, 4) 72°C 10 min, 1 cycle. For gene array analysis, purified RNA was transferred to the Functional Genomics Facility at the University of Chicago for analysis. RNA integrity and concentration were assessed using an Agilent Bioanalyzer 2100, and all RNA samples used for microarray analysis had an RNA Integrity Number > 9.0. Total RNA was processed into biotinylated cRNA using the Epicentre TargetAmp 2-Round Biotin-cRNA Amplification Kit

3.0 (TAB2R71024). The cRNA was hybridized to Illumina MouseRef8v2 arrays using Illumina provided protocols and scanned using an Illumina HiScan. Quantile normalized and background subtracted values were subsequently analyzed using Excel, R, and Illustrator. Genes whose expression value was under 10 were removed from the analysis.

2.10 Bone marrow chimeras

Recipient mice were irradiated with two doses or irradiation separated by 3 hours. The first dose was 500 cGy and the second dose was 550 cGy. The following day, bone marrow from donor mice was isolated. Mice were euthanized and the legs removed under sterile conditions. Tissue was removed to reveal the leg bones. Bones were separated and cleaned of remaining tissue. Femurs and tibias were either flushed with sterile PBS to remove the marrow, or crushed in a sterile mortar and pestle. Marrow was resuspended by vortexing or pipetting and filtered through a 70 micron filter. Bone marrow mononuclear cells were counted with a hemocytometer. Donor cells were resuspended to approximately $50x10^6$ mononuclear cells per mL in sterile PBS. Approximately $5x10^6$ cells were injected intravenously to irradiated mice in a total volume of 100 microliters via the tail vein. Mice were allowed to reconstitute for at least 6 weeks before experiments.

2.11 Splenocyte transfer to RAG2$^{-/-}$ mice

Spleens of donor mice were isolated under sterile conditions. Single cell suspensions were made by physical dissociation through a 70 micron filter. Sterile PBS was used to collect cells. Cells were centrifuged at 500 x g for 3 minutes to collect cell pellets. Red blood cells were lysed by resuspending the cell pellets with Geys solution for 2 minutes while shaking or vortexing at room temperature. Remaining splenocytes were counted with a hemocytometer. Splenocytes were reusupended at approximately $50x10^6$ cells per mL. Approximately $5x10^6$ splenocytes in a volume of 100 microliters were injected intravenously to RAG2$^{-/-}$ mice via

the tail vein. Mice were allowed to reconstitute for at least 6 weeks before being used for experiments.

2.12 Statistics

GraphPad Prism was used to compute all statistical tests. Data represent mean +/- SEM. Statistical significance was calculated with Mann-Whitney U tests, Kruskal-Wallis tests, or Two-Way ANOVA with Bonferroni correction, as appropriate. *P <0.05, **P $<$ 0.01, ***P $<$ 0.001, ****P $<$ 0.0001.

CHAPTER 3

RESULTS

3.1 Expression of inhibitory and costimulatory receptors on CD8$^+$ TIL

Tumor-infiltrating CD8$^+$ T cells express multiple inhibitory and costimulatory receptors (Speiser, 2016; Williams, 2017). One of these costimulatory receptors is 4-1BB, the activation of which can improve immune-mediated tumor control (Melero, 1997). To begin to explore the potential therapeutic mechanism of 4-1BB stimulation, we utilized a model in which B16 melanoma cells were transduced to express the model antigen SIYRYYGL (B16.SIY) was implanted subcutaneously into syngeneic C57BL/6 mice. This model enables tracking of antigen-specific CD8$^+$ T cell responses using peptide-MHC multimers, antigen-specific ELISPOT assays, and adoptive transfer of 2C TCR transgenic T cells specific for this antigen (Udaka, 1996). FACS analysis showed upregulation of inhibitory receptors CTLA-4 and PD-1, as well as 4-1BB on subsets of CD8$^+$ TIL in B16.SIY tumors (Figure 3.1A and 3.1B). We have previously shown that blockade of CTLA-4 and PD-L1 works by reinvigorating the CD8$^+$ T cells already within the tumor at the time of treatment (Spranger, 2014). Therefore we hypothesized that agonist 4-1BB antibodies might also work directly on tumor-infiltrating CD8$^+$ T cells.

3.2 Agonist anti-4-1BB antibody synergizes with blockade of either CTLA-4 or PD-L1 to promote potent tumor regression in vivo

As we had found that CTLA-4 and PD-1 (Figure 3.1A and 3.1B) were expressed on CD8$^+$ T cells infiltrating B16.SIY tumors that express 4-1BB, we evaluated whether agonist 4-1BB would synergize with blockade of either CTLA-4 or PD-L1 to promote B16.SIY tumor

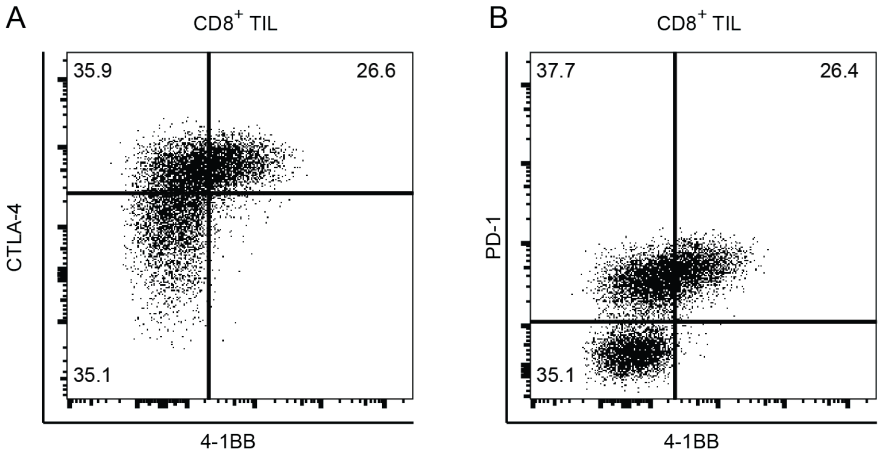

Figure 3.1: CD8$^+$ TIL express both inhibitory and costimulatory receptors
FACS plots showing expression of (A) 4-1BB and CTLA-4 or (B) 4-1BB and PD-1 on CD8$^+$ TIL isolated from B16.SIY tumor-bearing C57BL/6 mice.

control. Consistent with previous studies (Melero, 1997), we found that agonist anti-4-1BB alone provided some therapeutic effect compared to the untreated group (Figure 3.2A and 3.2B). Importantly, blockade of either CTLA-4 or PD-L1 combined with an agonistic anti-4-1BB antibody significantly enhanced tumor control compared to any single treatment arm (Figure 2A and 2B). Similarly potent tumor regression was seen in the MC38 tumor model with combination treatments (Figure 3.2C and 3.2D). Thus, agonist anti-4-1BB therapy can further enhance the benefits of neutralizing antibodies against CTLA-4 and the PD-1/PD-L1 axis.

3.3 Efficacy of anti-4-1BB combination plus blockade of either CTLA-4 or PD-L1 is dependent on $CD8^+$ T cells, but not $CD4^+$ T cells or natural killer (NK) cells

NK cells have been shown to participate in tumor control in syngeneic mouse models and human xenograft models treated with an agonist 4-1BB antibody (Melero, 1998; Wilcox, 2002), and more recently in combination therapies with an agonist 4-1BB antibody (Kohrt, 2011; Kohrt, 2012; Kohrt, 2014). To evaluate if NK cells were necessary for tumor control in the syngeneic B16.SIY model, we treated $RAG2^{-/-}$ mice, which lack B and T cells but contain NK cells, bearing B16.SIY tumors with agonist 4-1BB combined with either CTLA-4 or PD-L1 blockade. However, no anti-tumor effect was observed, arguing for dependence on adaptive immunity for tumor control (Figure 3.3A). To test whether NK cells were necessary in the context of an otherwise functional adaptive immune system, we depleted NK cells from WT mice. Depletion of NK cells did not interfere with the efficacy of anti-4-1BB combination immunotherapies (Figure 3.3B). To determine whether T cells were required, $CD4^+$ or $CD8^+$ cells were depleted prior to tumor inoculation, and the therapeutic antibodies were administered. $CD4^+$ cell depletion had no detrimental effect on tumor control after immunotherapy (Figure 3.4A), and in fact resulted in better tumor control compared to

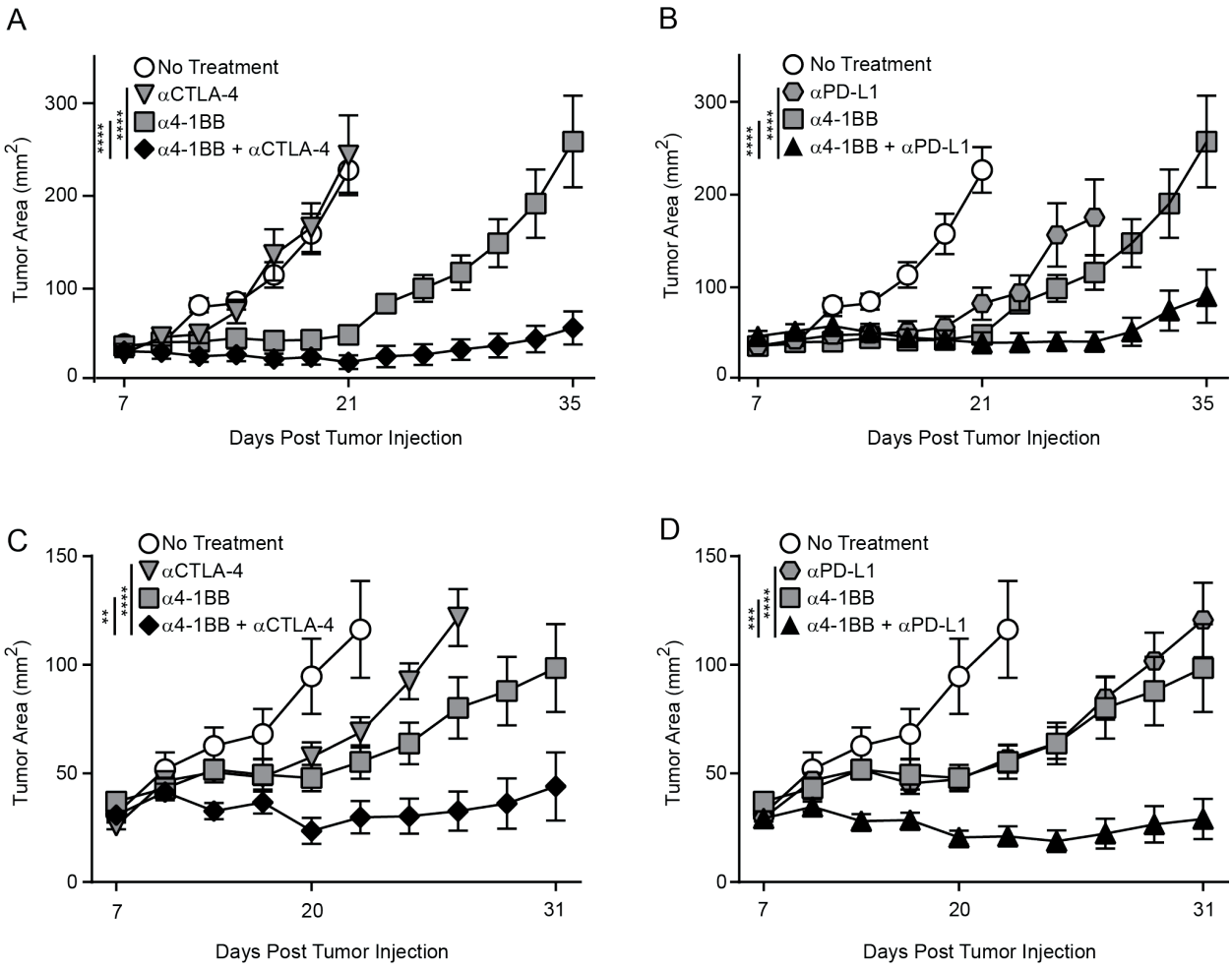

Figure 3.2: Agonist anti-4-1BB synergizes with blockade of either CTLA-4 or PD-L1 to promote potent B16.SIY tumor regression in vivo

C57BL/6 mice were subcutaneously inoculated with $2x10^6$ B16.SIY cells. Tumors were established for seven days, then cohorts were treated with either single antibodies against 4-1BB, CTLA-4, or PD-L1, or combinations of anti-4-1BB + anti-CTLA-4 (A) or anti-4-1BB + anti-PD-L1 (B). Antibodies were given intraperitoneally on days 7, 10, 13 and 16 post-tumor injection. Each mouse received 100 μg of each indicated antibody at each time point. Data are pooled from two individual experiments each with n = 5 mice per cohort. 2-way ANOVA with a Bonferroni correction was performed to determine statistical significance. No Treatment and anti-4-1BB curves are the same between (A) and (B). (C and D) C57BL/6 mice were subcutaneously inoculated with 2x10textsuperscript6 MC38 cells. Tumors were established for seven days, then cohorts were treated with either single antibodies against 4-1BB, CTLA-4, or PD-L1, or combinations of anti-4-1BB + anti-CTLA-4 (C) or anti-4-1BB + anti-PD-L1 (D). Antibodies were given intraperitoneally on days 7, 10, 13 and 16 post-tumor injection. Each mouse received 100 μg of each indicated antibody at each time point. Data are pooled from 2 individual experiments each with n=5 mice per cohort. 2-way ANOVA with a Bonferroni correction was performed to determine statistical significance. No Treatment and anti-4-1BB curves are the same between (C) and (D).

isotype control-treated mice, most likely due to the depletion of $CD4^+$ regulatory T cells as has been seen in previous studies (Bos, 2013). However, these mice still had increased tumor control upon immunotherapy, indicating that they were still able to respond to combination immunotherapy despite increased baseline tumor control (Figure 3.4A). $CD8^+$ cell depletion completely abrogated tumor control, indicating a requirement for $CD8^+$ T cells for efficacy of agonist anti-4-1BB combination immunotherapy (Figure 3.4B). Taken together with our previous results, 4-1BB-based immunotherapy depends on $CD8^+$ T cells for enhanced tumor control.

3.4 Blockade of CTLA-4 or PD-L1 combined with anti-4-1BB immunotherapy generates immunologic memory that requires $CD4^+$ T cells during rejection of the initial tumor

Several mice rejected their tumors completely with combination immunotherapy. Therefore we investigated whether these mice had generated protective immunological memory against tumor antigens. We compared tumor outgrowth of nave mice challenged with B16.SIY to outgrowth of B16.SIY in mice treated with combination immunotherapy that had rejected their tumors greater than 8 weeks previously. Secondary tumors were completely rejected in the vast majority of mice (6/7 for anti-4-1BB + anti-PD-L1, 4/4 for anti-4-1BB + anti-CTLA-4), suggesting that tumor antigen-specific $CD8^+$ T cells persisted and remained functional for long periods of time after immunotherapy (Figure 3.5A). Consistent with this notion, re-challenged mice also had expanded populations of detectable SIY-reactive $CD8^+$ T cells in their spleens as measured by IFN-γ ELISPOT (Figure 3.5B). Several mice depleted of $CD4^+$ cells also completely rejected their tumors. We compared tumor outgrowth of B16.SIY tumors in mice that had rejected their tumors over 8 weeks previously, and had either received antibody mediated depletion of $CD4^+$ cells or received isotype control antibody. Mice nave to B16.SIY served as control. Mice that rejected their tumors in the setting of CD4 deple-

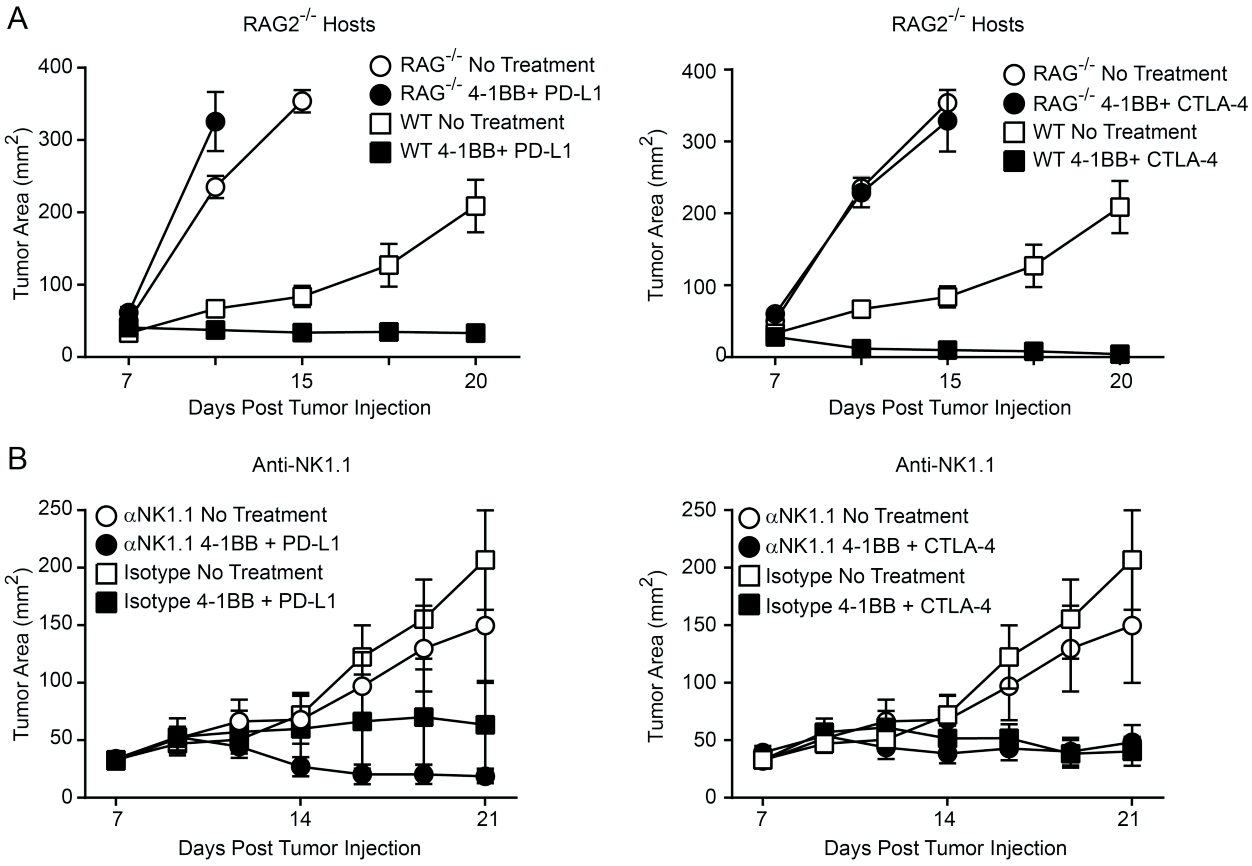

Figure 3.3: Efficacy of anti-4-1BB combination plus blockade of either CTLA-4 or PD-L1 is not dependent natural killer (NK) cells

(A) RAG2$^{-/-}$ or wild type (WT) mice were innoculated subcutaneously with 2x10^6 B16.SIY cells. Mice were treated with 100 μg of each therapeutic antibody on days 7, 10, 13 and 16 post tumor injection. RAG$^{-/-}$ NT n = 9, RAG$^{-/-}$ anti-4-1BB + anti-CTLA-4 n = 3, RAG$^{-/-}$ anti-4-1BB + anti-PD-L1 n = 4, WT no treatment n = 8, WT anti-4-1BB + anti-CTLA-4 n = 3, WT anti-4-1BB + anti-PD-L1 n = 5. No Treatment curves in (A) are the same between both panels. (B) C57BL/6 mice were given 250 μg of a depleting anti-NK1.1 antibody 24 hours before subcutaneous injection of 2x10^6 B16.SIY, and weekly thereafter for the duration of the experiment. Mice were treated with 100 μg of each therapeutic antibody on days 7, 10, 13 and 16 post tumor injection. n = 4-5 for each cohort. No Treatment curves in (B) are the same in each panel.

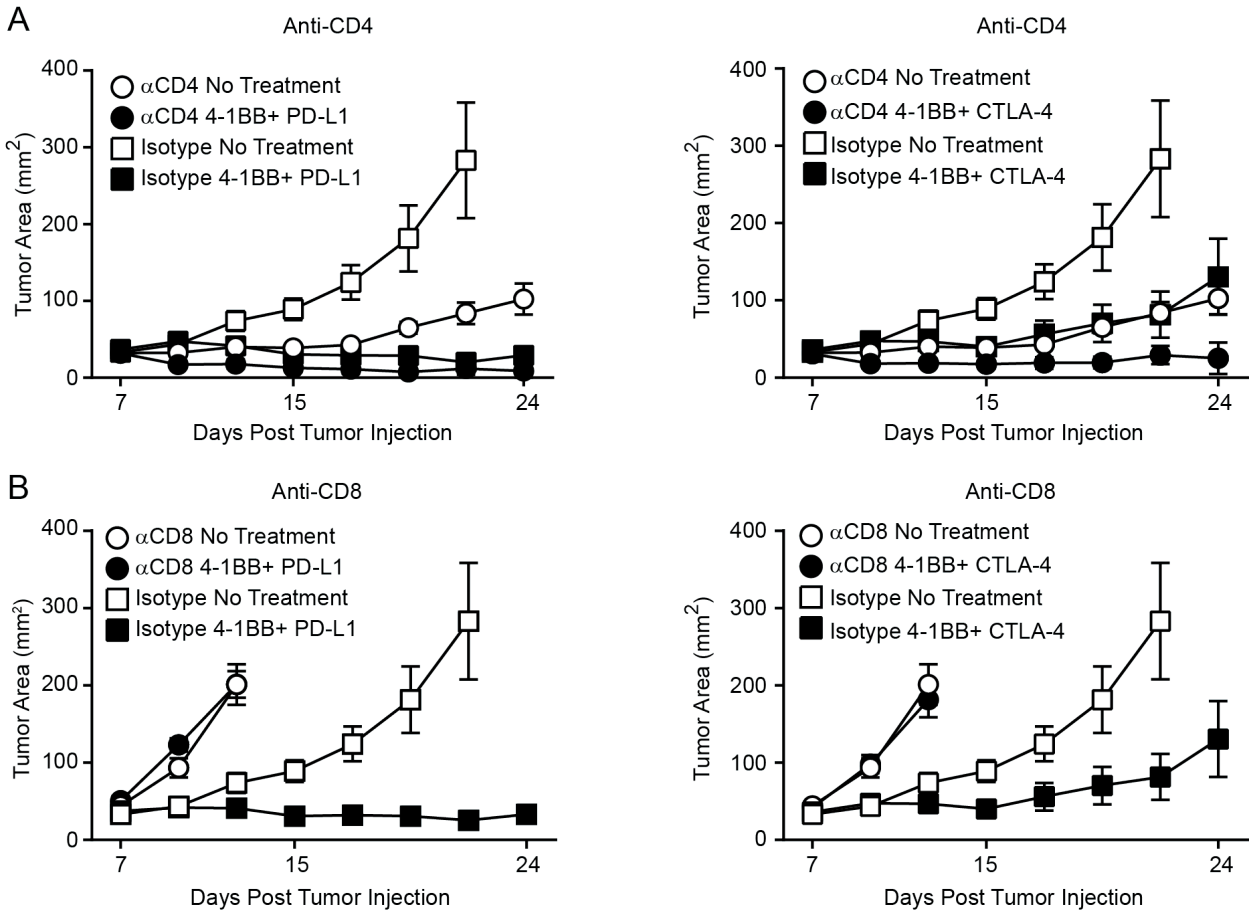

Figure 3.4: Efficacy of anti-4-1BB combination plus blockade of either CTLA-4 or PD-L1 is dependent on CD8$^+$ T cells but not on CD4$^+$ T cells
(A) Mice were given 250 μgrams of a depleting anti-CD4 antibody 24 hours before subcutaneous injection of 2x10^6 B16.SIY, and weekly thereafter for the duration of the experiment. Mice were treated with 100 μgrams of each therapeutic antibody on days 7, 10, 13 and 16 post tumor innoculation. Data are pooled from 2 experiments, each with n = 4-5 mice per cohort. No Treatment curves in (A) are the same in the two panels. (B) Mice were given 250 μgrams of a depleting anti-CD8 antibody 24 hours before subcutaneous injection of 2x10^6 B16.SIY cells, and weekly thereafter for the duration of the experiment. Mice were treated with 100 μgrams of each therapeutic antibody on days 7, 10, 13 and 16 post tumor injection. Data are pooled from 2 experiments, each with n = 4-5 per cohort. No Treatment curves in (B) are the same between the two panels.

tion did not form protective memory to a secondary challenge of B16.SIY (Figure 3.5C). These results suggest that $CD4^+$ cells were not required for rejecting the primary tumor, but played a role in forming protective immunologic memory.

3.5 Agonist 4-1BB plus neutralizing CTLA-4 or PD-L1 antibodies expand antigen-specific $CD8^+$ T cells in lymphoid tissues and within the tumor microenvironment

Our previous work revealed that combined CTLA-4 and PD-L1 blockade acts primarily on $CD8^+$ T cells in the tumor microenvironment (Spranger, 2013). As agonist anti-4-1BB combination immunotherapies were dependent on $CD8^+$ T cells for tumor control, we investigated whether 4-1BB agonist antibody combined with either CTLA-4 or PD-L1 blockade expanded $CD8^+$ T cells in the tumor microenvironment, in secondary lymphoid tissues, or both. Seventy-two hours after one antibody dose (Day 10 post tumor inoculation), the anti-4-1BB antibody cohort and the combination immunotherapy cohorts had increased numbers SIY-specific, IFN-γ-producing T cells in the spleen, as measured by IFN-γ ELISPOT (Figure 3.6A). Flow cytometry with SIY-K^b pentamers at the same time point revealed an increased frequency of splenic SIY-reactive $CD8^+$ cells in the combination immunotherapy groups (Figure 3.6B and 3.6D) as well as within tumor-draining lymph nodes and the tumor microenvironment (Figures 3.6C and 3.6E). These increases were seen at all interrogated anatomic locations after the combination immunotherapies, with only slight increases being observed in the single treatment cohorts (Figures 3.6C-3.6E). Similar results were obtained when analyzing the absolute numbers of SIY-reactive $CD8^+$ T cells in the tumor-draining lymph nodes, spleens, and tumors (Figures 3.6F-3.6H). A more detailed kinetic analysis was also performed. We found marked expansion of SIY-reactive $CD8^+$ T cells in the tumor-draining lymph nodes and spleens that peaked at Day 13 post-tumor inoculation with both combination immunotherapies (Figures 3.7A and 3.7B). We also found significant increases

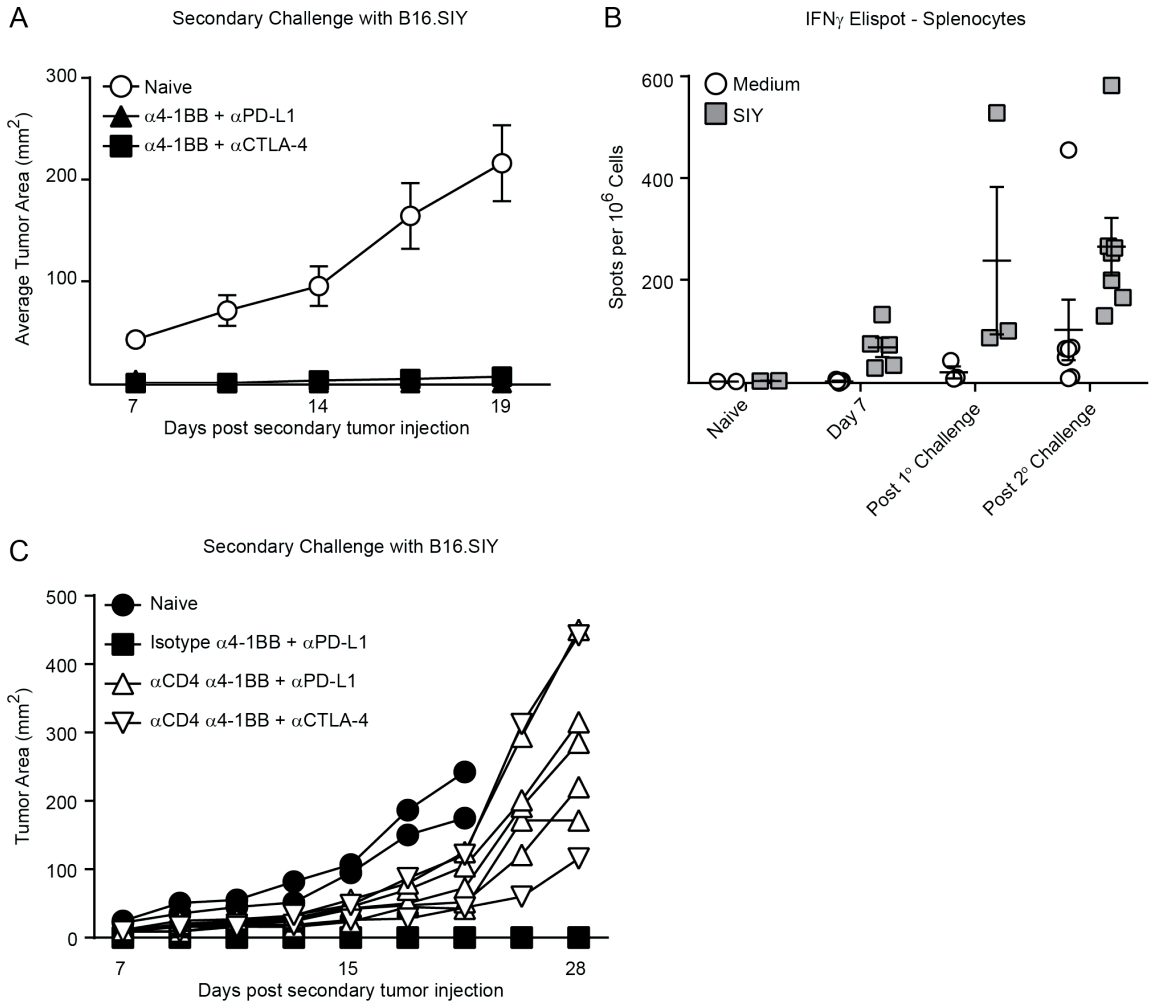

Figure 3.5: Complete tumor regression after anti-4-1BB combination immunotherapy generates immunologic memory that is dependent on CD4$^+$ cells (A) C57BL/6 mice that were either nave to B16.SIY or had rejected primary B16.SIY tumors from treatment with immunotherapy were challenged subcutaneously with 2x10^6 B16.SIY cells. Data are pooled from 2 independent experiments. Nave n=7, anti-4-1BB + anti-CTLA-4 n=4, anti-4-1BB + anti-PD-L1 n=7. (B) Mice were either nave, had been challenged subcutaneously with 2x10^6 B16.SIY cells seven days previously, had rejected primary B16.SIY tumors, or had rejected a secondary B16.SIY tumor. Mice were sacrificed and their splenocytes were used to perform an IFN-γ ELISPOT in response to SIY peptide. (C) C57BL/6 mice that were either nave to B16.SIY, had rejected primary B16.SIY tumors from treatment with immunotherapy plus isotype control antibody, or had rejected primary B16.SIY tumors from treatment with immunotherapy plus anti-CD4 depleting antibody, were challenged with 2x10^6 B16.SIY cells. Data are pooled from 2 independent experiments. Nave n=2, anti-PD-L1 + anti-4-1BB + isotype control n = 1, anti-4-1BB + anti-CTLA-4 + anti-CD4 n=2, anti-4-1BB + anti-PD-L1 n=5.

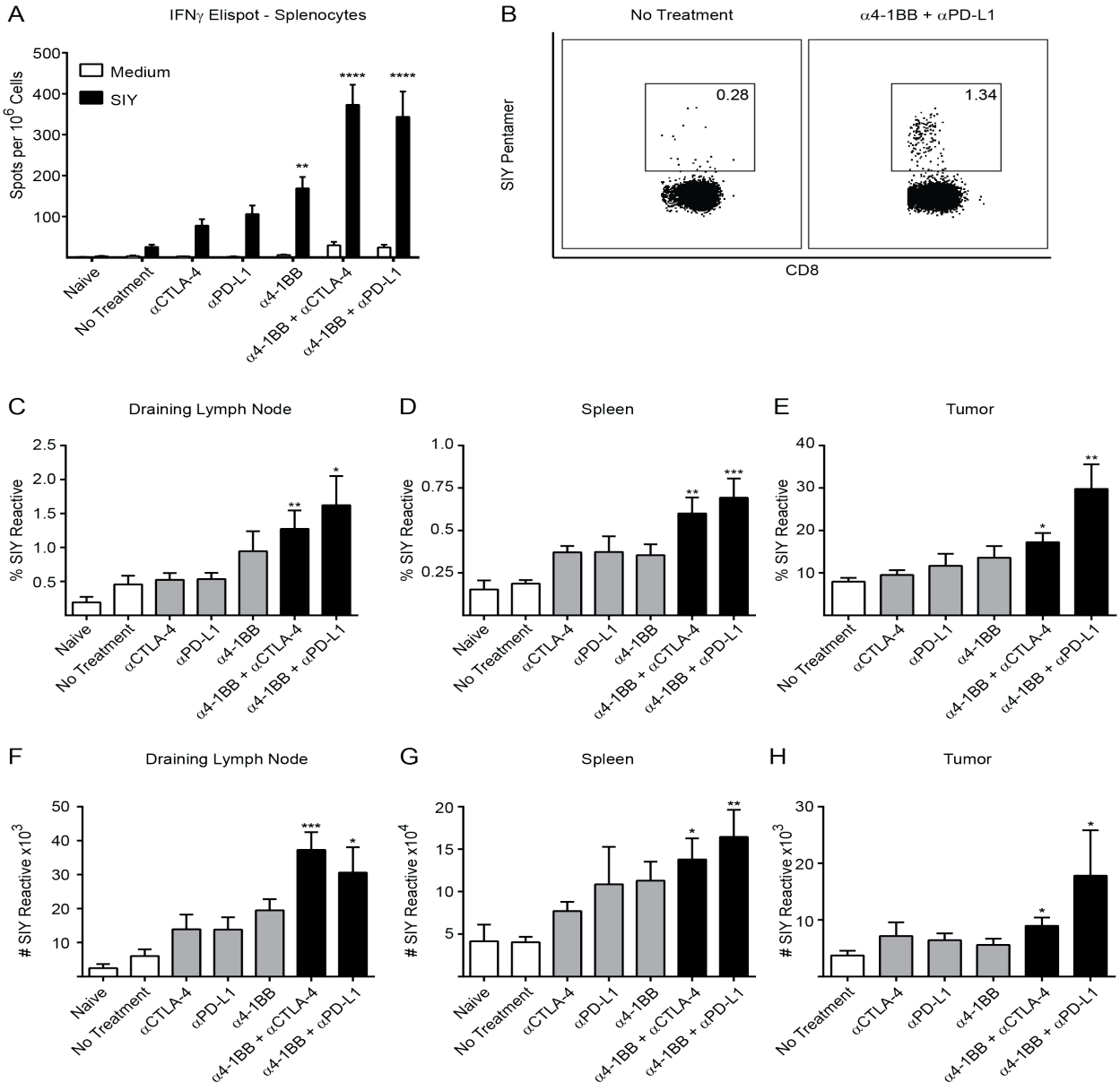

Figure 3.6: Agonist 4-1BB plus neutralizing CTLA-4 or PD-L1 antibodies expand antigen specific CD8$^+$ T cells in lymphoid tissues and within the tumor microenvironment

C57BL/6 mice were inoculated with 2x10^6 B16.SIY cells, given immunotherapy on day 7, and sacrificed on day 10. (A) Splenocytes were analyzed for IFN-γ production via ELISPOT. n=10, except "naive" where n=6. Statistical comparisons are made to the No Treatment group using 2-way ANOVA. (B) FACS plots from (A). Flow cytometry was used to detect the frequency (C-E) and number (F-H) of SIY-reactive CD8$^+$ cells in multiple anatomic locations in mice from (A). Statistical comparisons are made to the "No Treatment cohort using Kruskal-Wallis one-way ANOVA.

of SIY-reactive CD8$^+$ T cells within tumors, with the increase after anti-4-1BB + anti-PD-L1 peaking at Day 13 post tumor injection, earlier than after anti-4-1BB + anti-CTLA-4 (Figure 3.7C). The increase in specific CD8$^+$ cells in the tumor-draining lymph nodes prior to the tumor site led us to question whether the efficacy of agonist anti-4-1BB combination immunotherapy mainly enhanced the priming of SIY-reactive CD8$^+$ T cells in lymphoid tissues that subsequently migrated to the tumor to promote tumor regression.

3.6 Tumor rejection is driven by tumor-infiltrating T cells present in the tumor before immunotherapy begins

In order to determine if tumor regression after agonist 4-1BB combination immunotherapy was dependent on the arrival of recently primed T cells from tumor-draining lymph nodes, we used the S1P1 receptor agonist FTY720, which inhibits T cell egress from lymph nodes (Pinschewer, 2000; Brinkmann, 2002; Mandala, 2002; Matloubian, 2004). We inoculated mice with B16.SIY tumor cells and waited seven days for tumors to establish, to allow anti-tumor T cell priming and infiltration into tumors. Beginning seven days post tumor inoculation, mice were treated with FTY720 in order to prevent egress of T cells from lymph nodes into the tumor. Thus, only T cells already present within the tumor microenvironment prior to FTY720 treatment would be available to mediate anti-tumor effects. Despite the significant T cell expansion in tumor-draining lymph nodes during agonist 4-1BB combination immunotherapy, tumor control was completely preserved with concomitant FTY720 administration (Figure 3.8A). Despite the absence of circulating T cells during FTY720 administration (Figure 3.8B), we found an increased number of SIY-reactive CD8$^+$ TIL during immunotherapy (Figure 3.8C). These results suggested that tumor control after 4-1BB combination immunotherapy resulted from effects on T cells already within the tumor microenvironment.

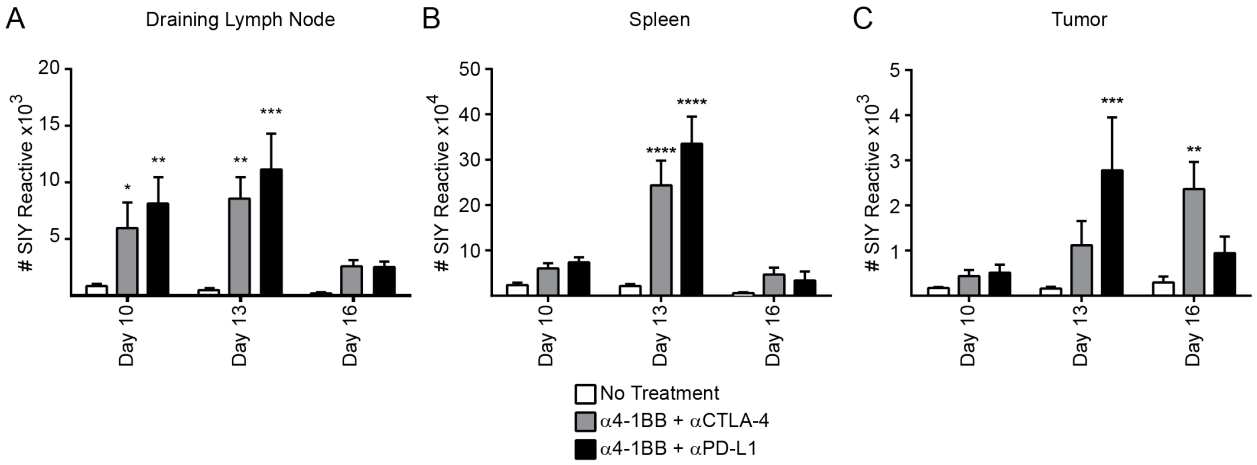

Figure 3.7: Agonist 4-1BB plus neutralizing CTLA-4 or PD-L1 antibodies expand the number of antigen specific CD8$^+$ T cells in lymphoid tissues and within the tumor microenvironment

The tumor draining lymph nodes (A), spleens (B), and tumors (C) from C57BL/6 mice innoculated subcutaneously with 2x10^6 B16.SIY were analyzed using flow cytometry to detect and enumerate SIY-reactive CD8$^+$ cells on day 10, 13 and 16. Immunotherapy began on day 7 post tumor injection and continued until mice were sacrificed. Data are pooled from 2 independent experiments with n=5 for each cohort per experiment. Statistical comparisons were made with 2-way ANOVA with a Bonferroni correction.

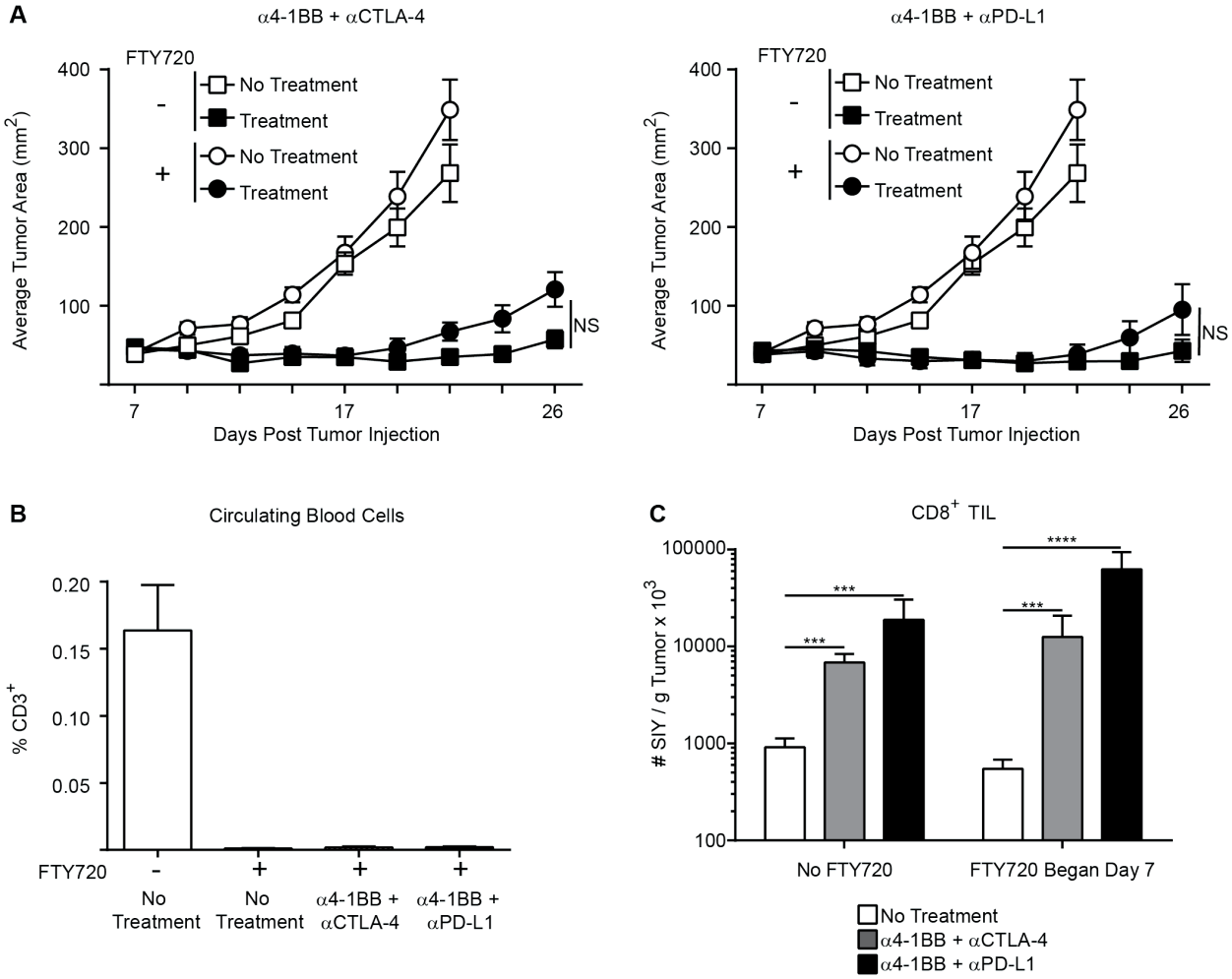

Figure 3.8: 4-1BB combination immunotherapy leads to tumor regression and CD8$^+$ TIL accumulation through an intratumoral process

C57BL/6 mice were inoculated subcutaneously with 2x10^6 B16.SIY cells. Tumors were established for 7 days, at which point daily oral administration of FTY720 was begun. Mice received immunotherapy intraperitoneally on days 7, 10, 13 and 16 post tumor injection. The day 7 treatments were given at least 2 hours after FTY720 administration began. (A) B16.SIY tumor outgrowth curves, n = 10. 2-way ANOVA with a Bonferroni correction. No Treatment curves are the same between the two panels. (B) Whole blood from mice from (A) was analyzed at the endpoint of the experiment for circulating CD3$^+$ cells using flow cytometry. (C) Mice received immunotherapy intraperitoneally on days 7 and 10 post tumor injection, and were analyzed on day 13. The accumulation of SIY-reactive CD8$^+$ TIL was analyzed with flow cytometry, n = 15, One-way ANOVA was performed to determine statistical significance.

3.7 Agonist 4-1BB plus neutralizing CTLA-4 or PD-L1 antibodies increases CD8$^+$ tumor-infiltrating T cell numbers through reduced apoptosis

As CD8$^+$ TIL accumulation was not due to new influx of peripheral T cells (Figure 3.8C), we reasoned that either increased proliferation or decreased apoptosis might be responsible for this expansion. To assess proliferation in situ, we pulsed mice with BrdU 24 hours before sacrifice and measured BrdU incorporation into CD8$^+$ T cells by flow cytometry. In tumor-draining lymph nodes and the spleens, a large increase in CD8$^+$ T cell proliferation was observed following 4-1BB combination immunotherapy, consistent with induced expansion of SIY specific CD8$^+$ T cells in these locations (Figure 3.9A and 3.9B). However, immunotherapy did not alter the proliferation of CD8$^+$ T cells within the tumor microenvironment (Figure 3.9C). We therefore performed a time course of CD8$^+$ TIL BrdU incorporation. While there was little BrdU incorporation seven days post tumor injection, we observed consistent BrdU incorporation by TIL between days 10 21 post tumor injection. Incorporation of BrdU was significantly greater in the TIL than in the spleen, indicating that TIL were being constantly driven to proliferate in the tumor microenvironment (Figure 3.10). To analyze antigen-specific TIL, we used K^b/SIY pentamers. Unfortunately, the BrdU staining interfered with the detection of pentamer-reactive cells. Previously, we found that expression of the surface receptors LAG-3 and 4-1BB identifies antigen-specific TIL (Williams, 2017), therefore we phenotyped TIL for LAG-3 and 4-1BB while measuring BrdU incorporation (Figure 11A). The subpopulations of TIL expressing LAG-3 were the most actively proliferating (Figure 11B), suggesting that antigen-specific TIL were proliferating within the tumor microenvironment during tumor progression. Consistent with our previous finding that this surface phenotype enriches for antigen specificity, a vast majority of SIY-reactive TIL expressed LAG-3, or LAG-3 and 4-1BB (Figure 11C), and conversely the PD-1$^+$LAG-3$^+$4-1BB$^+$ population was highly enriched for SIY-reactive TIL (Figure 3.11D).

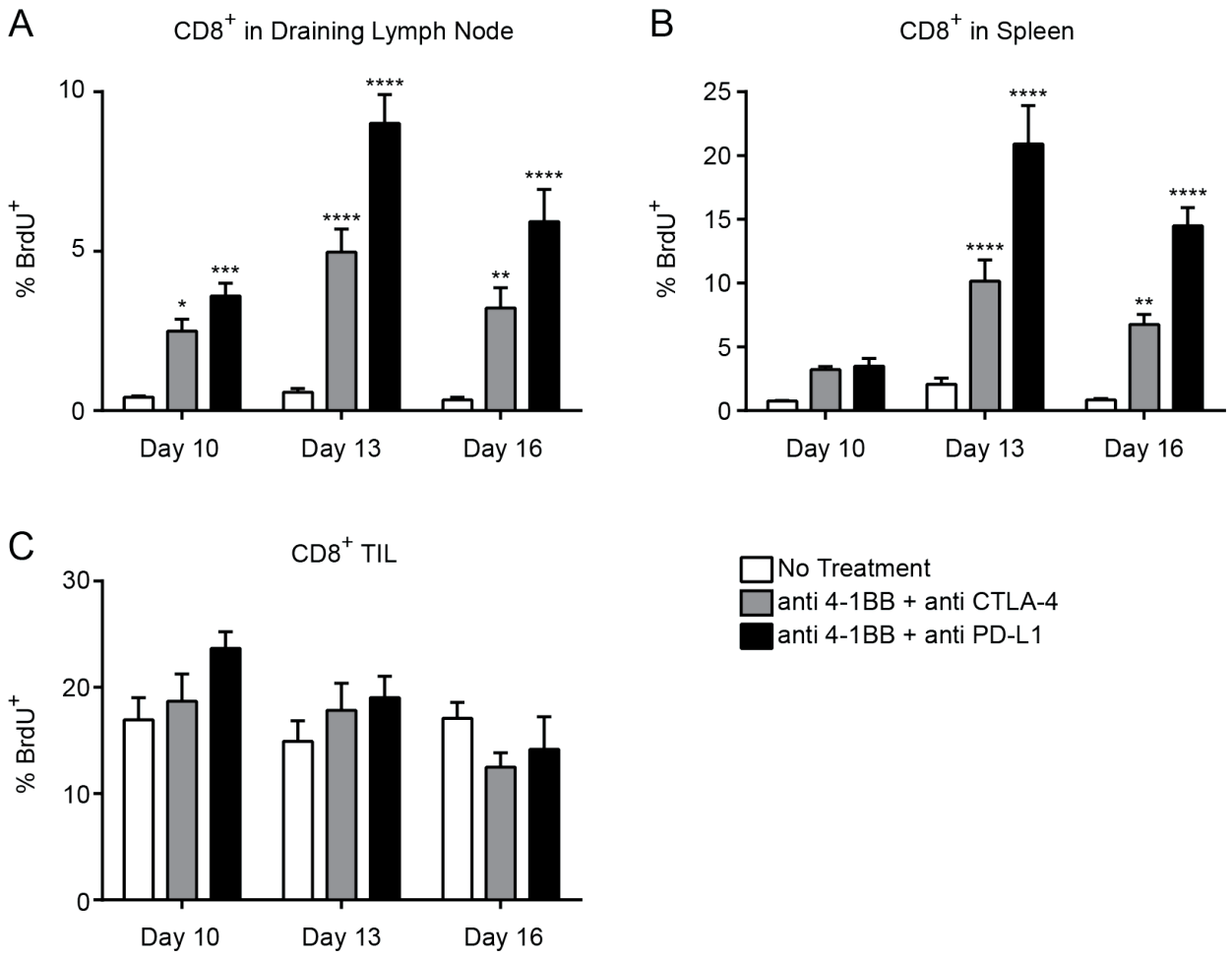

Figure 3.9: Agonist anti-4-1BB plus neutralizing anti-CTLA-4 or anti-PD-L1 antibodies increases CD8$^+$ T cell proliferation in secondary lymphoid tissues but not the tumor microenvironment

C57BL/6 mice were inoculated subcutaneously with 2x10^6 B16.SIY cells and treated with immunotherapy beginning on day 7 after tumor cell injection. 0.8 mg of BrdU per mouse was administered intraperitoneally 24 hours before sacrifice of each cohort. On day 10, 13, or 16 after tumor cell injection the tumor draining lymph nodes, spleens, and tumors of mice were analyzed using flow cytometry to detect and enumerate the CD8+ T cells with incorporated BrdU. Data are pooled from 2 independent experiments with n=5 mice per cohort for each experiment. 2-way ANOVA was used to compare statistical differences between cohorts.

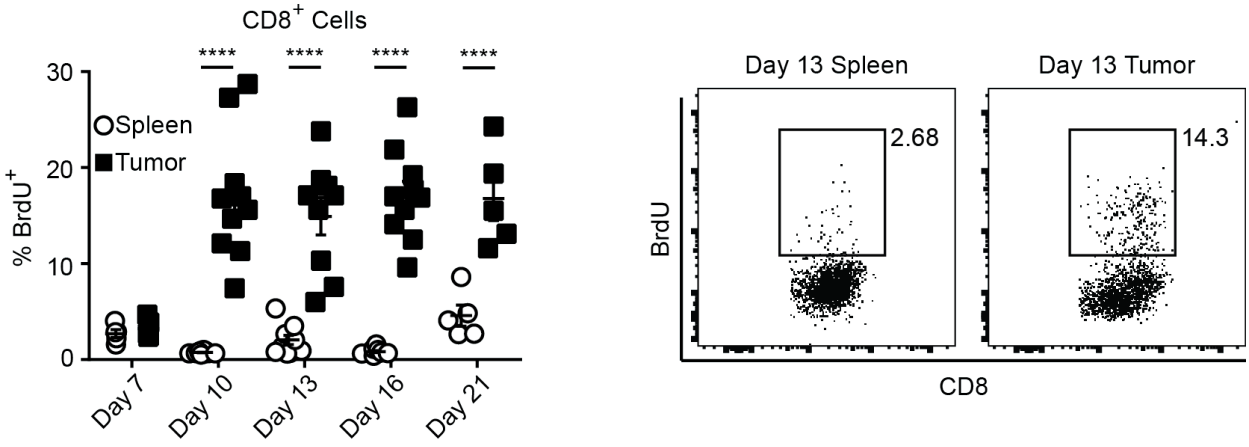

Figure 3.10: CD8$^+$ T cells proliferate in the tumor microenvironment without immunotherapy

C57BL/6 mice were injected subcutaneously with 2x10^6 B16.SIY tumor cells on day 0 and sacrificed at the indicated time points. One day prior to sacrifice, mice were injected intraperitoneally with 0.8 mg BrdU. Spleens and tumors of mice were analyzed via flow cytometry for BrdU incorporation in CD8$^+$ T cells. 2-way ANOVA with a Bonferroni correction was performed to determine statistical significance, n = 10 per time point.

To determine proliferation of antigen-specific TIL directly, we analyzed Ki-67 expression as an alternative indicator of proliferation, as Ki-67 staining was compatible with SIY staining. Nearly all SIY-reactive TIL expressed Ki-67 at every time point analyzed (Figure 11E).

The LAG-3-expressing populations remained the most proliferative subset of TIL over the course of tumor outgrowth (Figure 3.12A). This phenotype was consistent over all time points analyzed (Figure 3.12B), indicating that these antigen-specific TIL proliferate for the duration of tumor outgrowth. Despite this constant proliferative rate of TIL, there was no statistically significant accumulation of TIL or SIY-reactive TIL over the time points analyzed (Figure 3.13A and 3.13B). Therefore, some other process was restraining TIL accumulation despite constant proliferation.

Since tumor-specific $CD8^+$ T cells were actively proliferating but were not accumulating over time, we measured rates of TIL apoptosis. Caspase-3 is activated via cleavage during apoptosis, and it has been demonstrated that effector T cells containing active caspase-3 are undergoing cell death (Martin, 1996; Garrod, 2012). Therefore, we utilized flow cytometry to detect intracellular active caspase-3. We found that at day 13 post tumor injection, a large fraction of TIL and SIY-reactive TIL contained active caspase-3 within the tumor but not in the spleen (Figure 3.14A). To test if apoptosis of TIL occurred in non-transplantable tumor settings, we used an autochthonous, inducible B-Raf^{V600E}/$PTEN^{-/-}$ melanoma model. $CD8^+$ T cells within B-Raf^{V600E}/$PTEN^{-/-}$ melanomas also underwent apoptosis (Figure 3.14B) (Spranger, 2015). Thus, $CD8^+$ T cell apoptosis occurs specifically in the tumor microenvironment of tumor models with very different developmental origins and latency times.

In order to better understand the relationship between TIL phenotype, proliferation, and apoptosis, we performed a phenotypic analysis of $CD8^+$ TIL. TIL co-expressing LAG-3 and 4-1BB showed the highest rate of apoptosis (Figure 3.14C), which suggested that antigen-specific TIL were simultaneously proliferating and dying. This result suggested that the acquisition of this phenotype in the tumor environment was associated with high

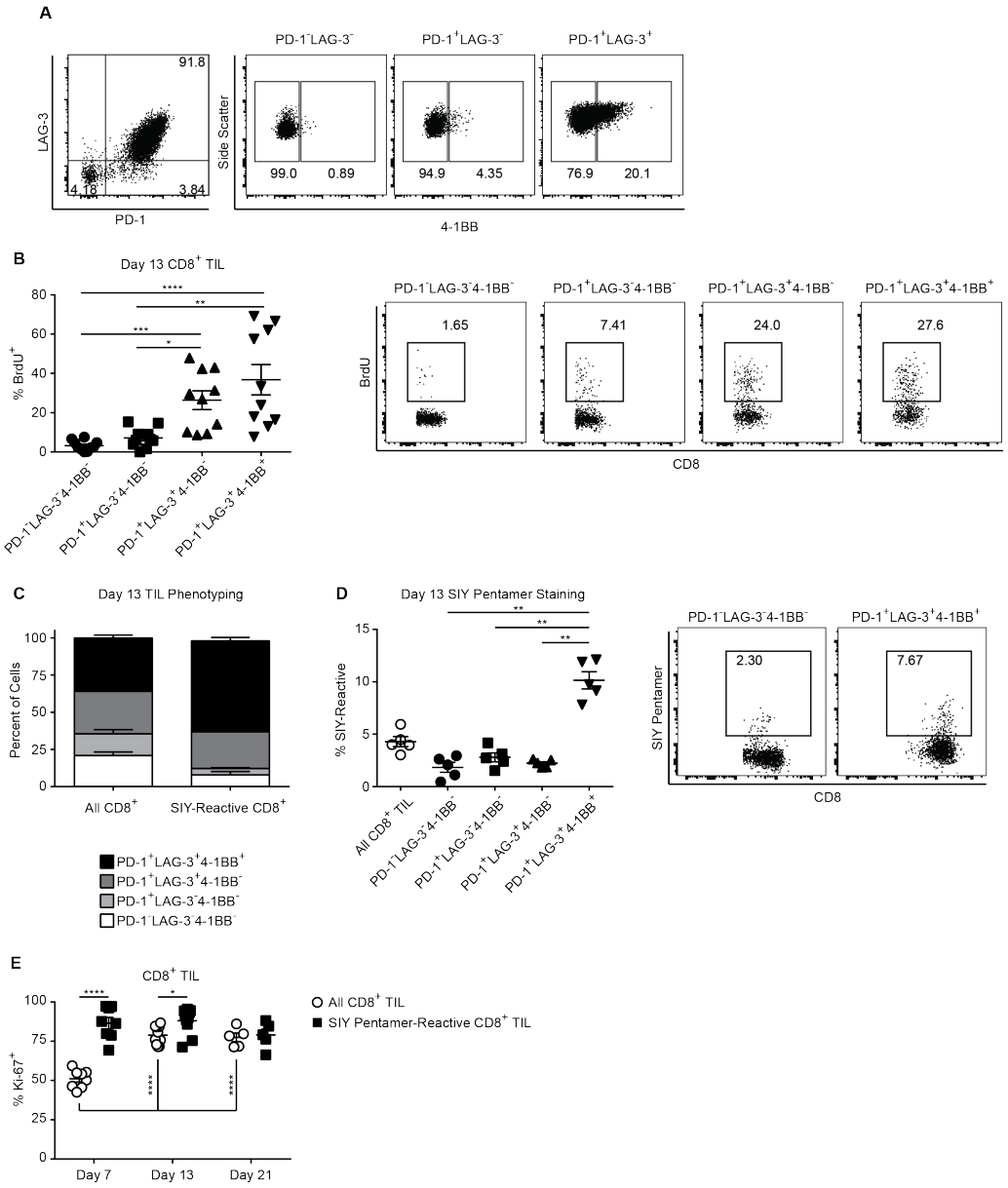

Figure 3.11: Antigen-specific CD8$^+$ T cells proliferate in the tumor microenvironment

(A) Representative FACS plots of PD-1, LAG-3, and 4-1BB expression on CD8$^+$ TIL isolated from B16.SIY tumors. (B) Analysis of TIL for the incorporation of BrdU on day 13, combined with phenotyping for the expression of PD-1, LAG-3 and 4-1BB. One-way ANOVA, n = 10. (C) and (D) TIL were stained with SIY pentamer and analyzed for the expression of PD-1, LAG-3, and 4-1BB on day 13 post tumor injection, n = 5, one-way ANOVA. (E) Tumors of mice bearing B16.SIY tumors for 13 days were analyzed for SIY pentamer-reactive cells and Ki-67 expression via flow cytometry, day 7 n = 8, day 13 n = 10, day 21 n = 5. Two-way ANOVA.

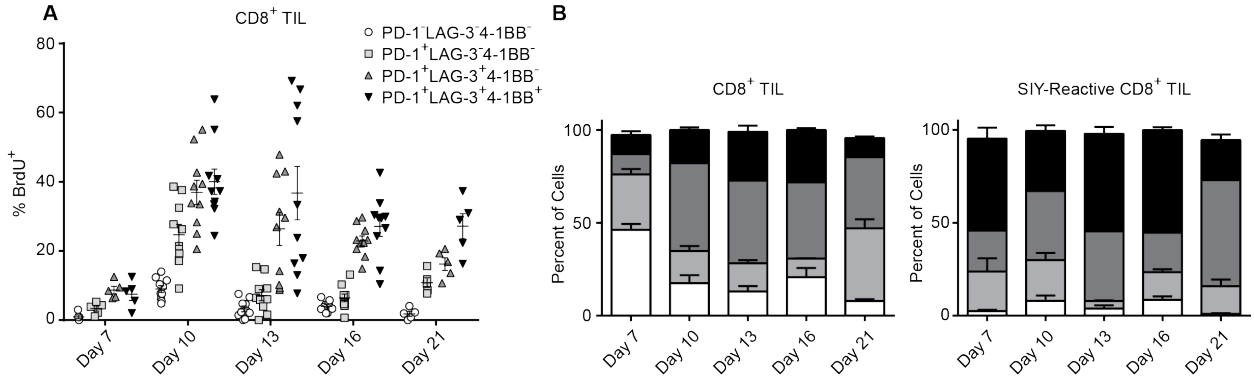

Figure 3.12: Time course of CD8$^+$ TIL phenotype and proliferation
(A) Time course of CD8$^+$ TIL BrdU incorporation by CD8$^+$ TIL expressing PD-1, LAG-3, or 4-1BB. Day 7 n = 5, day 10 n = 10, day 13 n = 10, day 16 n = 10, day 21 n = 5. (B) Time course of PD-1, LAG-3, and 4-1BB phenotypes of CD8$^+$ and SIY-reactive CD8$^+$ TIL. Day 7 n = 8, day 10 n = 10, day 13 n = 10, day 16 n = 5, day 21 n = 10.

rates of proliferation and apoptosis. Direct measurement of active caspase-3 in SIY-reactive TIL revealed similar patterns of increased apoptosis in LAG-3^+4-1BB$^+$ cells (Figure 14D). Antigen-specific TIL were therefore undergoing both proliferation and apoptosis in the tumor microenvironment.

We also stained TIL with annexin V and a cell-impermeable viability dye to measure different stages of apoptosis. The LAG-3+4-1BB+ population contained decreased numbers of non-apoptotic, annexin V$^-$ cells, and far more cells in later stages of apoptosis that were annexin V$^+$ and ef780$^+$ (Figure 3.14E). This result was important, as it confirmed that the eventual fate of LAG-3^+4-1BB$^+$ TIL was indeed death.

Both proliferating and dying TIL were LAG-3^+4-1BB$^+$, suggesting that the same TIL were undergoing both proliferation and apoptosis. To directly confirm this, we measured active caspase-3 and Ki-67 expression in TIL and SIY-reactive TIL. Active caspase-3 was highest among TIL that were Ki-67$^+$, directly indicating that apoptosis of proliferating cells was occurring (Figure 3.14F). Antigen-specific TIL were therefore trapped in a cycle of proliferation and apoptosis that potentially limited TIL accumulation and immune-mediated tumor destruction.

Caspase-3 staining of CD8$^+$ T cells was consistent throughout tumor growth (Figure 15A). LAG-3^+4-1BB$^+$ TIL maintained the highest rates of apoptosis over time (Figure 3.15B), even at the earliest time points analyzed.

Interestingly, following anti-4-1BB combination immunotherapy, there was a striking decrease in the fraction of apoptotic CD8$^+$ T cells, both in the overall population and within the SIY-reactive subset (Figure 3.16A and 3.16B). Together, these results indicate that the accumulation of CD8$^+$ TIL after anti-4-1BB combination immunotherapy was not a result of increased proliferation, but rather due to decreased apoptosis. Analysis of cohorts treated with only single monoclonal antibodies revealed that the increased survival of CD8$^+$ TIL was mediated primarily by the agonist anti-4-1BB antibody. Only this cohort had a statistically significantly reduced fraction of SIY-reactive CD8$^+$ TIL containing active caspase-3,

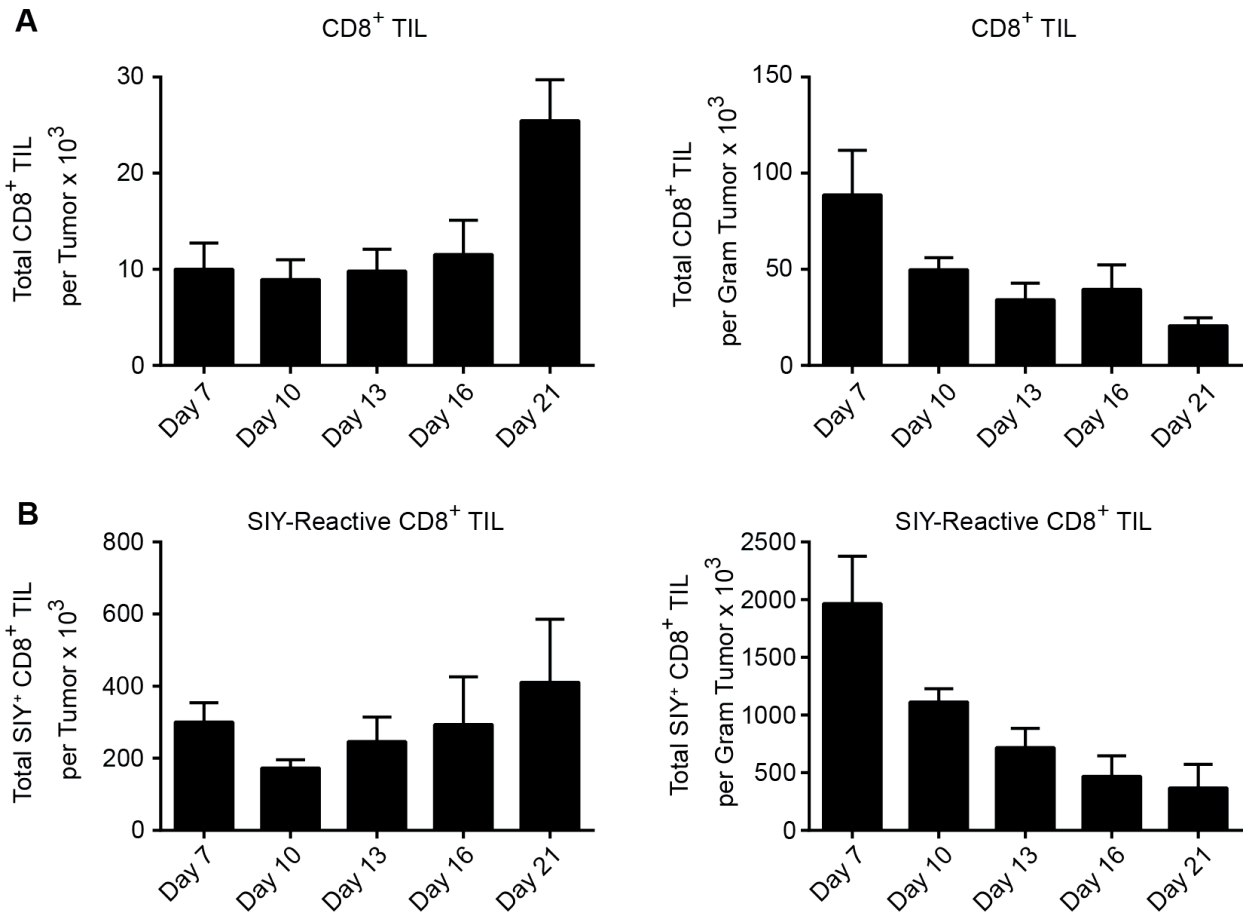

Figure 3.13: Time course of CD8$^+$ TIL accumulation in B16.SIY tumors
C57BL/6 mice were injected subcutaneously with 2x10^6 B16.SIY tumor cells on day 0 and sacrificed at the indicated time points. Flow cytometry was used to enumerate the total numbers of CD8textsuperscript+ TIL (A) and SIY-reactive CD8$^+$ TIL (B).

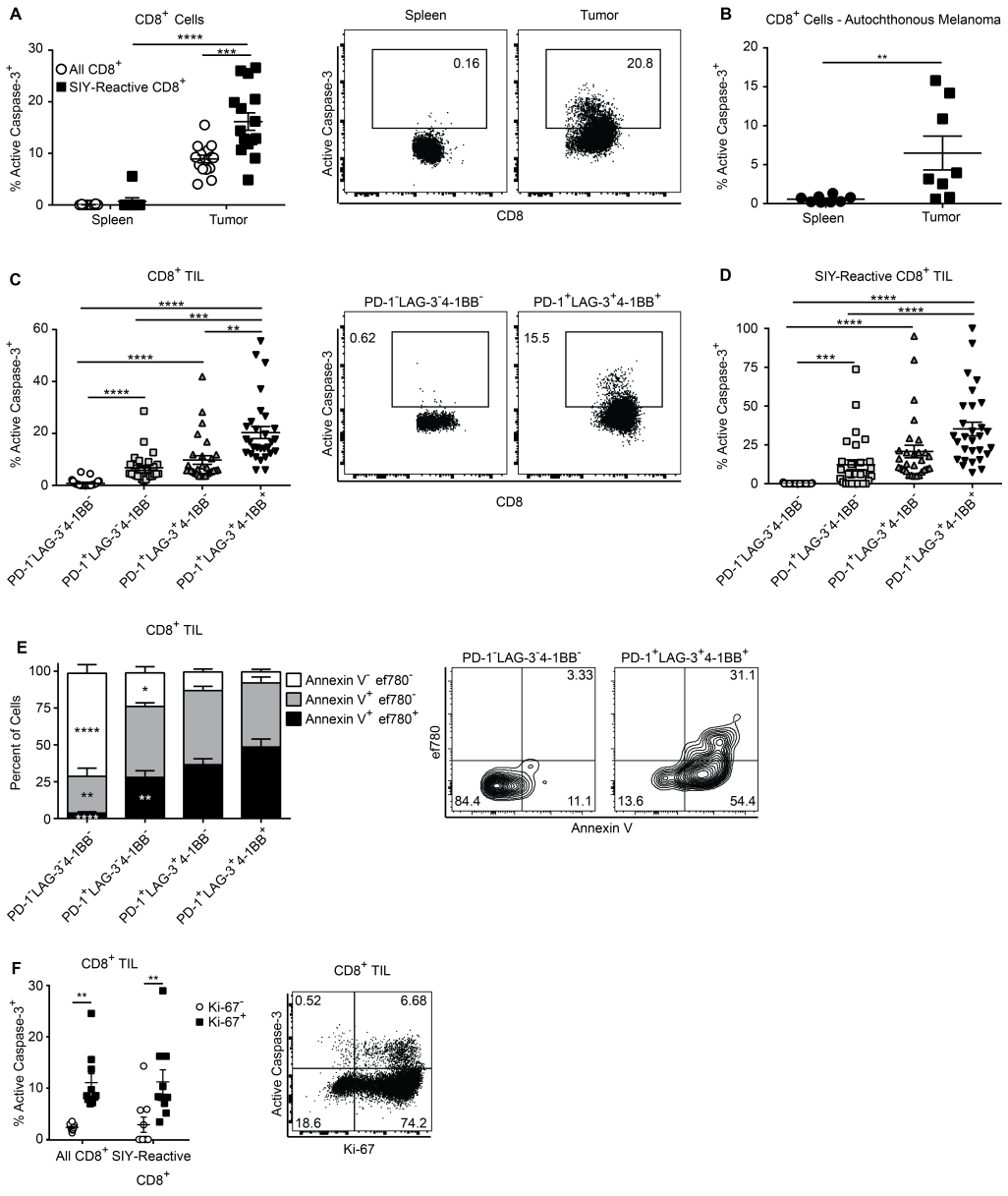

Figure 3.14: CD8$^+$ T cells undergo apoptosis in the tumor microenvironment (A) Tumors and spleens from B16.SIY-bearing mice were analyzed on day 13 for the presence of active caspase-3 via flow cytometry. Two-way ANOVA with a, n = 15. (B) Spleens and tumors from an autochthonous melanoma model were analyzed for active caspse-3. Mann-Whitney U test, n = 8. (C) TIL and (D) SIY-reactive TIL from B16.SIY tumor-bearing mice were analyzed for active caspase-3 as in (A) and for expression of PD-1, LAG-3 and 4-1BB via flow cytometry. One-way ANOVA, n = 29. (E) TIL from B16.SIY were analyzed for PD-1, LAG-3, and 4-1BB, as well as binding to Annexin V and Fixable Viability Dye eFluor 780, n = 10. Two-way ANOVA. The indicated statistical differences are compared to the PD-1$^+$LAG-3$^+$4-1BB$^+$ populations. (F) TIL B16.SIY tumors were analyzed for Ki-67 and active caspase-3 via flow cytometry, n=10. Two-way ANOVA with a Bonferroni correction.

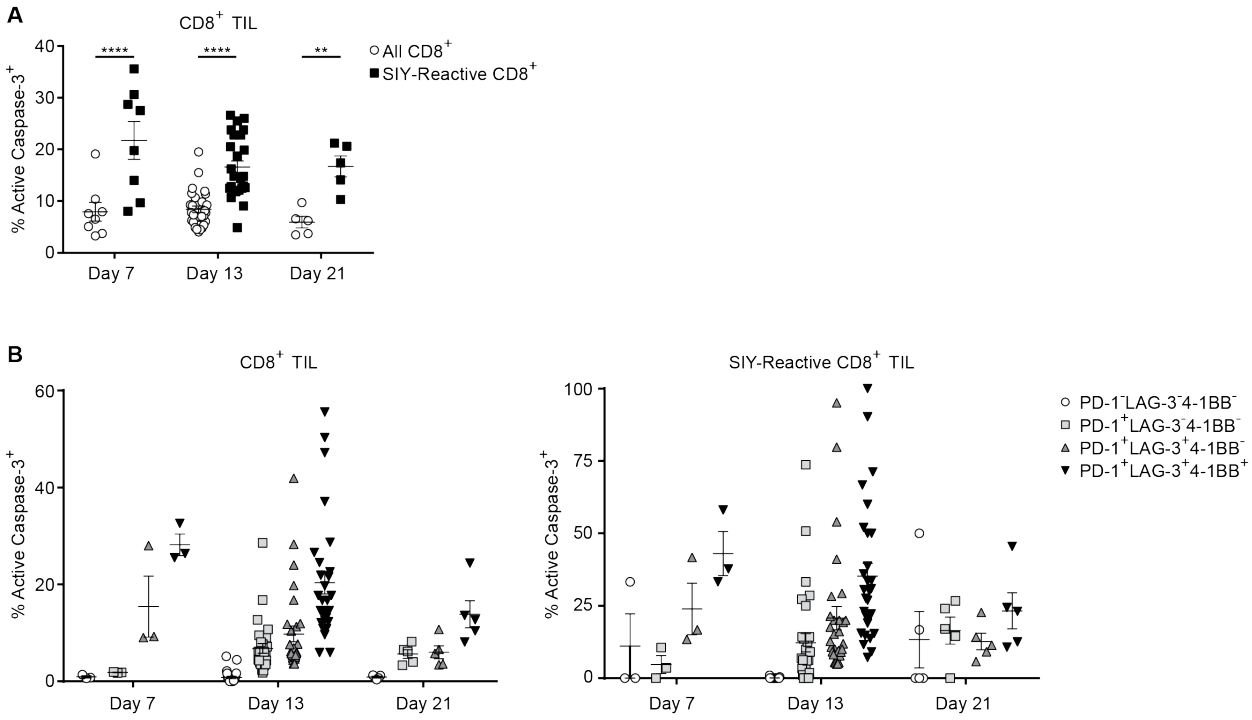

Figure 3.15: Time course of active caspase-3 and phenotype of CD8$^+$ TIL and SIY-reactive CD8$^+$ TIL

(A) Time course of active caspase-3 in CD8$^+$ and SIY-reactive CD8$^+$ TIL as measured by flow cytometry. Day 7 n = 8, day 13 n = 30, day 21 n = 5. 2-way ANOVA with a Bonferroni correction was used to determine statistical significance. (B) Time course of active caspase-3 in CD8$^+$ TIL expressing PD-1, LAG-3, or 4-1BB. Day 7 n = 3, day 13 n = 29, day 21 n = 5.

and a corresponding increase in the number of SIY-reactive $CD8^+$ TIL (Figure 3.17A and 3.17B). Anti-PD-L1 showed a slight but not statistically significant reduction in caspase-3 levels in SIY-reactive TIL, while anti-CTLA-4 had negligible effects on SIY-reactive TIL caspase-3 activation (Figure 3.17A). Similarly, anti-PD-L1 showed a slight but not statistically significant increase in SIY-reactive TIL number, and anti-CTLA-4 alone had negligible effects on SIY-reactive TIL number (Figure 3.17B). Thus, the agonist anti-4-1BB antibody appears to drive increased survival of tumor antigen-specific $CD8^+$ TIL culminating in their accumulation in the tumor microenvironment.

3.8 Decreased $CD8^+$ TIL apoptosis leads to increased TIL accumulation and tumor control

We wished to determine if there was a relationship between apoptosis, accumulation of $CD8^+$ TIL, and immune-mediated tumor control in an immunotherapy-free context. We began by studying TIL apoptosis in syngeneic, regressor tumor cell lines MC57.SIY and 1969.SIY. These spontaneously rejected tumors allowed a comparison of TIL apoptosis in progressing versus regressing tumors. Seven days following tumor inoculation, we measured SIY-reactive TIL abundance in MC57.SIY, 1969.SIY, or B16.SIY tumors. When compared to progressing B16.SIY tumors, a much larger expansion of SIY-reactive TIL was observed in MC57.SIY and 1969.SIY tumors (Figure 3.18A). Interestingly, this expansion did not appear to be the result of changes in proliferation, as the Ki-67^+ fraction of T cells was similar (Figure 3.18B). However, apoptosis was only observed among TIL from B16.SIY progressing tumors (Figure 3.18C). These results indicate that spontaneous TIL apoptosis is a feature of progressing and not regressing tumors.

To modulate apoptosis in T cells, we used a transgenic Lck^{pr} - Bcl-x_L mouse that over-expresses Bcl-x_L in T cells (Bcl-x_L mice). Bcl-x_L mice challenged with B16.SIY tumors had significantly reduced apoptosis of $CD8^+$ TIL (Figure 3.19A), and an increase in the

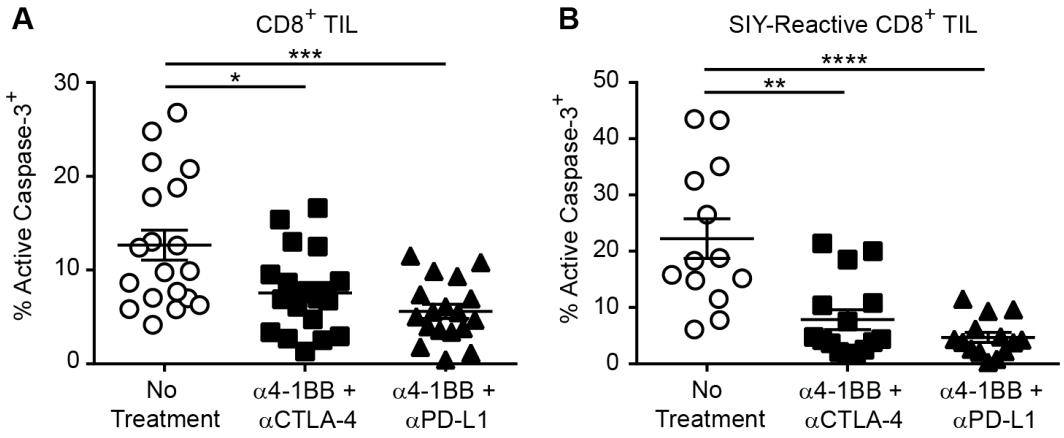

Figure 3.16: Anti-4-1BB combination immunotherapy decreases CD8$^+$ TIL apoptosis

(A) C57BL/6 mice were inoculated subcutaneously with 2x10^6 B16.SIY cells and treated with immunotherapy on day 7 and day 10 post tumor cell injection. On day 13 after tumor cell injection the tumors were analyzed using flow cytometry to detect CD8$^+$ T cells for the presence of active capase-3 via flow cytometry No Treatment n=19, anti-4-1BB + anti-CTLA-4 n=20, anti-4-1BB + anti-PD-L1 n=18. One-way ANOVA with a Bonferroni correction was performed to determine statistical significance. (B) As in (A), but CD8$^+$ TIL were analyzed for the presence of active capase-3 and SIY-reactivity via flow cytometry. No Treatment n=13, anti-4-1BB + anti-CTLA-4 n=15, anti-4-1BB + anti-PD-L1 n=14. One-way ANOVA was performed to determine statistical significance.

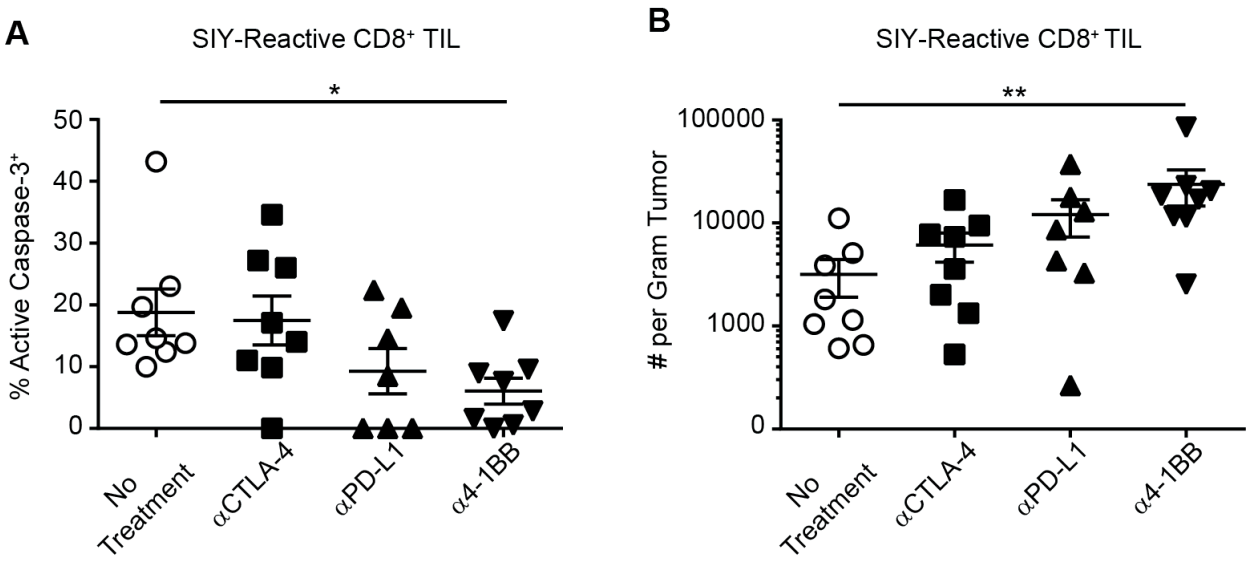

Figure 3.17: Decreased CD8$^+$ TIL apoptosis is mostly driven by anti-4-1BB
C57BL/6 mice were injected subcutaneously with 2x10^6 B16.SIY cells on day 0. Mice were treated with 100 μgrams anti-4-1BB, anti-PD-L1, or anti-CTLA-4 on days 7 and 10, and analyzed on day 13 via flow cytometry to enumerate SIY-reactive CD8$^+$ TIL and the fraction of CD8$^+$ TIL that contained active caspase-3. No Treatment n = 8, anti-CTLA-4 n = 8, anti-PD-L1 n = 7, anti-4-1BB n = 8. One-way ANOVA was performed to determine statistical significance.

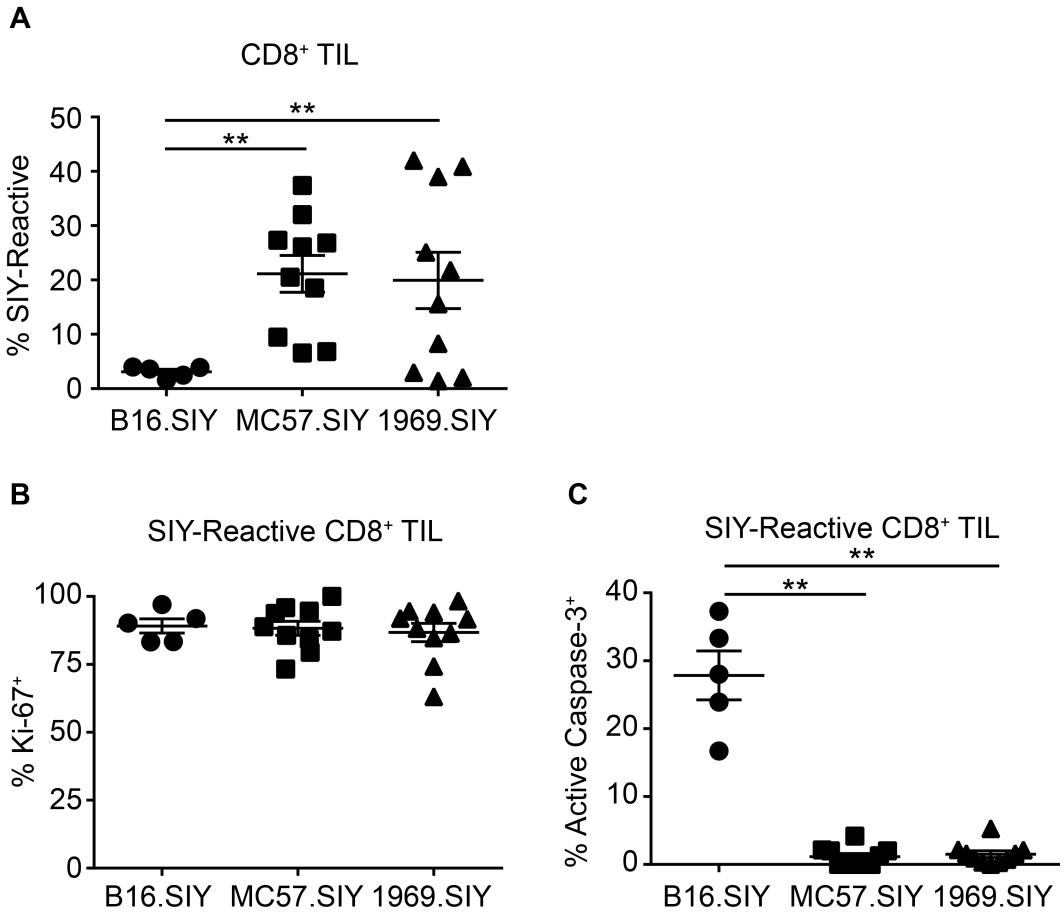

Figure 3.18: Spontaneous tumor rejection is associated with decreased CD8$^+$ TIL apoptosis

(A) C57BL/6 mice were injected with 2x10^6 B16.SIY, 2x10^6 MC57.SIY, or 2x10^6 1969.SIY cells on day 0. On day 7, mice were sacrificed and analyzed for SIY-reactive CD8$^+$ TIL via flow cytometry. One-way ANOVA was performed to determine statistical significance, B16.SIY n=5 MC57.SIY and 1969.SIY n=10. (B) Similar conditions to (A) Ki-67 expression of SIY-reactive CD8$^+$ TIL is shown. One-way ANOVA was performed to determine statistical significance, B16.SIY n=5 MC57.SIY and 1969.SIY n=10. (C) As in (A), the fraction of SIY-reactive cells with active caspase-3 is shown. One-way ANOVA was performed to determine statistical significance, B16.SIY n=5 MC57.SIY and 1969.SIY n=10.

number of infiltrating $CD8^+$ TIL (Figure 3.19B). However, these mice paradoxically had a reduced percentage of SIY-reactive $CD8^+$ TIL (Figure 3.19C), suggesting that Bcl-xL was enabling expansion or survival of T cells having non-SIY specificities. In order to restrict Bcl-x_L expression to tumor antigen-specific $CD8^+$ T cells, we crossed Bcl-x_L mice to 2C TCR transgenic mice, whose T cells express the 2C TCR that recognizes the SIY peptide in the context of K^b (2C Bcl-x_L mice). Splenic T cells from either 2C or 2C Bcl-x_L mice were activated in vitro with αCD3/αCD28 antibodies to generate primed effector cells, then were transferred (1 x 10^6 cells per mouse) intravenously to mice bearing seven-day established B16.SIY tumors. Bcl-x_L expression in 2C T cells resulted in significantly improved tumor control than wild type 2C cells, indicating that inhibiting effector T cell apoptosis is sufficient for more effective immune-mediated tumor destruction in vivo (Figure 3.19D).

3.9 $CD8^+$ TIL accumulate DNA damage

To better understand the mechanisms behind TIL apoptosis, we compared gene expression profiles between the PD-1^+LAG-3^-4-1BB$^-$ and the PD-1^+LAG-3^+4-1BB$^+$ $CD8^+$ T cell populations. We chose these populations as their shared expression of PD-1 indicates they have recently encountered cognate antigen, but the PD-1+LAG-3+4-1BB+ population is both much more proliferative and apoptotic. Using The Database for Annotation, Visualization and Integrated Discovery (DAVID) v6.8, we determined enriched gene ontology (GO) terms from 1616 genes upregulated 2 fold or more in the PD-1^+LAG-3^+4-1BB$^+$ TIL. Interestingly, the two GO terms with the highest enrichment scores were associated with DNA damage (Figure 3.20A). As DNA damage can lead to apoptosis, we were interested to determine if there was increased DNA damage in TIL. Phosphorylated histone 2A, also known as μH2AX, is a marker of double stranded DNA than in the Ki-67^- TIL (Figure 3.20D). However, there was no difference in γH2AX levels between $CD8^+$ splenocytes that were Ki-67^+ and Ki-67^-, indicating that proliferation itself was not innately linked to the accumulation of DNA damage. To test directly whether increased proliferation alone was responsible for increased DNA

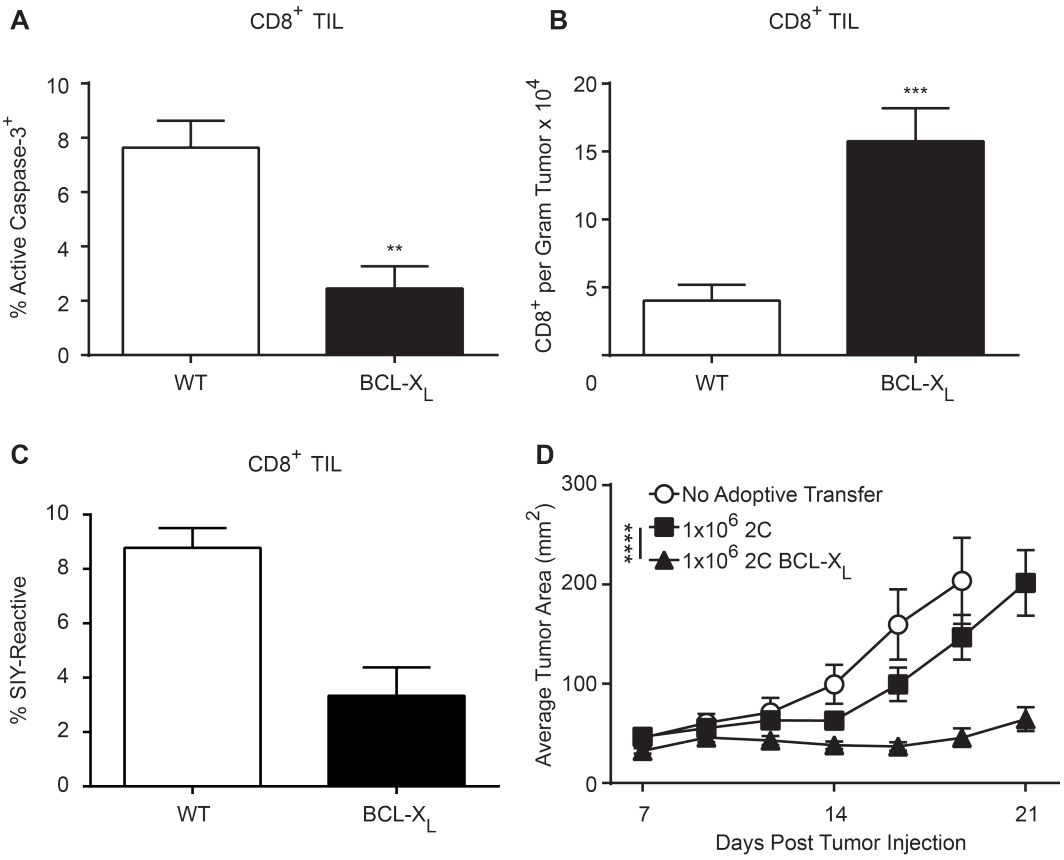

Figure 3.19: Expression of Bcl-x_L in $CD8^+$ TIL leads to decreased apoptosis and increased tumor control

(A and B) Bcl-x_L or WT mice were injected with $2x10^6$ B16.SIY cells on day 0. On day 13, mice were sacrificed and analyzed for active caspase-3 expression and to enumerate the number of $CD8^+$ TIL. Mann-Whitney U test was performed to determine statistical significance, n=9. (C) The mice from (A) were also analyzed for the percentage of $CD8^+$ TIL that were SIY-reactive. (D) 2C or 2C Bcl-x_L splenocytes were activated in vitro with plate bound αCD3 and αCD28 antibodies to generate activated effector $CD8^+$ T cells. $1x10^6$ T cells were transferred to mice bearing seven-day established B16.SIY tumors and tumor growth was measured over time. Two-way ANOVA with a Bonferroni correction was performed to determine statistical significance. No Adoptive Transfer n = 10, 2C n = 10, 2C Bcl-x_L n = 20.

damage, we used agonist 4-1BB combination immunotherapy to induce high levels of proliferation in the $CD8^+$ T cells in spleens and tumor-draining lymph nodes. Immunotherapy greatly increased the proliferation of these T cells, as measured by increased Ki-67 expression (Figure 3.20E). However, γH2AX levels in $CD8^+$ T cells in the spleen and lymph nodes were not significantly increased after immunotherapy (Figure 3.20F), indicating that even high levels of proliferation in these locations are insufficient to lead to high levels of DNA damage. Therefore, DNA damage in proliferating $CD8^+$ T cells occurs at high levels specifically in the tumor microenvironment, a potential cause of TIL apoptosis.

3.10 4-1BB combination immunotherapy induces phenotypic changes in $CD8^+$ TIL

We wanted to determine how 4-1BB combination immunotherapy changed the phenotypic and functional properties of $CD8^+$ TIL. We began by assessing the expression of the surface markers PD-1 and LAG-3, as co-expression of these markers has been linked to dysfunction of $CD8^+$ TIL (Williams, 2017). After agonist 4-1BB combination immunotherapy, we found a significant decrease in the fraction of $CD8^+$ TIL expressing both PD-1 and LAG-3, and a corresponding increase in the fraction expressing PD-1 but not LAG-3 (Figure 3.22A, 3.22B, and 3.22C). The PD-1^+LAG-3^- phenotype is not associated with dysfunction in our previous studies, indicating an increase in $CD8^+$ TIL functionality after agonist 4-1BB combination immunotherapy. Studies with single treatments found that these changes in phenotype were largely due to the agonist 4-1BB antibody, as $CD8^+$ TIL were phenotypically similar between anti-4-1BB only and anti-4-1BB + anti-CTLA-4, and anti-4-1BB + anti-PD-L1 (Figure 3.22D). Interestingly, anti-PD-L1 or anti-CTLA-4 alone did not affect $CD8^+$ TIL phenotype, indicating potential differences in how these immunotherapies affect $CD8^+$ TIL. We next investigated other inhibitory receptors, and found that agonist 4-1BB combination immunotherapy was associated with decreased surface expression of other in-

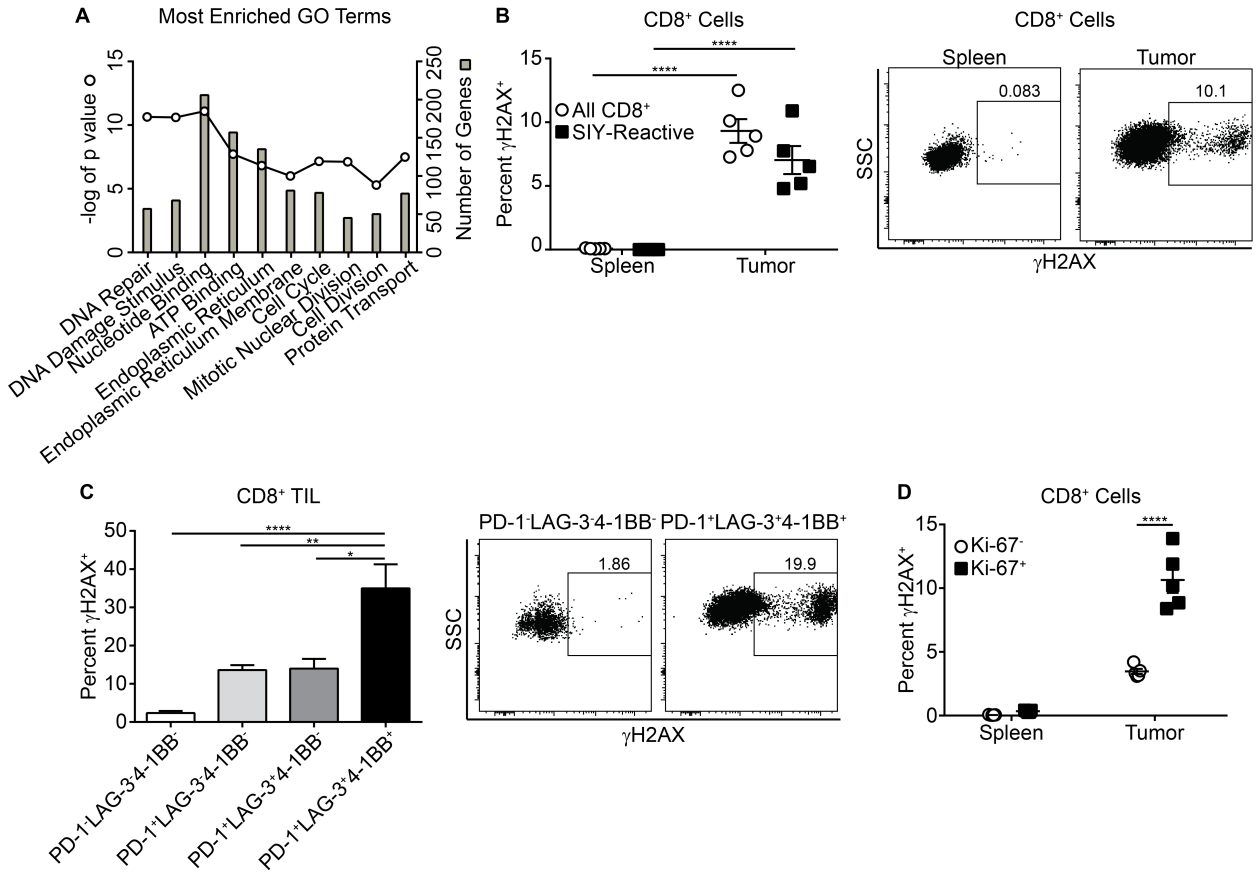

Figure 3.20: CD8$^+$ TIL accumulate DNA damage
(A) The top 10 enriched GO terms identified by DAVID from genes upregulated in PD-1$^+$LAG-3$^+$4-1BB$^+$ TIL compared to PD-1$^+$LAG-3$^-$4-1BB$^-$ TIL, the log(p value) of each, and the number of genes from the upregulated genes that were included the each GO term. (B) Day 13 CD8$^+$ cells from the spleens and tumors of mice were analyzed for γH2AX, n = 5, two-way ANOVA. (C) TIL from day 13 tumors were analyzed for expression of PD-1, LAG-3, 4-1BB, and γH2AX, n = 10, one-way ANOVA. (D) Day 13 CD8$^+$ cells were analyzed for expression of Ki-67 and γH2AX, n = 5, two-way ANOVA.

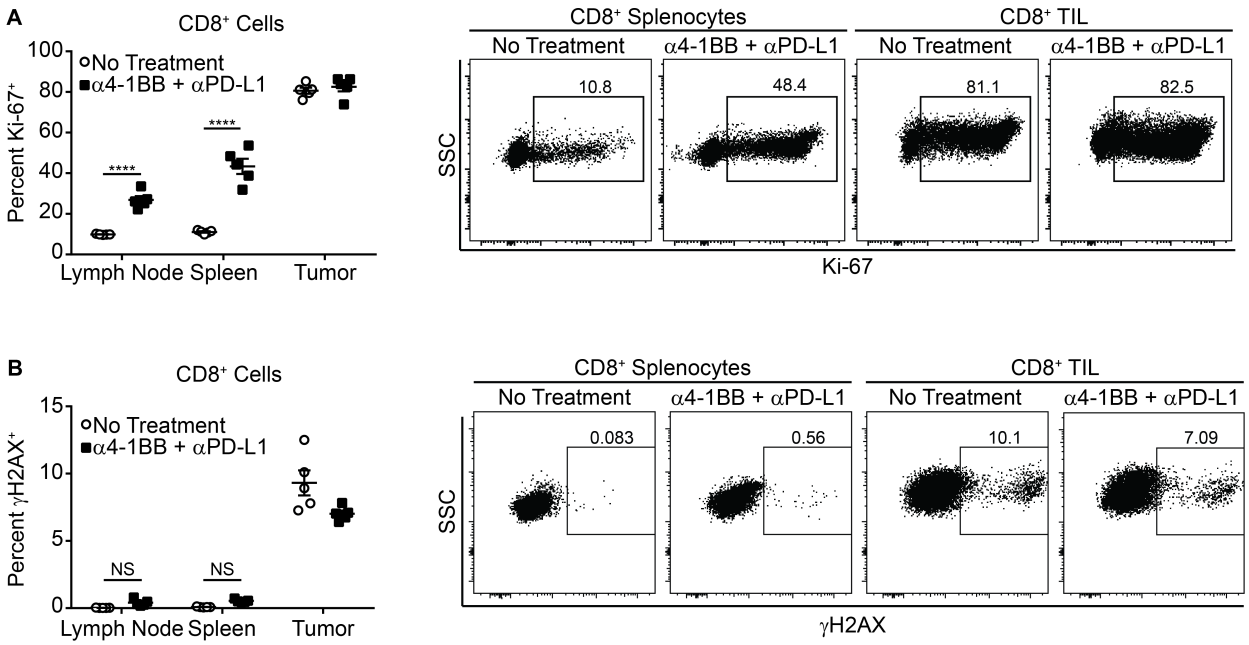

Figure 3.21: DNA damage accumulates in proliferating CD8$^+$ T cells only in the tumor microenvironment

(A) C57BL/6 mice were inoculated with B16.SIY cells on day 0, and given immunotherapy on days 7 and 10. On day 13, CD8$^+$ cells were analyzed for expression of Ki-67, or (B) γH2AX, n = 5, two-way ANOVA. Representative No Treatment FACS plots in (3.20A) and (3.21B) are from the same samples.

hibitory receptors including 2B4, TIM-3, and TIGIT, indicating that immunotherapy that includes agonist anti-4-1BB may lower the inhibitory signals T cells receive from the tumor microenvironment (Figure 3.22E). Interestingly, agonist 4-1BB combination immunotherapy was also associated with increased expression of the surface receptor KLRG1, indicating that perhaps $CD8^+$ TIL were becoming more effector-like as a result of immunotherapy (Figure 3.23).

3.11 Agonist anti-4-1BB antibody drives gene expression changes in $CD8^+$ TIL

To gain a deeper understanding of the molecular changes in $CD8^+$ TIL following immunotherapy with agonist anti-4-1BB antibody, we performed gene expression profiling of $CD8^+$ TIL from untreated mice, or those that received agonist 4-1BB antibody, anti-4-1BB + anti-CTLA-4, or anti-4-1BB + anti-PD-L1. We began immunotherapy at day 7 post B16.SIY tumor innoculation, and sorted cells on day 13. To ensure that we captured only changes in $CD8^+$ TIL, and not changes reflective of new homing of lymphocytes into the tumor microenvironment, we performed the experiment with daily FTY720 dosing, beginning on day 7. We sorted cells directly into lysis buffer to best preserve their in vivo gene expression. Clustering the top 100 differentially regulated genes showed that all samples that received immunotherapy clustered together (Figure 3.24), although differences were obvious between the immunotherapy and "no treatment" groups. This indicated to us that similar to the changes in surface phenotype, agonist anti-4-1BB therapy wasdriving the transcriptional reprogramming of $CD8^+$ T cells. This indicated that 4-1BB signaling changed gene expression levels in $CD8^+$ T cells more than blockade of CTLA-4 or PD-L1.

We next used qPCR and verified the upregulation of a selected group of genes that were upregulated during immunotherapy. Using independent biological samples from the gene array experiment, we tested gene expression changes resulting from 4-1BB combination

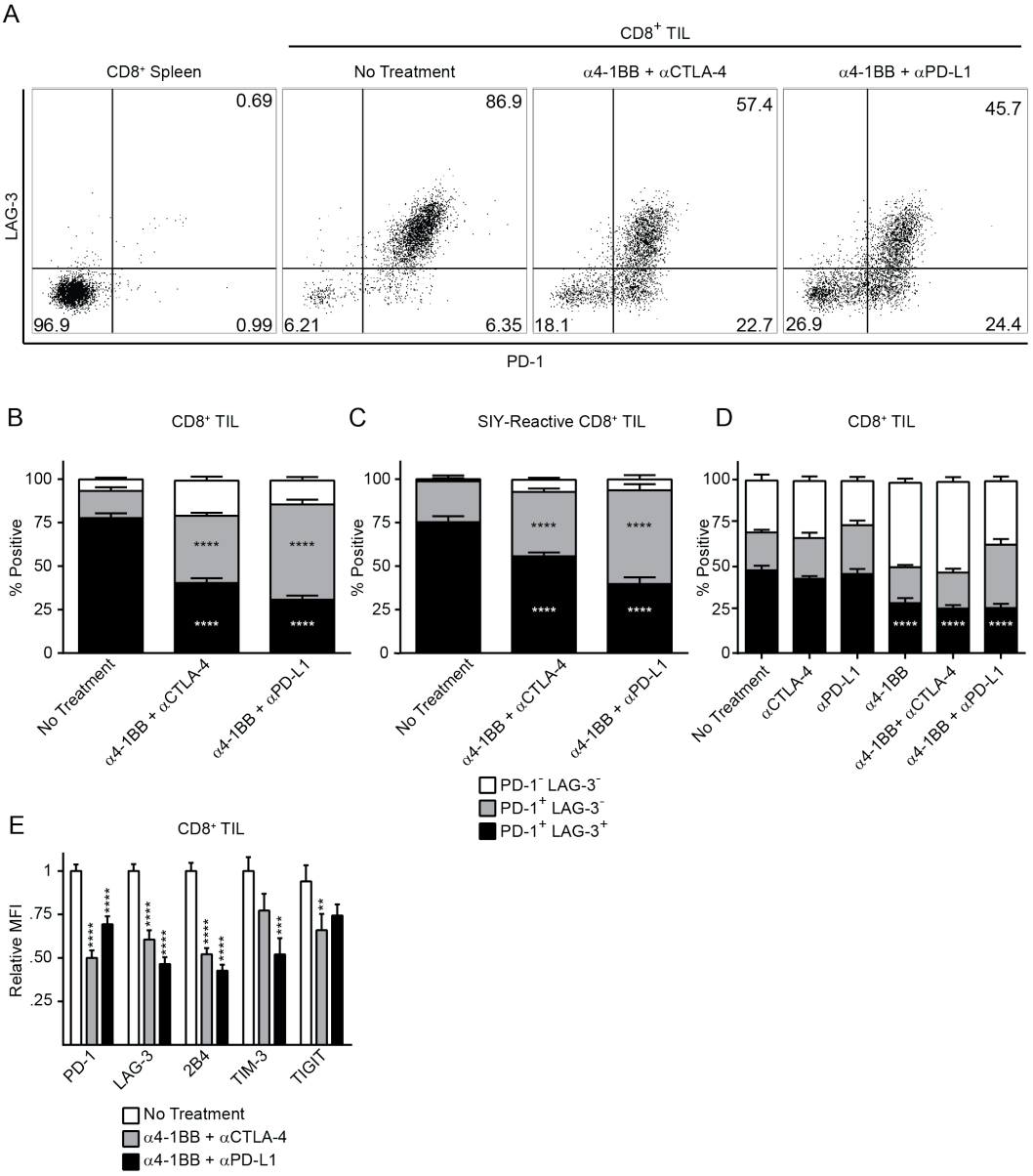

Figure 3.22: Anti-4-1BB combination immunotherapy decreases CD8$^+$ TIL inhibitory receptor expression

(A) Representative FACS plots of PD-1 and LAG-3 expression in CD8$^+$ TIL. (B) Quantification of CD8$^+$ TIL and (C) SIY-reactive CD8$^+$ TIL phenotype without and after immunotherapy, n=10. (D) Quantification of CD8$^+$ TIL phenotype comparing single and combination immunotherapy treatments. (E) Displayed MFI values were obtained by normalizing the MFI of each inhibitory receptor to the average of the No Treatment groups in each experiment. Pooled data from multiple experiments. PD-1 n=25, LAG-3 n=15, 2B4 n=10, TIM-3 n=5 TIGIT n=10. 2-way ANOVA with a Bonferroni correction was performed to determine statistical differences between cohorts.

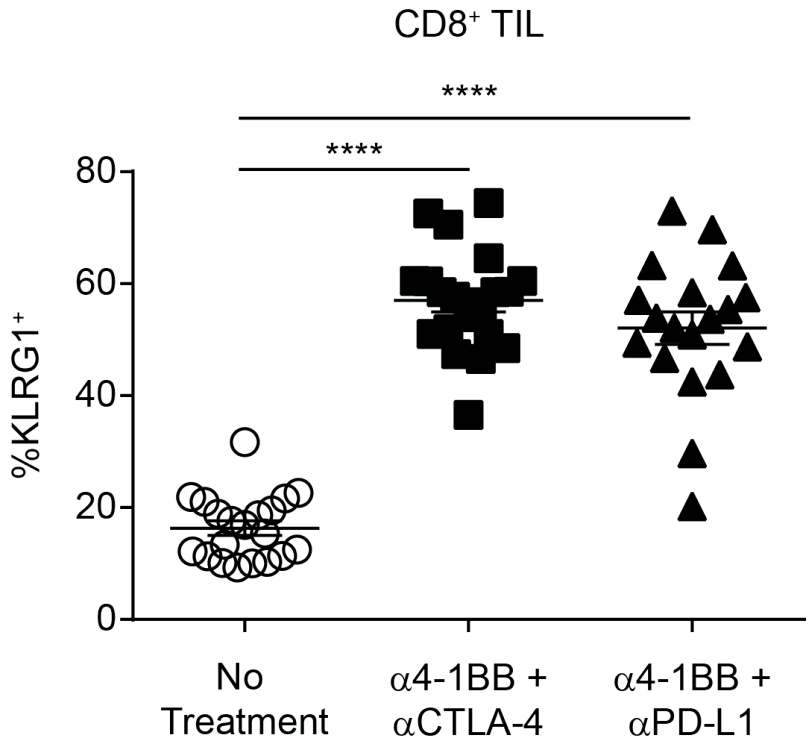

Figure 3.23: Anti-4-1BB combination immunotherapy increases KLRG1 expression on CD8$^+$ TIL

C57BL/6 mice were injected subcutaneously with 2x10$^+$ B16.SIY cells and treated with immunotherapy on day 7 and day 10 after tumor implantation. On day 13, TIL were analyzed using flow cytometry for the expression of KLRG1. Data is pooled from 4 independent experiments. No Treatment n = 20, anti-4-1BB + anti-CTLA-4 n = 20, anti-4-1BB + anti-PD-L1 n = 19. Statistical comparisons are made using Kruskal-Wallis one-way ANOVA.

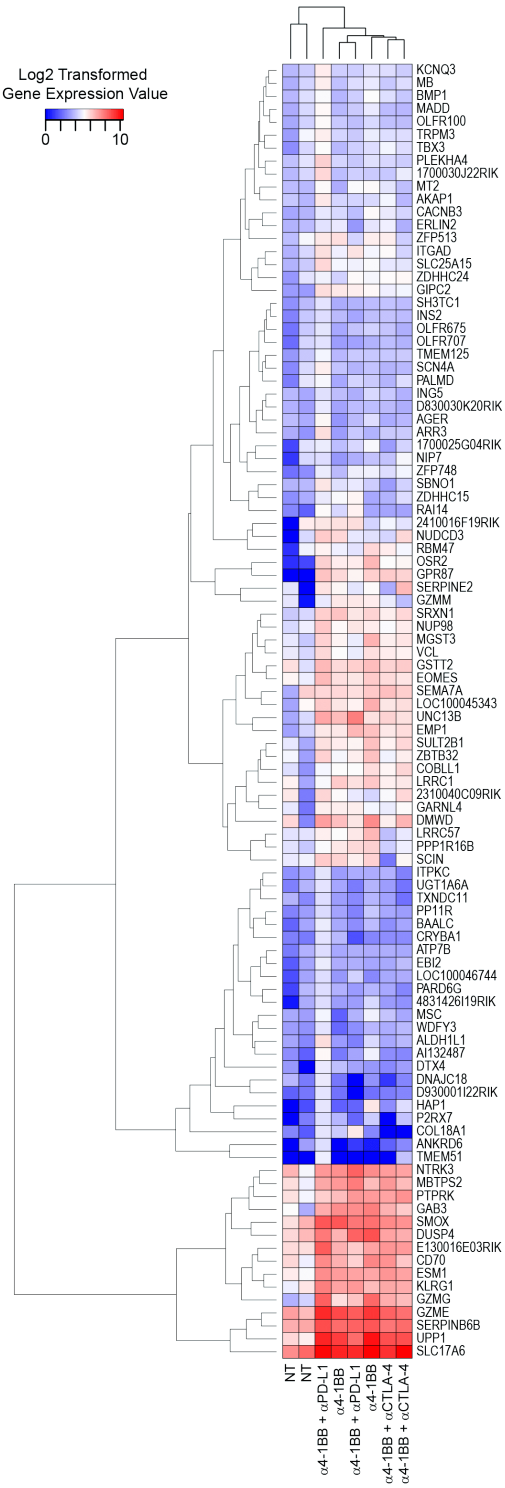

Figure 3.24: Gene expression profiling reveals differentially regulated genes after 4-1BB combination immunotherapy

Gene expression profiling of CD8$^+$ TIL. Non-hierarchical clustering of the 100 genes most upregulated by immunotherapy.

immunotherapy in $CD8^+$ TIL. The tested genes showed a similar pattern of upregulation as compared to the gene array, indicating that the gene array results were consistent across multiple different biological samples and represented consistent changes that resulted from 4-1BB combination immunotherapy (Figure 3.25).

We next wanted to infer patterns of molecular changes based on gene expression profiling. Ingenuity Pathway Analysis was utilized to determine which molecular pathways were affected by agonist 4-1BB combination immunotherapy. We found major hubs of genes surrounding the IL-2 signaling and NF-κB signaling pathways (Figure 3.26). These were interesting results, as we have previously found consistent upregulation of IL-2 production in $CD8^+$ TIL after immunotherapy (Spranger, 2014; Williams, 2017). NF-κB was also interesting, because the NF-κB pathway has been shown to be required in T cells for a spontaneous anti-tumor immune response, and forced NF-κB pathway activity in T cells has been reported to lead to superior immune-mediated tumor control (Barnes, 2015; Evaristo, 2016). We therefore focused on these pathways for functional studies.

3.12 Expression levels of IL-2 and CD25 after 4-1BB combination immunotherapy

Reports from other laboratories have found that agonist 4-1BB engagement of $CD8^+$ T cells leads to a feedback loop where T cells upregulated both IL-2 and CD25, enhancing their accumulation in vivo (Oh, 2015). We have also previously found that multiple types of immunotherapy can lead to an increased ability of $CD8^+$ TIL to produce IL-2 (Spranger, 2014; Williams, 2017). However, these experiments involved the ex-vivo restimulation of $CD8^+$ TIL. To determine if $CD8^+$ TIL were producing more IL-2 in vivo, we sorted $CD8^+$ TIL directly into lysis buffer and extracted RNA. We found an increased IL-2 mRNA levels in $CD8^+$ TIL from mice that had received anti-4-1BB + anti-CTLA-4 or anti-4-1BB + anti-PD-L1 compared to $CD8^+$ TIL from untreated mice (Figure 3.27). We also found CD25

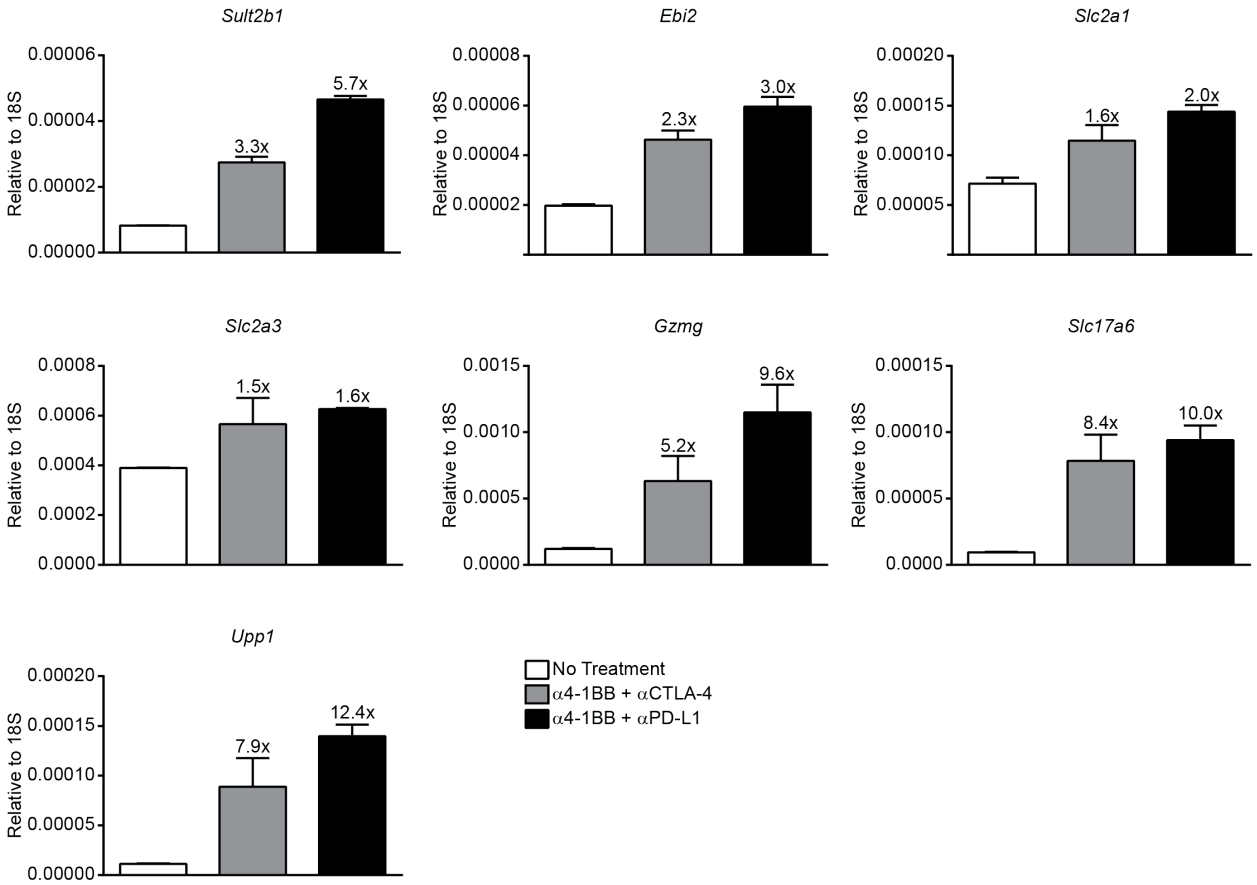

Figure 3.25: qPCR confirmation of selected genes from gene array
C57BL/6 mice were injected subcutaneously with 2x10^6 B16.SIY cells and treated with immunotherapy on day 7 and day 10 after tumor implantation. On day 13, $CD8^+$ TIL were FACS sorted directly into lysis buffer for RNA extraction. qPCR was used to analyze the expression of Sult2b1, Ebi2, Slc2a1, Slc2a3, Gzmg, Slc17a6, and Upp1. Data are pooled from 2 independent experiments, each using pooled TIL from n=5 mice per cohort.

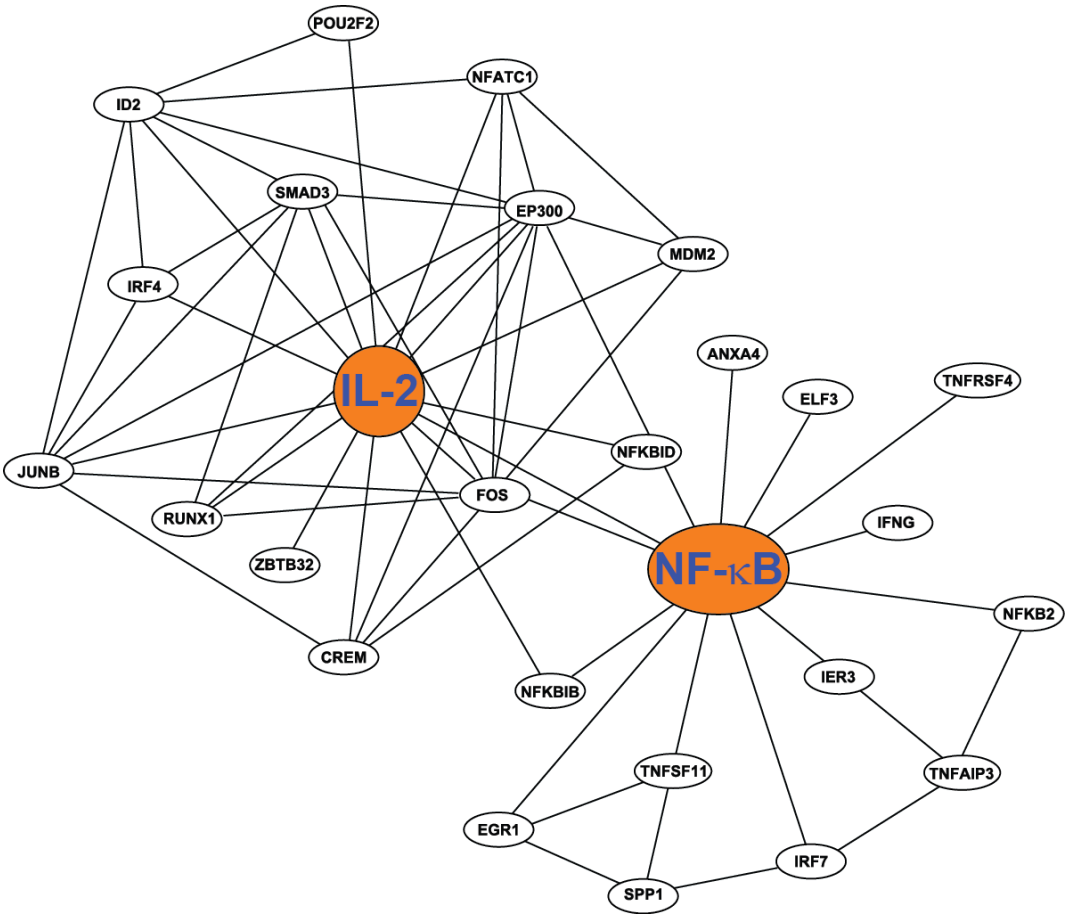

Figure 3.26: Pathway analysis of genes upregulated after immunotherapy reveals nodes around IL-2 and NF-κB pathways

Genes upregulated in both anti-4-1BB + anti-CTLA-4 and anti-4-1BB + anti-PD-L1 treatment groups were analyzed with Ingenuity Pathway Analysis. Pathway analysis revealed hubs around IL-2 and NF-κB signaling.

expression on $CD8^+$ TIL and SIY-reactive $CD8^+$ TIL (Figure 3.28). Many of the CD25 expressing cells also expressed 4-1BB, raising the possibility that increased IL-2 expression after the delivery of agonist 4-1BB signals was acting in autocrine loop to stimulate $CD8^+$ TIL. We found that CD25 expression was not altered after immunotherapy, suggesting that increased IL-2 production after immunotherapy could result in engagement of IL-2R already expressed by $CD8^+$ TIL (Figure 3.29).

3.13 IL-2 – CD25 signaling is not required for the efficacy of agonist 4-1BB combination immunotherapy

To test if IL-2 signaling was necessary for efficacy of agonist 4-1BB combination immunotherapy, we injected B16.SIY bearing mice with two anti-IL-2 antibodies, JES6-1A12 and SB46-1, which bind two different epitopes of IL-2 that interact with either CD25 or CD122 (Boyman, 2012). Systemic administration of these IL-2 neutralizing antibodies had no effect on tumor outgrowth in either control or anti-4-1BB + anti-PD-L1 treated mice (Figure 3.30A), but it was difficult to confirm that all IL-2 was successfully inhibited. To ensure that IL-2 antibodies were reaching the tumor site, we administered immunotherapy systemically, but injected the anti-IL-2 antibodies directly into the tumor site. With intratumoral administration, we found that anti-IL-2 antibodies significantly increased tumor growth in control mice, but had no effect on tumor outgrowth of anti-4-1BB + anti-PD-L1 treated mice (Figure 3.30B). These experiments indicated to us that IL-2 signaling was most likely not necessary for the response to 4-1BB combination immunotherapy. However, it was interesting that intratumoral administration of anti-IL-2 neutralizing antibodies decreased tumor control, suggesting that IL-2 signaling may play a role in endogenous anti-tumor immunity.

To better ensure that all IL-2 – CD25 signaling on $CD8^+$ TIL was blocked during agonist 4-1BB combination immunotherapy, we used a genetically engineered mouse strain that lacks CD25 expression. Because these mice develop fatal autoimmunity with increasing age

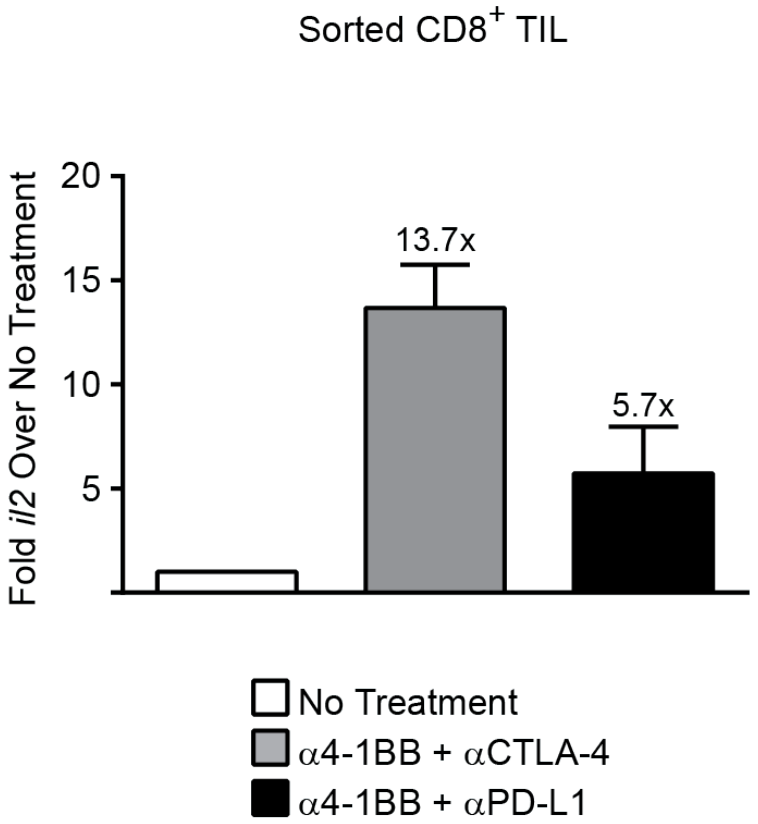

Figure 3.27: Anti-4-1BB combination immunotherapy increases *il2* expression in CD8$^+$ TIL

C57BL/6 mice were injected subcutaneously with 2x10^6 B16.SIY cells and treated with immunotherapy on day 7 and day 10 after tumor implantation. On day 13, CD8$^+$ TIL were FACS sorted directly into lysis buffer for RNA extraction. qPCR was used to analyze the expression of IL-2 mRNA. Data are pooled from 2 independent experiments, each using pooled TIL from n=5 mice per cohort.

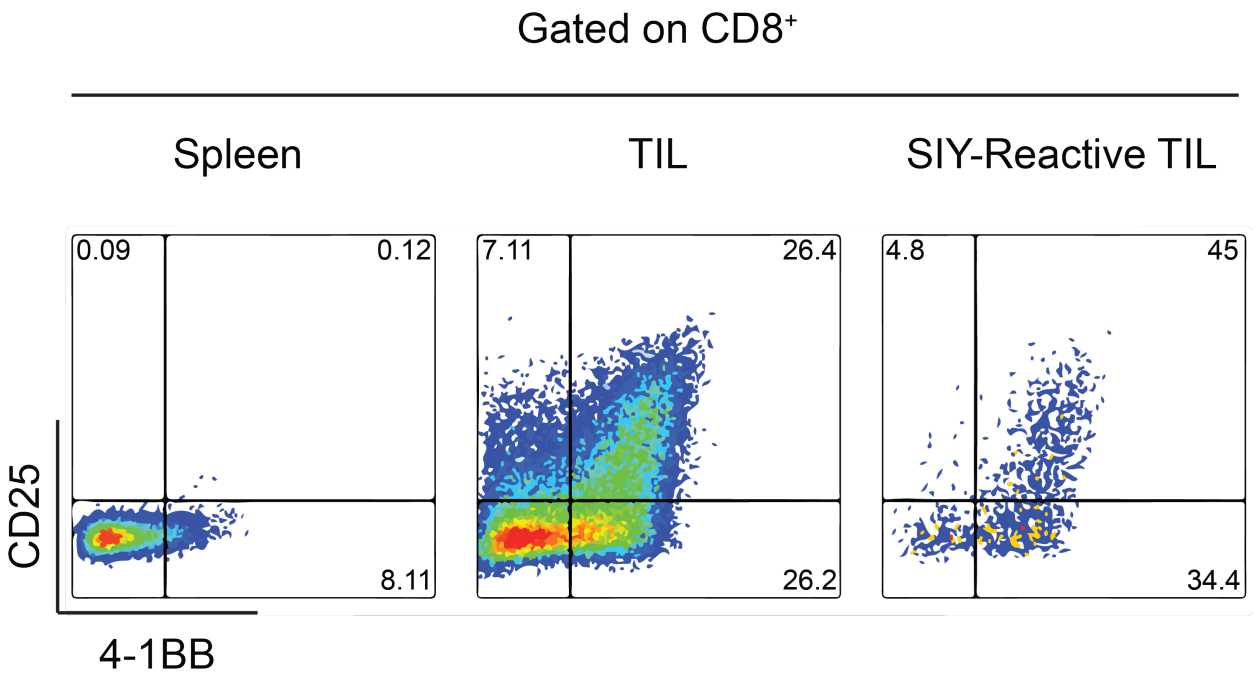

Figure 3.28: CD8$^+$ TIL express 4-1BB and CD25
C57BL/6 mice were injected subcutaneously with 2x10^6 B16.SIY cells. On day 13, post tumor injection, CD8$^+$ T cells were isolated from tumors and spleens and stained with SIY pentamer, anti-4-1BB and anti-CD25 antibodies. Shown are example FACS plots of CD8$^+$ T cells demonstrating co-expression of 4-1BB and CD25 on CD8$^+$ TIL and SIY-reactive CD8$^+$ TIL.

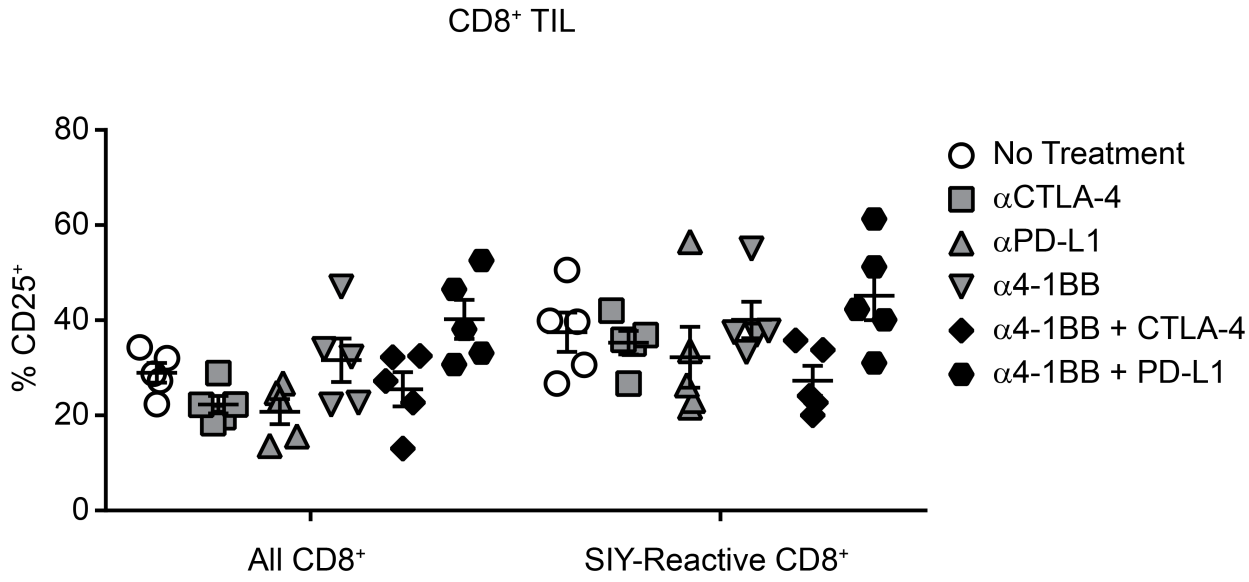

Figure 3.29: Immunotherapy does not alter CD25 expression on CD8$^+$ TIL
C57BL/6 mice were injected subcutaneously with 2x10^6 B16.SIY cells. Antibodies against CTLA-4, PD-L1, or 4-1BB were administered on days 7 and 10 after tumor implantation. On day 13, post tumor injection, CD8$^+$ T cells were isolated from tumors and spleens and stained with SIY pentamer, anti-4-1BB and anti-CD25 antibodies. For all groups n = 5.

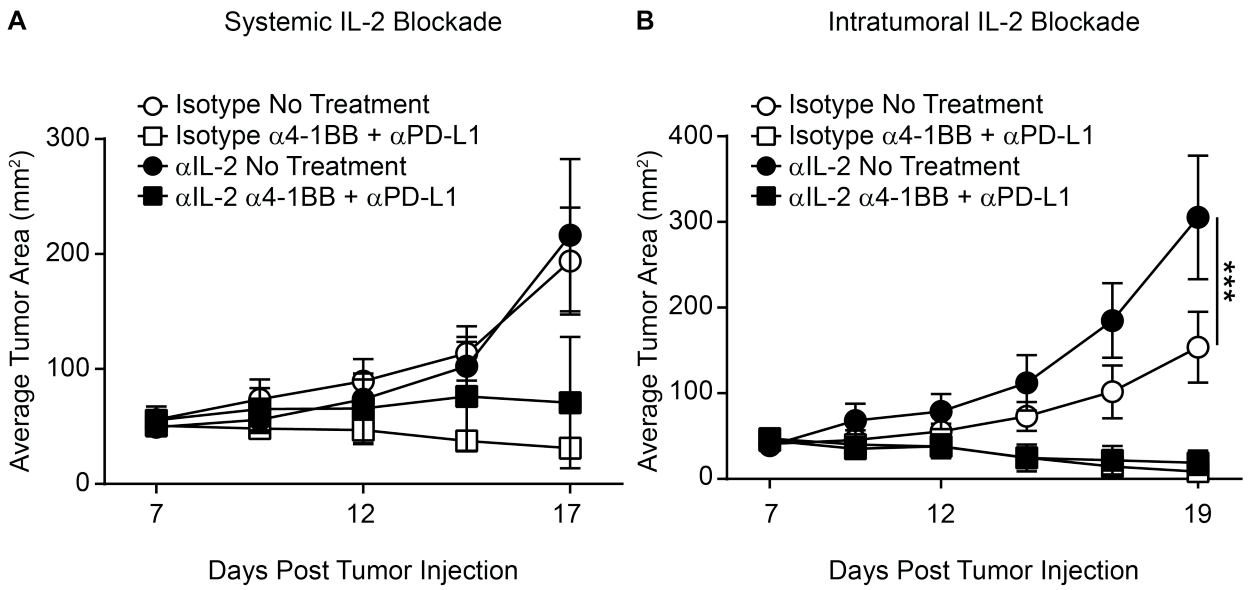

Figure 3.30: Antibody-mediated blockade of IL-2 does not affect the therapeutic efficacy of anti-4-1BB + anti-PD-L1

C57BL/6 mice were subcutaneously injected with 2x10^6 B16.SIY cells. Tumors were established for seven days, then cohorts were treated with anti-4-1BB + anti-PD-L1. At the same time, anti-IL-2 antibodies JES6-1A12 and SB46-1 were administered either systemically via the peritoneum (A) or directly into the tumor microenvironment (B). Both anti-IL-2 and therapeutic antibodies were given intraperitoneally on days 7, 10, 13 and 16 post-tumor injection at a dose of 100 μg per antibody per mouse per time point.

due to lack of regulatory T cells (Willerford, 1995; Furtado, 2002), we generated mixed bone marrow chimeras by transferring a 1:1 mixture of WT and CD25$^{-/-}$ bone marrow cells into lethally irradiated congenic recipients. Because these mice still retained WT CD8^{+} T cells, we could not test the effects of lack of CD25 on tumor outgrowth. However, we could compare the expansion of SIY-reactive WT and CD25$^{-/-}$ cells in the same animal, to determine if IL-2 was necessary for the expansion of antigen-specific TIL after agonist 4-1BB combination immunotherapy. After reconstitution, we subcutaneously inoculated chimeric mice with B16.SIY cells and treated mice with immunotherapy on days 7 and 10 after tumor injection. On day 13, we analyzed the tumors and spleens of these mice. We found that reconstitution of CD8^{+} T cells in chimeric mice favored the WT bone marrow, as there were more WT CD8^{+} T cells in both the tumors and the spleens of tumor bearing mice (Figure 30A and 30B). The ratios of WT to CD25$^{-/-}$ cells were largely unaffected by agonist 4-1BB combination immunotherapy (Figure 3.31A and 3.31B).

Examining the CD8^{+} TIL populations, we found that in addition to being less abundant, the CD25$^{-/-}$ CD8^{+} TIL displayed qualitative differences from the WT CD8^{+} TIL. A lower percentage of CD25$^{-/-}$ CD8^{+} TIL bound the SIY-pentamer, indicating that CD25 may play a role in maintaining endogenous antigen-specific CD8^{+} T cells in the tumor microenvironment (Figure 3.32A and 3.32B). Fewer CD25$^{-/-}$ CD8^{+} TIL expressed KLRG1, indicating fewer effector-like CD8^{+} T cells in the absence of CD25 signaling (Figure 3.33A and 3.33B). Despite these differences during the endogenous anti-tumor immune response, we found that CD25$^{-/-}$ CD8^{+} TIL were able to respond normally to 4-1BB combination therapies. After agonist anti-4-1BB immunotherapy, CD25$^{-/-}$ CD8^{+} TIL were able to expand their SIY-reactive fractions to achieve near WT levels, both in percentage and absolute number (Figure 3.34A-3.34C). Interestingly, when measuring the fold increase of SIY-reactive CD8^{+} TIL, the CD25$^{-/-}$ cells actually expanded more compared to untreated CD25$^{-/-}$ TIL than the WT cells did (3.34B and 3.34C). KLRG1 upregulation was also normal in CD25$^{-/-}$ cells, indicating that CD25 signaling was not necessary for the expansion of tumor antigen-

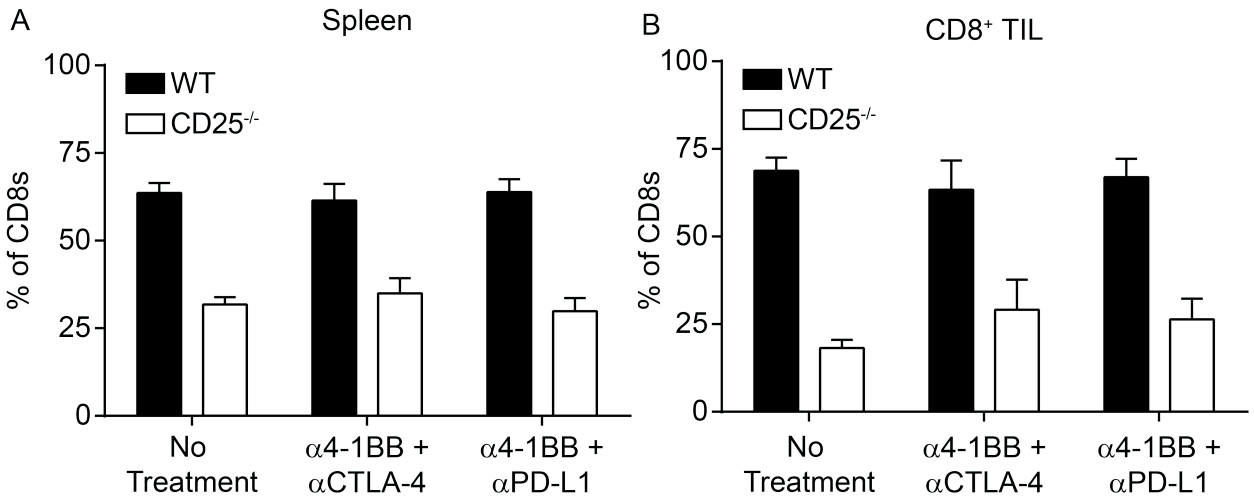

Figure 3.31: Increased numbers of WT CD8$^+$ T cells than CD25$^{-/-}$ CD8$^+$ T cells after reconstitution of mixed bone marrow chimeras

C57BL/6 mice were lethally irradiated. 24 hours later, mice were intravenously injected with approximately 5x10^6 bone marrow cells at a 1:1 ratio of WT:CD25$^{-/-}$ bone marrow. After reconstitution, mice were subcutaneously injected with 2x10^6 B16.SIY cells. Mice were treated with immunotherapy on day 7 and day 10 after tumor implantation. On day 13, the spleens and tumors of mice were analyzed. (A) The percent chimerism of the CD8$^+$ T cell lineage in spleens of chimeric mice, as measured by flow cytometry. (B) The CD8$^+$ TIL were analyzed via flow cytometry to determine the percent chimerism in tumors of chimeric mice.

specific CD8$^+$ TIL or their change in phenotype in response to agonist 4-1BB combination immunotherapy (3.35A and 3.35B).

3.14 NF-κB activation in T cells recapitulates many aspects of agonist 4-1BB immunotherapy

To ask if increased NF-κB signaling was responsible for the efficacy of agonist 4-1BB combination immunotherapy, we used mice that express a constitutively active form of IKKβ in the T cell compartment (IKKβ-CA mice). We innoculated IKKβ-CA mice and littermate controls with B16.SIY tumors and assessed the phenotype of CD8$^+$ TIL. The CD8$^+$ TIL from IKKβ-CA mice recapitulated many aspects of agonist 4-1BB immunotherapy. An increased fraction of CD8$^+$ TIL from IKKβ-CA were SIY-reactive compared to WT mice (Figure 3.36A). Additionally, fewer CD8$^+$ TIL from these mice contained active caspase-3, indicating increased survival of CD8$^+$ TIL (Figure 3.36B). There was no change in Ki-67 expression (Figure 3.36C). Phenotypically, CD8$^+$ TIL from IKKβ-CA mice were similar to TIL that received agonist 4-1BB immunotherapy (Figure 3.22B), with fewer PD-1$^+$LAG-3$^+$ TIL (Figure 3.36D) and a significant increase in TIL KLRG1 expression (Figure 3.36E). Interestingly, there was increased γH2AX staining in IKKβ-CA mice (Figure 3.36F), indicating that NF-κB signaling increased TIL survival despite the presence of DNA damage. Together with published results indicating that T cell-intrinsic NF-κB signaling is required for immune-mediated tumor rejection (Barnes, 2015; Evaristo, 2016), these results suggest that the mechanism by which agonist anti-4-1BB immunotherapy enhances tumor control might be through the NF-κB pathway.

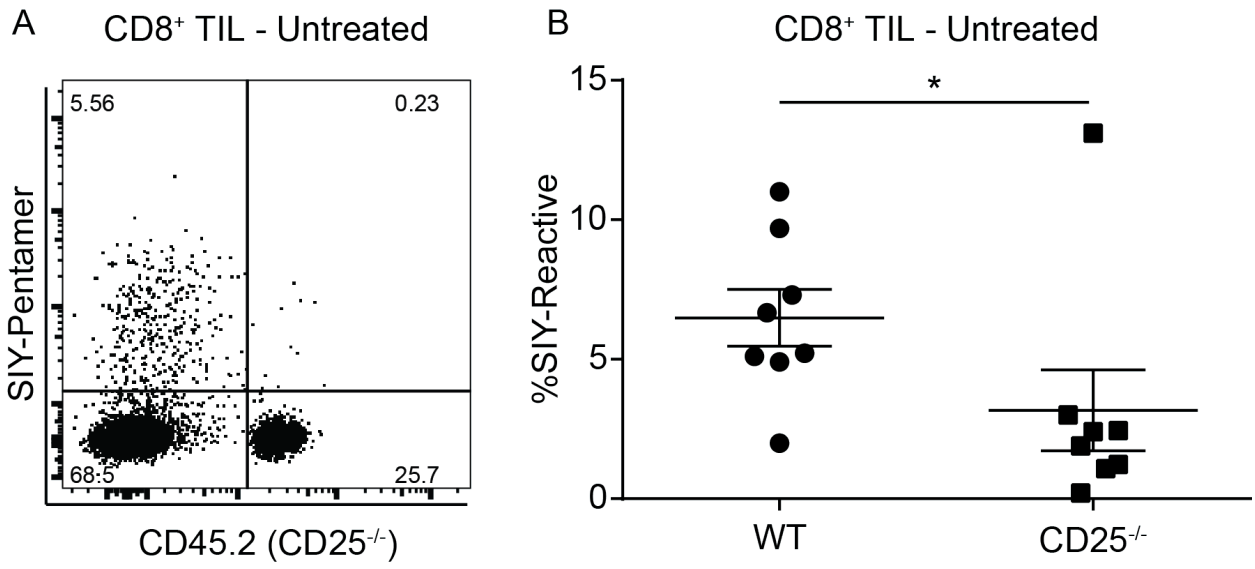

Figure 3.32: A lower percentage of CD25$^{-/-}$ CD8^{+} TIL are SIY-reactive
C57BL/6 mice were lethally irradiated. 24 hours later, mice were intravenously injected with approximately 5x10^{6} bone marrow cells at a 1:1 ratio of WT:CD25$^{-/-}$ bone marrow. After reconstitution, mice were subcutaneously injected with 2x10^{6} B16.SIY cells (A) Representative flow plots of SIY-pentamer staining of WT and CD25$^{-/-}$ CD8^{+} TIL. (B) Quantification of SIY-pentamer reactivity of WT and CD25$^{-/-}$ CD8^{+} TIL. (B) CD8^{+} TIL KLRG1 expression was quantified via flow cytometry

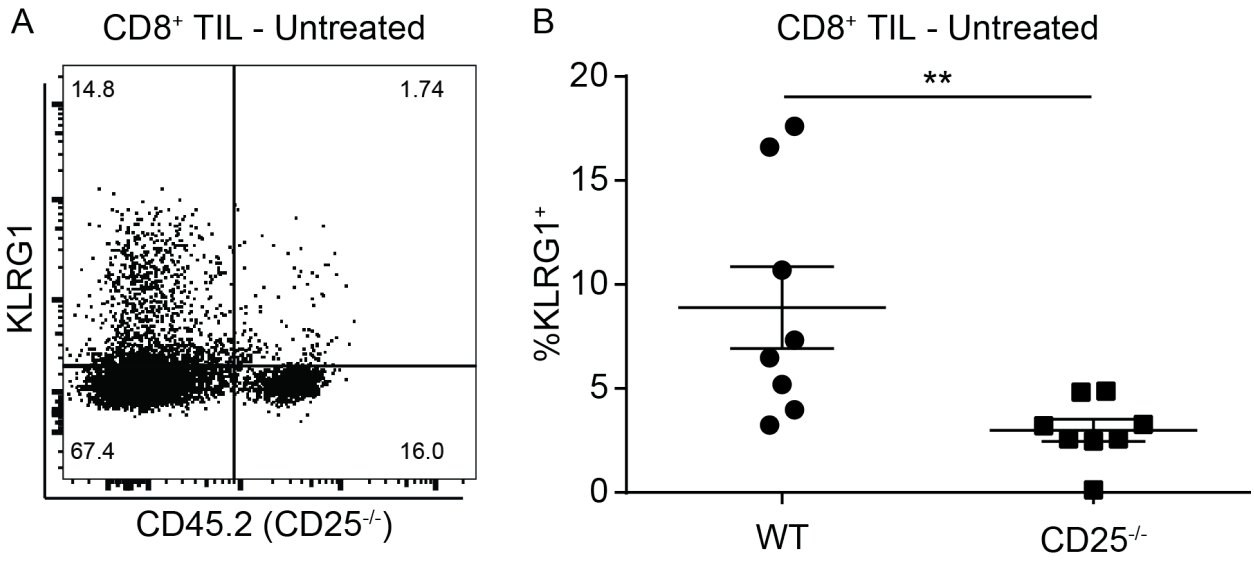

Figure 3.33: A lower percentage of CD25$^{-/-}$ CD8^{+} TIL express KLRG1
C57BL/6 mice were lethally irradiated. 24 hours later, mice were intravenously injected with approximately 5x10^{6} bone marrow cells at a 1:1 ratio of WT:CD25$^{-/-}$ bone marrow. After reconstitution, mice were subcutaneously injected with 2x10^{6} B16.SIY cells (A) Representative flow plots of KLRG1 staining of WT and CD25$^{-/-}$ CD8^{+} TIL. (B) Quantification of KLRG1 expression on WT and CD25$^{-/-}$ CD8^{+} TIL.

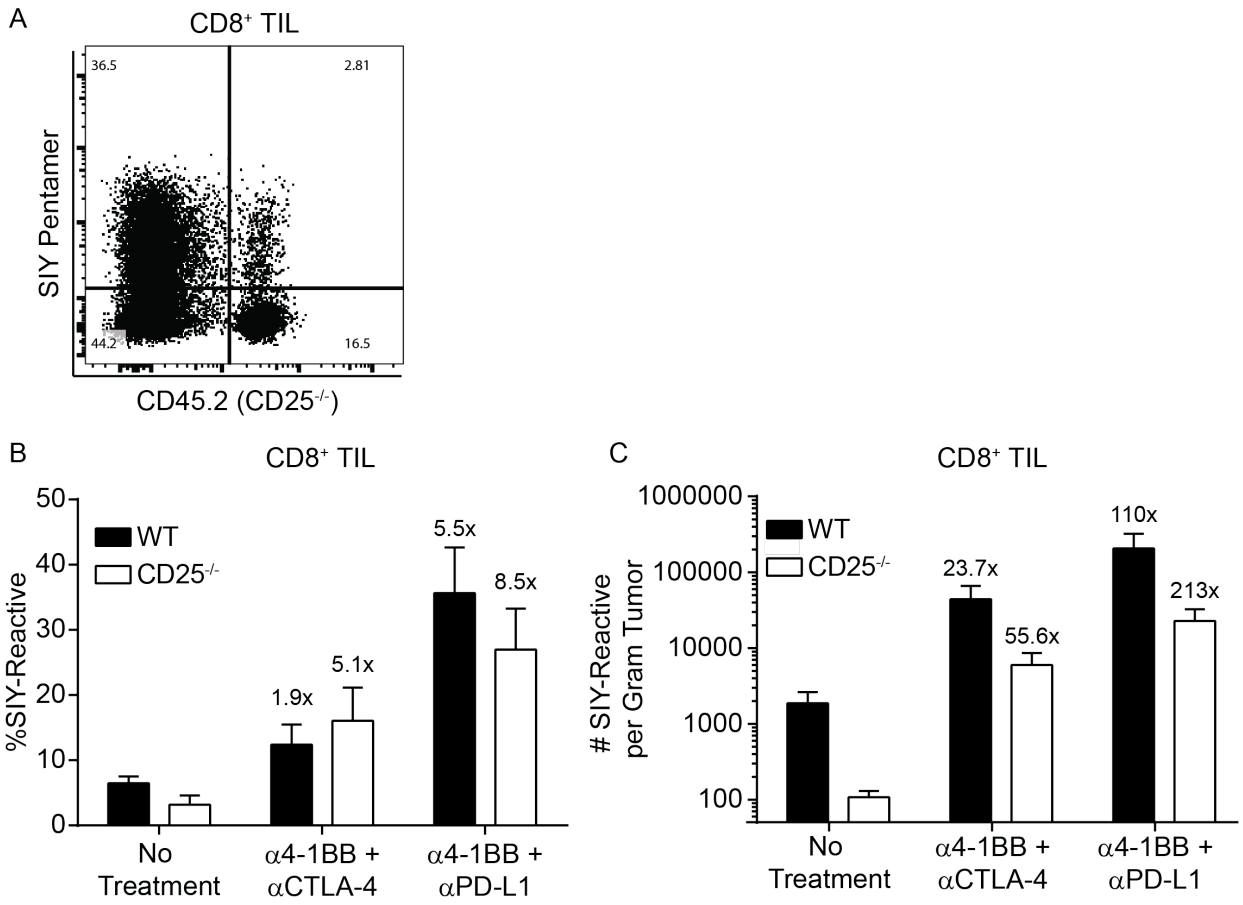

Figure 3.34: No deficit in expansion of CD25$^{-/-}$ SIY-reactive CD8^{+} TIL after immunotherapy

C57BL/6 mice were lethally irradiated. 24 hours later, mice were intravenously injected with approximately 5x10^{6} bone marrow cells at a 1:1 ratio of WT:CD25$^{-/-}$ bone marrow. After reconstitution, mice were subcutaneously injected with 2x10^{6} B16.SIY cells. Mice were treated with immunotherapy on day 7 and day 10 after tumor implantation, and analyzed on day 13. (A) Representative FACS plot of SIY-pentamer staining of WT and CD25$^{-/-}$ CD8^{+} TIL. (B) The percentage of WT and CD25$^{-/-}$ CD8^{+} TIL that bind the SIY-pentamer as measured by flow cytometry. (C) The number of SIY-reactive CD8^{+} TIL per gram tumor.

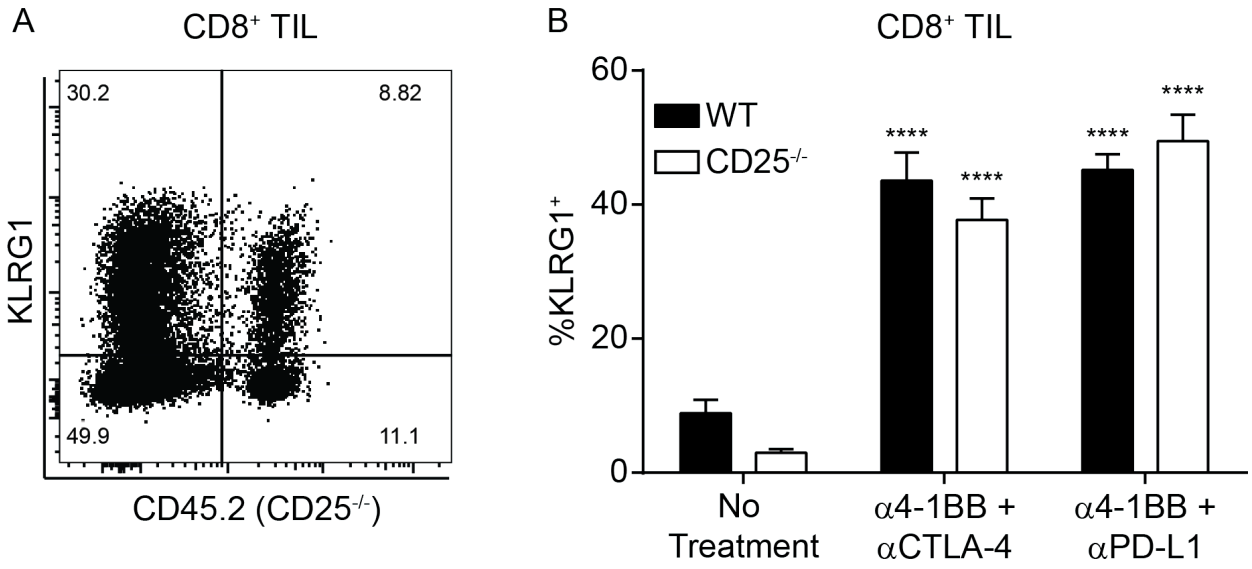

Figure 3.35: No deficit in KLRG1 upregulation on CD25$^{-/-}$ CD8^{+} TIL after immunotherapy

C57BL/6 mice were lethally irradiated. 24 hours later, mice were intravenously injected with approximately 5x10^{6} bone marrow cells at a 1:1 ratio of WT:CD25$^{-/-}$ bone marrow. After reconstitution, mice were subcutaneously injected with 2x10^{6} B16.SIY cells. Mice were treated with immunotherapy on day 7 and day 10 after tumor implantation, and analyzed on day 13. (A) Representative FACS plot of KLRG1 staining of WT and CD25$^{-/-}$ CD8^{+} TIL. (B) The percentage of CD8^{+} TIL that are either WT or CD25$^{-/-}$ that express KLRG1.

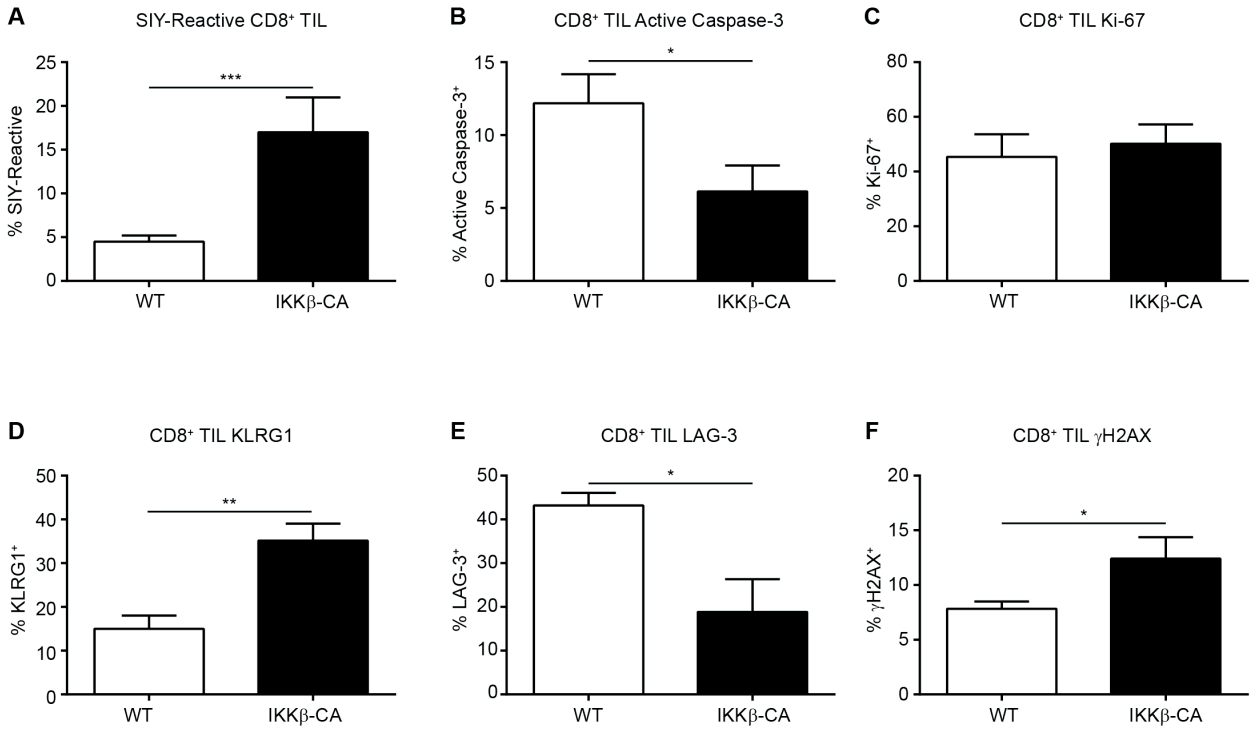

Figure 3.36: The effects of constitutive IKKβ expression in T cells mimic those of agonist 4-1BB combination immunotherapy

WT or CD4-cre IKKβ (IKKβ-CA) mice were given subcutaneous B16.SIY tumors. On day 10, the CD8$^+$ TIL were analyzed with flow cytometry for (A) the percentage that bound SIY/K^b pentamer, (B) the fraction that contained active caspase-3, (C) Ki-67 expression, (D) KLRG1 expression, (E) LAG-3 expression and (F) the presence of γH2AX. Mann-Whitney U tests were performed for all comparisons. For (A), (B), (D), and (E), WT n = 15, IKKβ-CA n = 8. For (C) WT n = 3, IKKβ -CA n = 4. For (F) WT n = 12, IKKβ-CA n = 4.

3.15 Agonist 4-1BB antibody requires 4-1BB expression on hematopoietic cells for tumor control

Studies have suggested that 4-1BB is expressed on tumor endothelium and other non-hematopoietic cells, and that 4-1BB on endothelial cells can be targeted by agonist 4-1BB antibodies to enhance recruitment of T cells to the tumor microenvironment (Palazon, 2011; Blank, 2015). We therefore investigated whether 4-1BB expression on non-hematopoietic cells contributed to tumor control after agonist 4-1BB antibody administration. To test this, we generated bone marrow chimeras using WT mice as recipients, and either WT or 4-1BB$^{-/-}$ bone marrow donors to generate mice where 4-1BB would be expressed either on all cells or only on non-hematopoietic cells. Seven days post sub-cutaneous injection with B16.SIY, we began treating with agonist 4-1BB antibody. As expected, agonist 4-1BB antibody treatment led to improved tumor control in the mice that received WT bone marrow (Figure 3.37A). However, in mice that received 4-1BB$^{-/-}$ bone marrow, no increase in tumor control by agonist 4-1BB antibody was observed. Therefore, 4-1BB expression on hematopoietic cells is required for the anti-tumor effects of agonist 4-1BB antibodies (Figure 3.37B).

3.16 Agonist 4-1BB antibody acts on CD8$^+$ T cells in a cell-intrinsic manner

We next investigated whether CD8$^+$ T cells were being affected directly by agonist 4-1BB antibody. We generated mixed bone marrow chimeras by transplanting a 1:1 mixture of 4-1BB$^{-/-}$ and WT bone marrow into lethally irradiated congenic hosts. This allowed us to determine if agonist 4-1BB antibody expanded antigen-specific CD8$^+$ TIL, and if 4-1BB$^{-/-}$ T cells could respond to agonist 4-1BB immunotherapy. Six to eight weeks after reconstitution, we innoculated B16.SIY cells subcutaneously into chimeric mice. Seven days post-tumor injection, we initiated agonist 4-1BB immunotherapy. On day 13 post-tumor injection, the

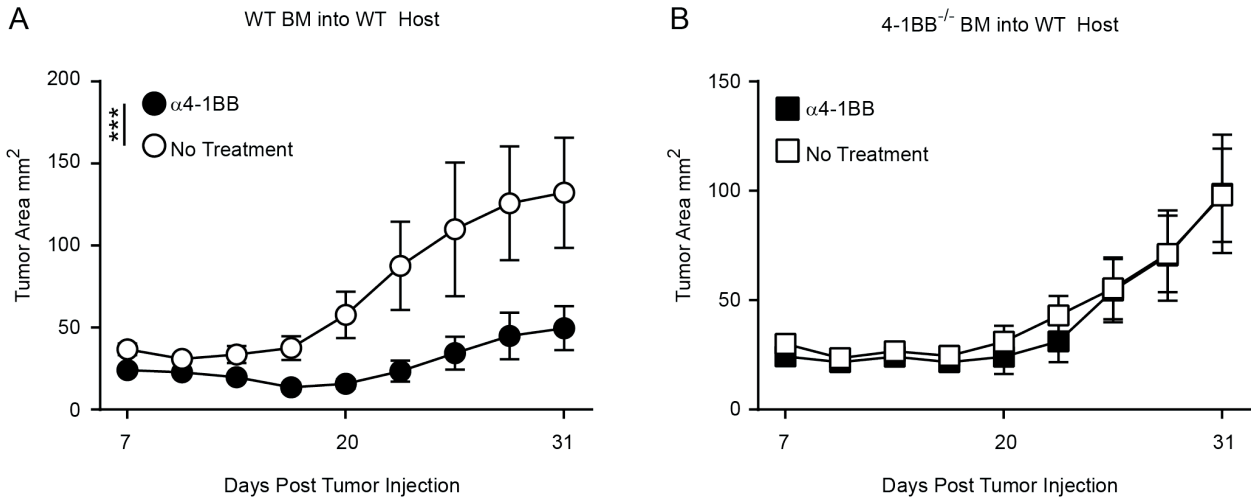

Figure 3.37: Agonist 4-1BB antibody requires 4-1BB expression on hematopoietic cells for tumor control

(A) Lethally irradiated WT mice were reconstituted with WT bone marrow. 6-8 weeks after reconstitution, mice were subcutaneously inoculated with B16.SIY. Tumors were allowed to establish for seven days, and then 100 μg agonist 4-1BB antibody was administered on days 7, 10, 13 and 16. (B) Lethally irradiated WT mice were reconstituted with 4-1BB$^{-/-}$ bone marrow. 6-8 weeks after reconstitution, mice were subcutaneously inoculated with B16.SIY. Tumors were allowed to establish for seven days, and then 100 μg agonist 4-1BB antibody was administered on days 7, 10, 13 and 16. Results are pooled from two independent experiments. WT into WT No Treatment n = 6, WT into WT anti-4-1BB n = 10, 4-1BB$^{-/-}$ into WT No Treatment n = 9, 4-1BB into WT anti-4-1BB$^{-/-}$ n = 10.

mice were sacrificed and their T cells analyzed to determine the frequency of SIY-reactive $CD8^+$ T cells. In all anatomic locations analyzed, the frequency of antigen-specific $CD8^+$ T cells was significantly higher in the WT compartment compared to the 4-$1BB^{-/-}$ compartment after agonist 4-1BB immunotherapy (Figure 3.38A, 3.38B, and 3.38C). There were no significant changes between the treated and untreated 4-$1BB^{-/-}$ SIY-reactive $CD8^+$ T cells, indicating that agonist 4-1BB immunotherapy acts in a $CD8^+$ T cell-intrinsic manner, and requires 4-1BB expression on T cells to expand an antigen-specific population (Figure 3.38A, 3.38B, and 3.38C). KLRG1 is upregulated on $CD8^+$ TIL by agonist 4-1BB signaling (Curran, 2013; Williams, 2017). In our mixed bone marrow chimeras, KLRG1 was upregulated only on WT $CD8^+$ TIL, and not on 4-$1BB^{-/-}$ TIL, indicating T cell-intrinsic signaling was necessary for increased KLRG1 expression in response to agonist 4-1BB immunotherapy (Figure 3.38D).

Comparing the reconstitution efficiency of the transferred WT and 4-$1BB^{-/-}$ cells also revealed interesting information. In the spleen and tumor draining lymph nodes, 4-$1BB^{-/-}$ cells made up a significantly higher proportion of the $CD8^+$ T cells than WT cells (Figure 3.39A and 3.39B). This is consistent with a previous study showing that 4-$1BB^{-/-}$ cells can have higher proliferation rates than their WT counterparts (Kwon, 2002). However, WT and 4-$1BB^{-/-}$ TIL were present at equal ratios, indicating that despite their lower prevalence in the spleen, WT $CD8^+$ T cells were superior to 4-$1BB^{-/-}$ $CD8^+$ T cells at residing in the tumor. (Figure 3.39C). And in the presence of agonist 4-1BB antibody, WT $CD8^+$ TIL dominated over the 4-$1BB^{-/-}$ $CD8^+$ TIL (Figure 3.39C). This indicated that 4-1BB on T cells both in steady state and in the presence of agonist 4-1BB antibody provides signals that help to maintain $CD8^+$ T cell numbers in the tumor microenvironment. This finding was further highlighted by comparing the SIY-reactive cell numbers in the spleens and tumors of chimeric animals. In the spleens, 4-$1BB^{-/-}$ SIY-reactive cells outnumbered their WT counterparts (Figure 3.40A). In the tumor however, both in the absence and presence of agonist 4-1BB, WT SIY-reactive $CD8^+$ TIL outnumbered the 4-$1BB^{-/-}$ $CD8^+$

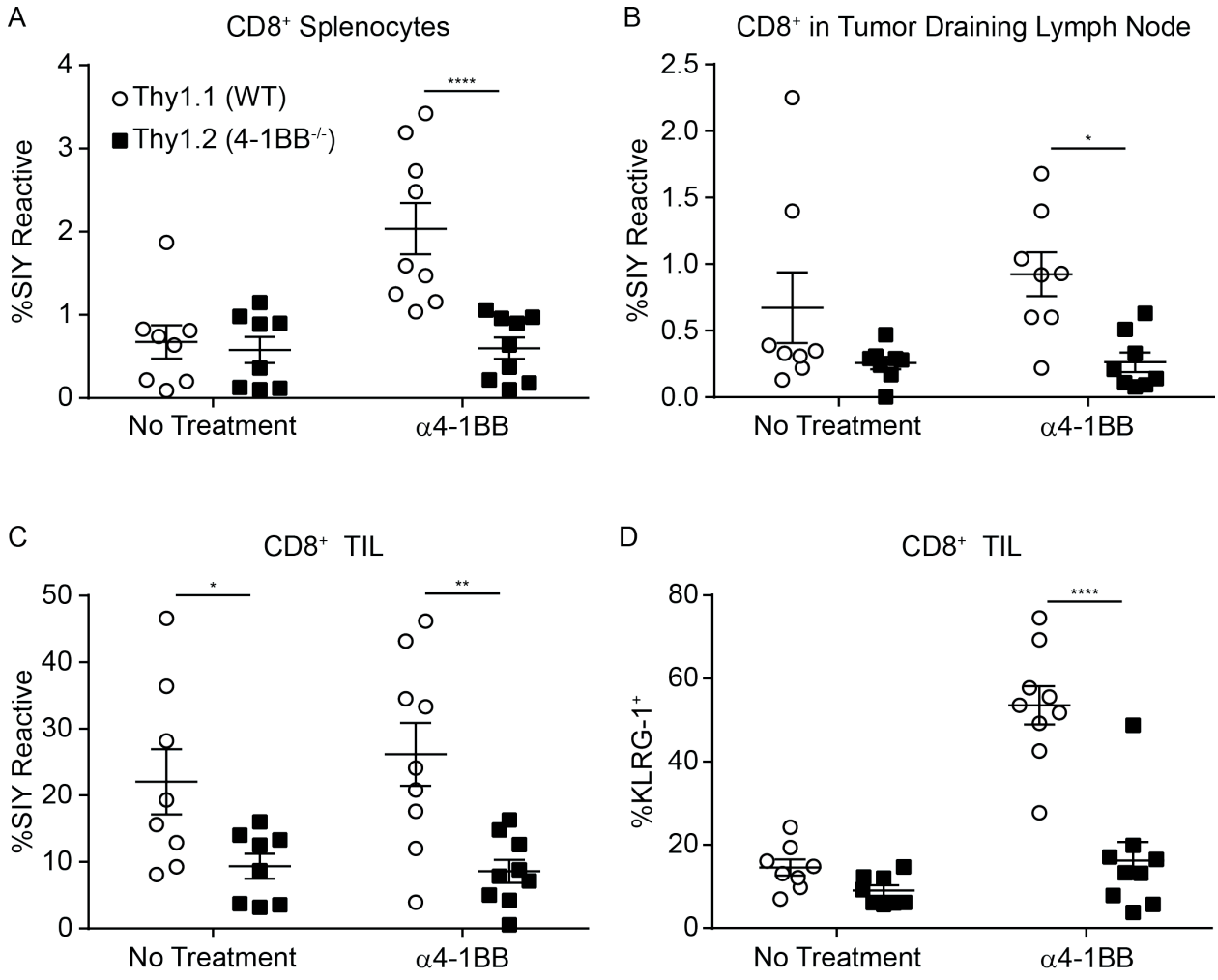

Figure 3.38: Agonist anti-4-1BB antibody expands antigen specific T cells in a T cell intrinsic manner

Mixed bone marrow chimeras were generated by transferring a 1:1 ratio of WT and 4-1BB$^{-/-}$ marrow into lethally irradiated WT hosts. Chimeric mice were then subcutaneously injected with B16.SIY and treated with agonist anti-4-1BB antibody seven and ten days post tumor injection. On day 13 post tumor injection, the expansion of SIY-reactive CD8$^+$ T cells was measured via flow cytometry in the (A) spleen, (B) tumor draining lymph nodes, and (C) tumor. (D) KLRG1 upregulation was measured via flow cytometry on CD8$^+$ TIL.

TIL, indicating that 4-1BB signaling helped to maintain tumor antigen-specific $CD8^+$ TIL (Figure 3.40B).

3.17 4-1BB$^{-/-}$ mice generate but cannot maintain normal numbers of $CD8^+$ TIL

We next tested if 4-1BB$^{-/-}$ mice would be able to generate a normal immune response against transplanted tumors. We inoculated B16.SIY cells subcutaneously and monitored immune responses at day 7 and day 13 post tumor injection. On day 7, we performed an IFN-μ elispot using splenocytes as a measure of $CD8^+$ T cell priming against SIY. There was no statistically significant difference between the WT and 4-1BB$^{-/-}$ spleens, indicating that the 4-1BB$^{-/-}$ mice were able to prime normal numbers of SIY-reactive $CD8^+$ T cells (Figure 3.41A). This result was confirmed using SIY-K^b pentamer staining and flow cytometry. On both day 7 and day 13 post tumor injection, we found no significant differences in numbers of SIY-reactive $CD8^+$ T cells in the spleen, indicating that 4-1BB$^{-/-}$ mice were capable of generating normal numbers of tumor-specific $CD8^+$ T cells in secondary lymphoid tissues (Figure 3.41B). 4-1BB$^{-/-}$ mice also had normal numbers of $CD8^+$ TIL on day 7 post-tumor injection, indicating that 4-1BB$^{-/-}$ mice could initially generate TIL and that TIL were capable of migrating to the tumor site in normal numbers (Figure 3.41C). However, at day 13, 4-1BB$^{-/-}$ mice had decreased $CD8^+$ TIL numbers compared to WT animals (Figure 3.41C), as well as SIY-reactive $CD8^+$ TIL (Figure 3.41D). Therefore, it appeared that while 4-1BB$^{-/-}$ SIY-reactive $CD8^+$ cells were able to generate normal numbers in the spleen, they were not able to maintain normal numbers in the tumor over time. This was similar to the mixed bone marrow chimera data, and indicated again that 4-1BB$^{-/-}$ $CD8^+$ T cells were specifically disadvantaged in the ability to be maintained in the tumor microenvironment. Phenotyping of the $CD8^+$ TIL on day 7 (Figure 3.41E) and day 13 (Figure 3.41F) revealed that the 4-1BB$^{-/-}$ mice had fewer LAG-3^+ TIL. The LAG-3^+ TIL population has been shown

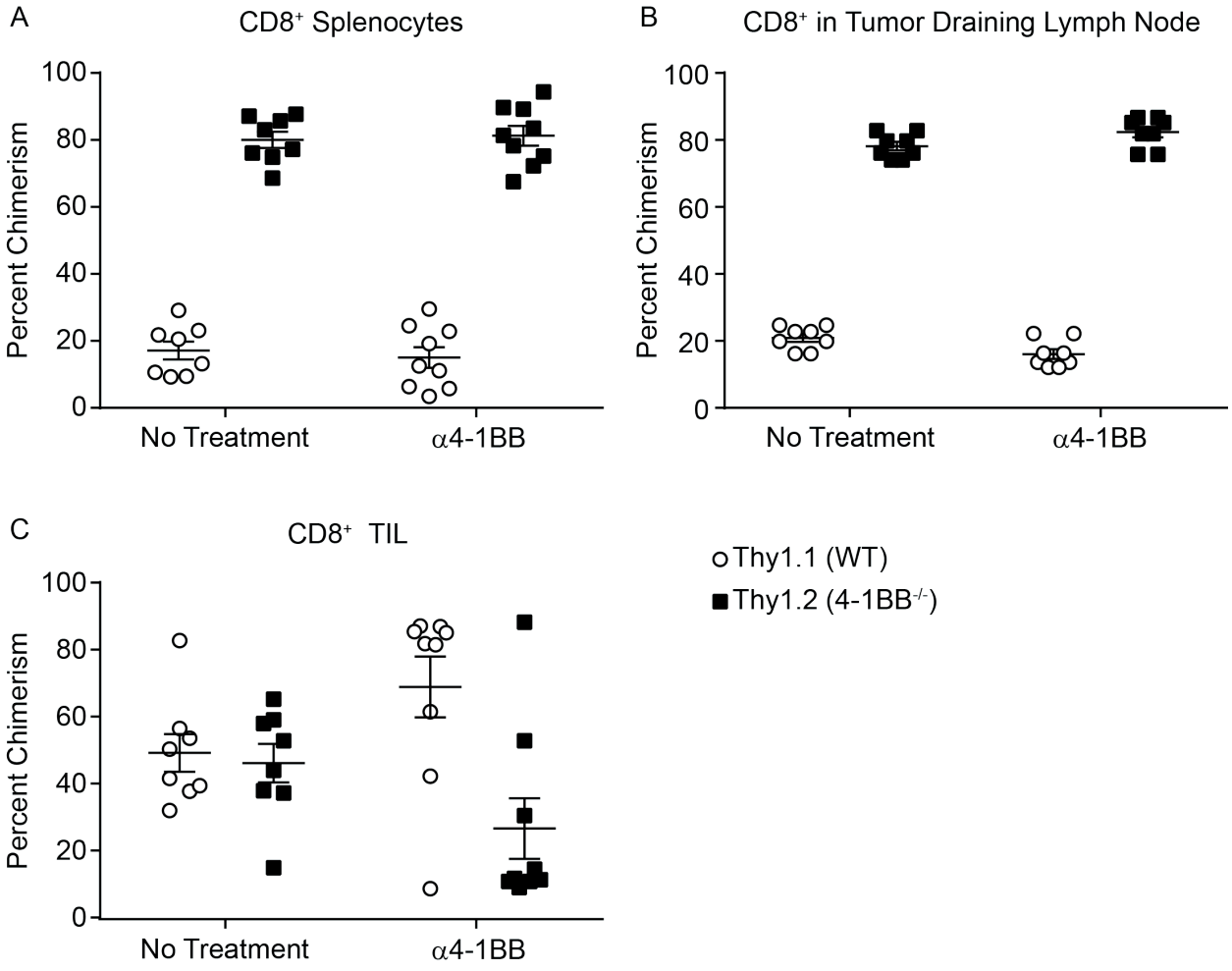

Figure 3.39: 4-1BB signaling advantages CD8$^+$ T cells in the tumor microenvironment

The percent chimerism between transferred WT and 4-1BB$^{-/-}$ bone marrow was measured in the (A) spleens, (B) tumor draining lymph nodes, and (C) tumors.

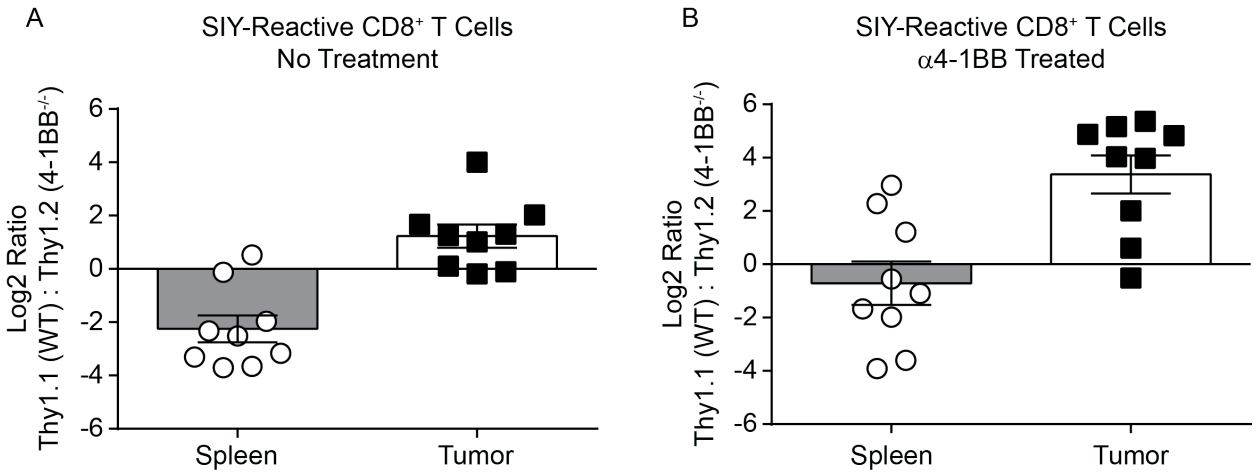

Figure 3.40: WT SIY-reactive CD8$^+$ T cells dominate the tumor microenvironment despite being outnumbered in secondary lymphoid tissues
The log2-adjusted ratios of WT:4-1BB$^{-/-}$ SIY-reactive CD8$^+$ cells was compared between the spleens and tumors in (A) untreated mice or with (B) agonist anti-4-1BB antibody treatment.

to be tumor antigen-specific T cells (Williams, 2017). Thus, the lack of LAG-3$^+$ TIL was another indication of the lackof maintenance of antigen-specific CD8$^+$ TIL in the absence of 4-1BB. Correspondingly, 4-1BB$^{-/-}$ mice had larger tumors on day 13 than WT mice (Figure 3.41G), indicating that the low levels of antigen-specific CD8$^+$ TIL were associated with a functional decrease in tumor control.

3.18 4-1BBL signals to CD8$^+$ TIL during the spontaneous immune response against B16.SIY

The results from mixed bone marrow chimeras as well as 4-1BB$^{-/-}$ mice revealed that CD8$^+$ T cell-intrinsic 4-1BB signaling during the endogenous anti-tumor immune response allowed for greater accumulation of SIY-reactive CD8$^+$ TIL. We therefore wanted to determine if there was active 4-1BBL engagement of 4-1BB that contributed to tumor control and the accumulation of CD8$^+$ TIL during the anti-tumor immune response. Using C57BL/6 mice bearing subcutaneous B16.SIY tumors, we administered 200 μg per mouse of a blocking antibody against 4-1BBL on days 7, 10, 13, and 16 post-tumor injection. We found that blockade of 4-1BBL resulted in a subtle but statistically significant enhancement of tumor outgrowth, indicating that 4-1BBL signaling contributed to tumor control (Figure 3.42A). Consistently, when we analyzed these tumors, we found that mice treated with anti-4-1BBL had fewer infiltrating CD8$^+$ TIL and SIY-reactive CD8$^+$ TIL (Figure 3.42B and 3.42C).

To determine if 4-1BBL signaling was important for CD8$^+$ TIL, or was exerting effects in secondary lymphoid tissues, we repeated the tumor outgrowth experiments while simultaneously administering daily FTY720 beginning on day 7 post tumor injection. The results from these experiments were very similar to experiments without FTY720. We found a statistically significant increase in tumor growth with anti-4-1BBL antibody (Figure 3.43A), and anti-4-1BBL treated tumors contained fewer CD8$^+$ TIL and SIY-reactive CD8$^+$ TIL (Figure 3.43B and 3.43C). Taken together, these results indicated that 4-1BBL signaling to 4-1BB

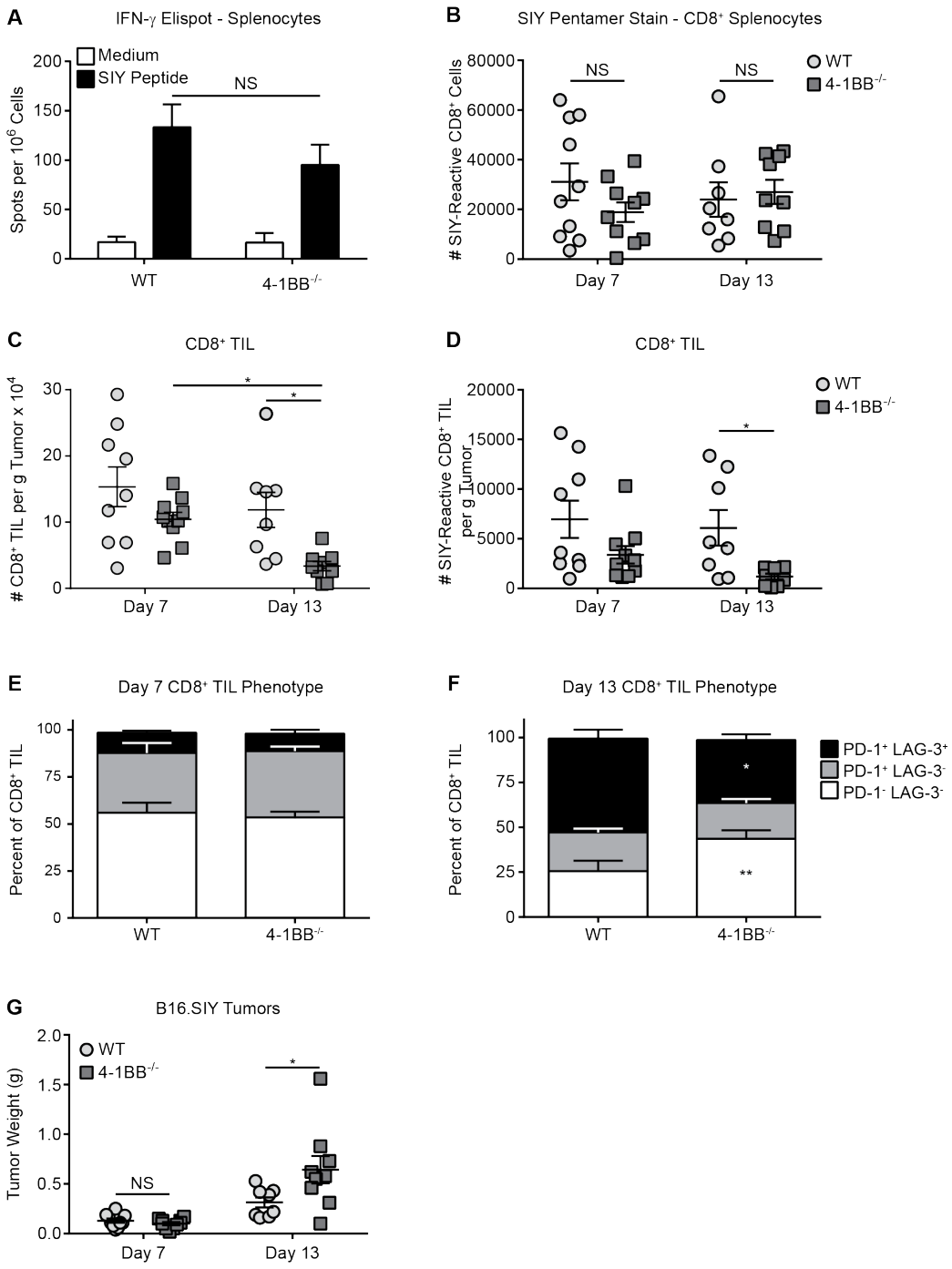

Figure 3.41: 4-1BB$^{-/-}$ mice generate but cannot maintain normal numbers of CD8$^+$ TIL

(A) IFN-γ ELISPOT performed on day 7 splenocytes. (B) Flow cytometry was used to quantify the number of SIY-reactive CD8$^+$ T cells in the spleen (C) CD8$^+$ TIL, and (D) SIY-reactive CD8$^+$ TIL. (E) PD-1 and LAG-3 expression of CD8$^+$ TIL and (F) SIY-reactive CD8$^+$ TIL. (G) Tumor weights. WT day 7 n = 9, 4-1BB$^{-/-}$ day 7 n = 10, WT day 13 n = 8, 4-1BB$^{-/-}$ day 13 n = 9, two-way ANOVA.

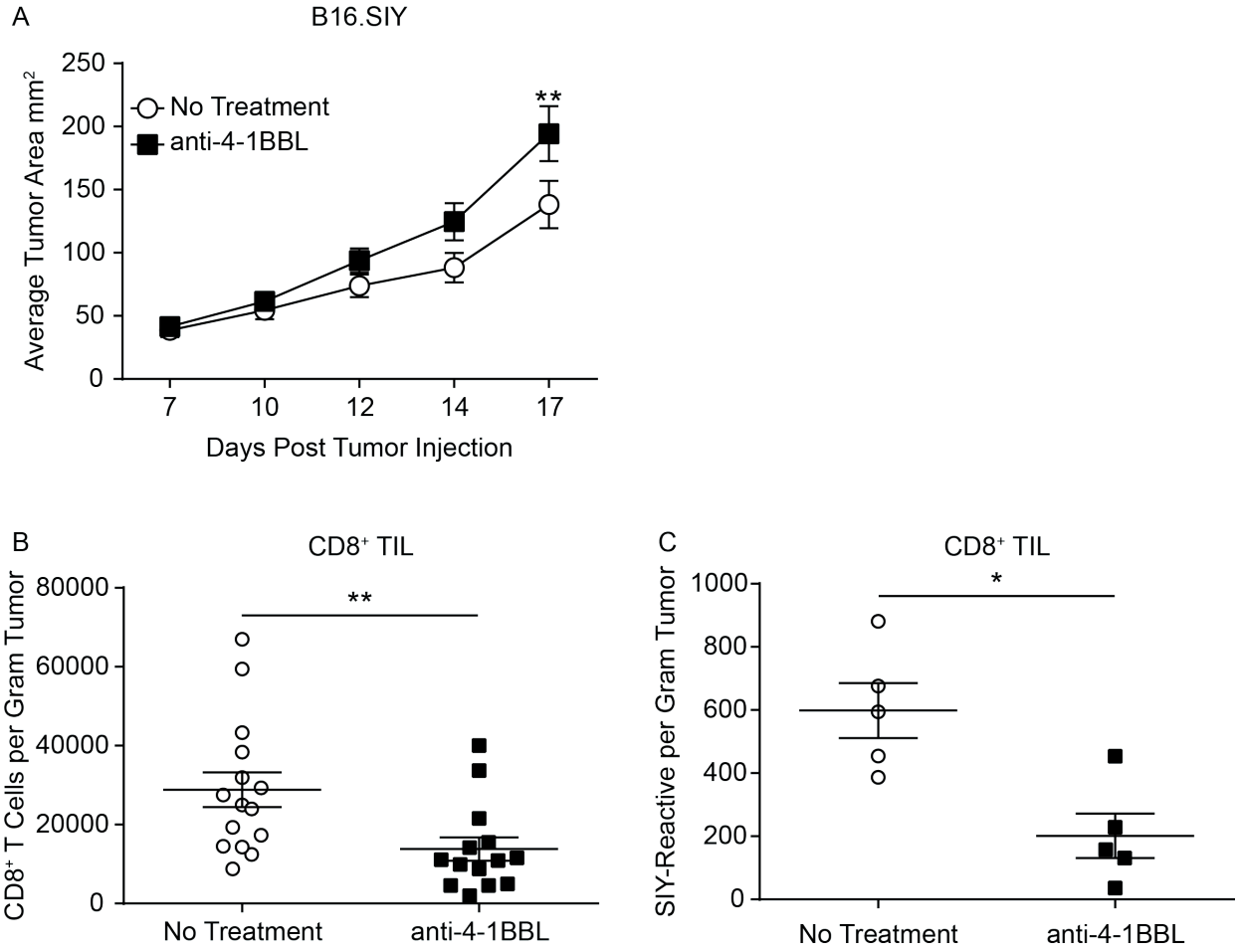

Figure 3.42: Blockade of 4-1BBL worsens tumor control and decreases CD8$^+$ TIL numbers

C57BL/6 mice were subcutaneously injected with 2x10^6 B16.SIY on day 0. Mice were treated with 200 μg anti-4-1BBL antibody on days 7, 10, 13, and 16 post tumor injection. (A) Outgrowth of B16.SIY tumors in untreated or anti-4-1BBL treated mice. Data is pooled from 3 independent experiments. 2-way ANOVA with a Bonferroni correction was used to calculate statistical significance. (B) Analysis of CD8$^+$ TIL after tumor outgrowth studies were complete. Data is pooled from 3 independent experiments. Statistical significance was computed with Mann-Whitney t test. (C) Representative data from one experiment enumerating the number of SIY-reactive CD8$^+$ TIL after tumor outgrowth studies were complete. Statistical significance was computed with Mann-Whitney t test.

expressed on $CD8^+$ TIL is important for maintaining the maximum number of $CD8^+$ T cells in the tumor microenvironment. Interestingly, in a cohort of metastatic melanoma samples from the clinic, *4-1BBL* expression also correlated with *CD8A* gene expression (Figure 3.44). This result, combined with results from 4-1BB$^{-/-}$ mice and blockade of 4-1BBL, suggests that 4-1BBL may play a functional role in maintaining $CD8^+$ TIL in both mouse and human tumors. The correlation in human tumors between 4-1BBL expression and infiltration of $CD8^+$ T cells should be studied further. It should be determined if 4-1BB signaling plays a functional role in maintaining $CD8^+$ TIL numbers.

3.19 4-1BB is required on lymphocytes for therapeutic efficacy of anti-PD-L1 antibodies

We next wanted to investigate whether endogenous 4-1BB engagement was important for the therapeutic efficacy of checkpoint blockade immunotherapy. Co-stimulation through CD28 was recently found to be necessary for the anti-tumor effect of anti-PD-L1 antibody (Kamphorst, 2017). As 4-1BB also delivers costimulatory signals to T cells, we tested if 4-1BB$^{-/-}$ mice would have reduced tumor growth in response to antibody blockade of PD-L1. We inoculated WT or 4-1BB$^{-/-}$ mice subcutaneously with B16.SIY and measured tumor growth in control mice and in mice that received anti-PD-L1 antibody. There were no significant differences in tumor growth between untreated WT and 4-1BB$^{-/-}$ mice (Figure 3.45). However, while the WT mice showed significantly better tumor control in response to anti-PD-L1 antibody, there were no effects of anti-PD-L1 in the 4-1BB $^{-/-}$ mice (Figure 3.45). These experiments indicate that 4-1BB signaling is required for increased tumor control after anti-PD-L1 immunotherapy, and generally that co-stimulatory signals other than CD28 are required for the efficacy of anti-PD-L1 antibodies.

We wanted to determine if the lack of therapeutic efficacy of anti-PD-L1 in 4-1BB$^{-/-}$ mice was the result of 4-1BB deficiency on adaptive immune cells. To test this, we transferred

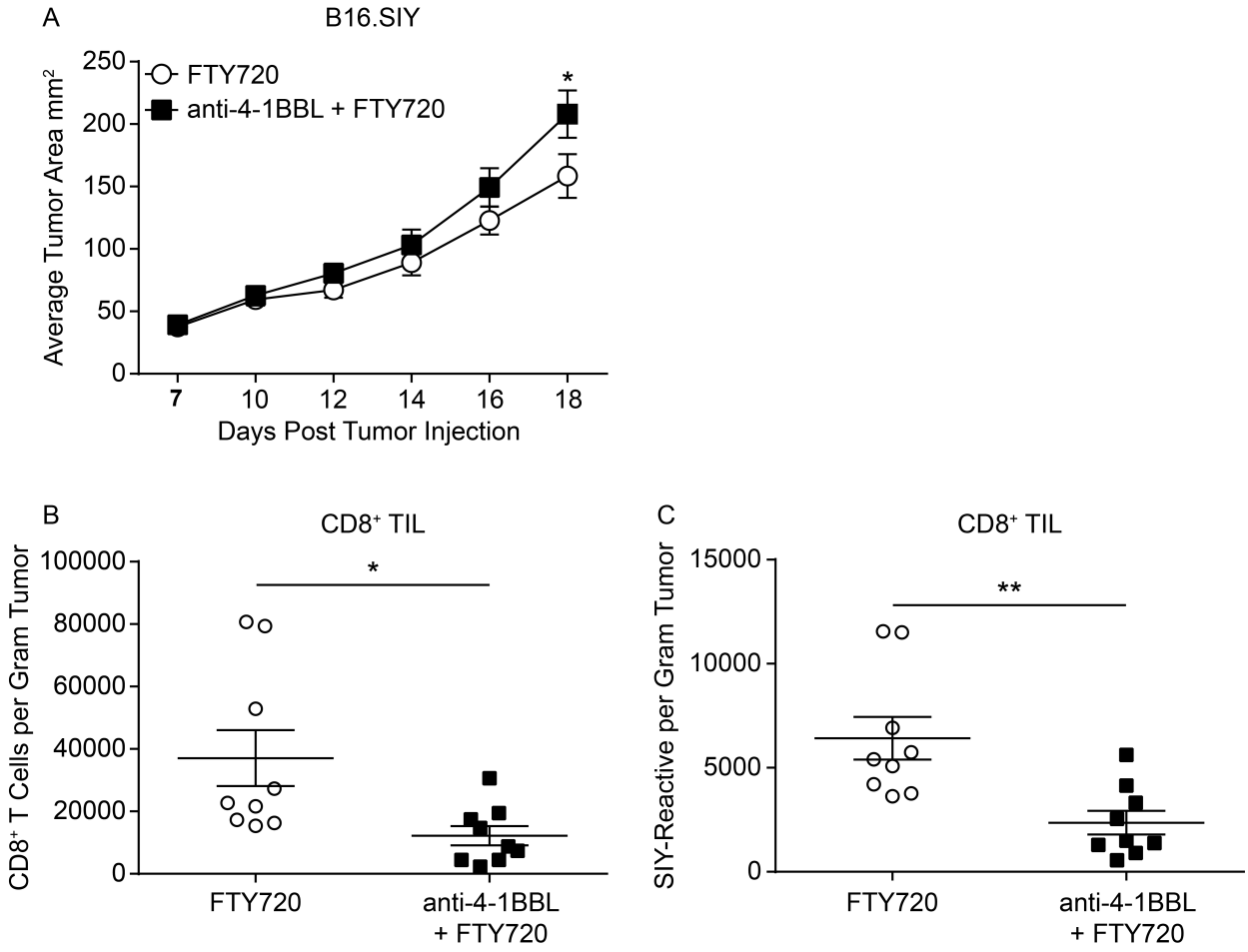

Figure 3.43: 4-1BBL blockade decreases tumor control and decreases CD8$^+$ TIL numbers with concomitant FTY720 administration
C57BL/6 mice were subcutaneously injected with 2x10^6 B16.SIY on day 0. Daily FTY720 administration began seven days post tumor injection. Mice were treated with 200 μg anti-4-1BBL antibody on days 7, 10, 13, and 16 post tumor injection. (A) Outgrowth of B16.SIY tumors in untreated or anti-4-1BBL treated mice. Data is pooled from 2 independent experiments. 2-way ANOVA with a Bonferroni correction was used to calculate statistical significance. (B) Analysis of CD8$^+$ TIL after tumor outgrowth studies were complete. Data is pooled from 2 independent experiments. Statistical significance was computed with Mann-Whitney t test. (C) Analysis enumerating the number of SIY-reactive CD8$^+$ TIL after tumor outgrowth studies were complete. Data is pooled from 2 independent experiments. Statistical significance was computed with Mann-Whitney t test.

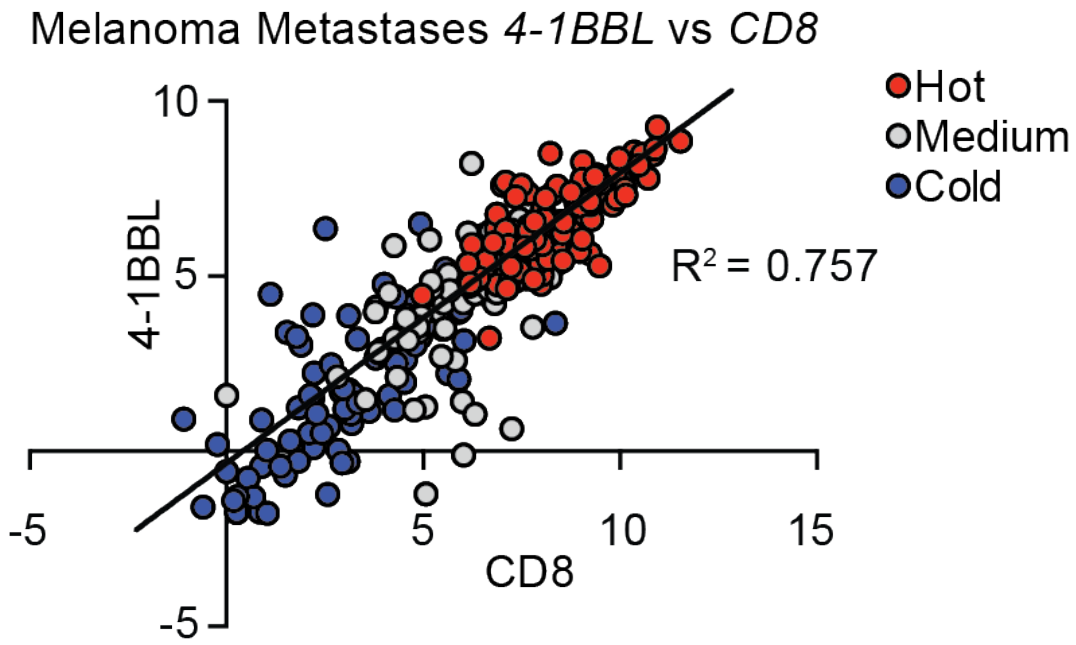

Figure 3.44: *4-1BBL* expression correlates with *CD8A* expression in human melanoma metastases
Transcriptional profiling from human melanoma metastases revealed that expression of *4-1BBL* and *CD8A* were highly correlated with each other.

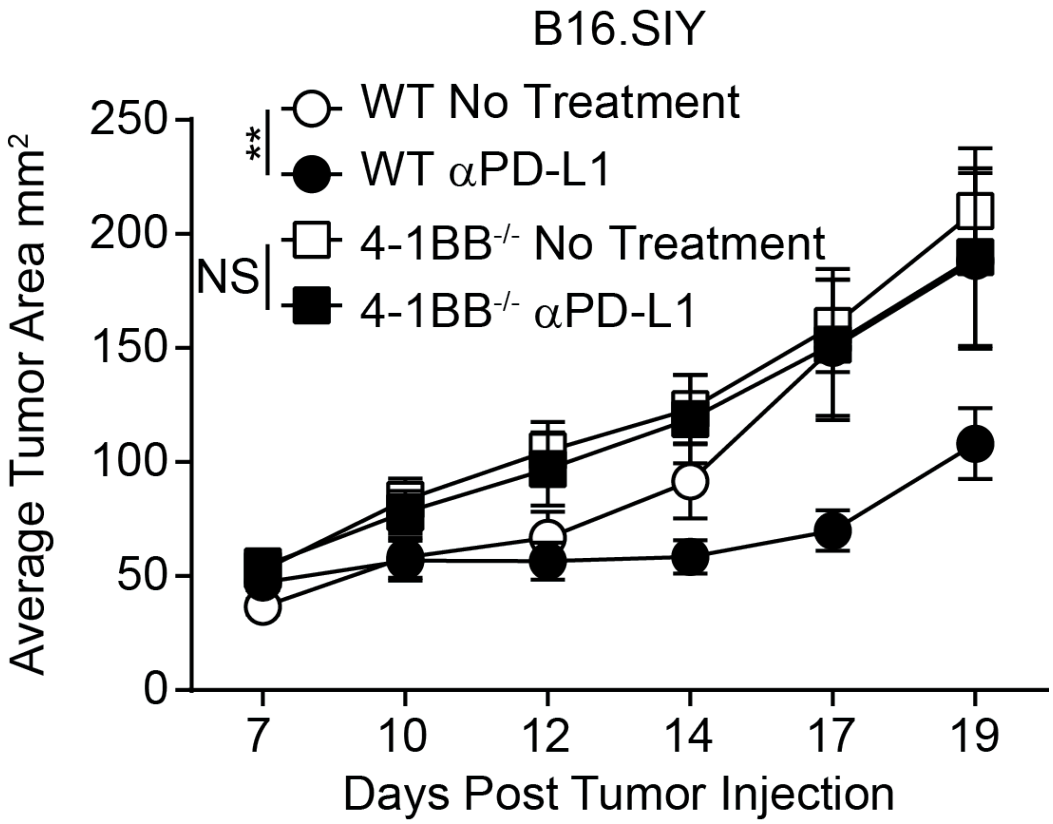

Figure 3.45: 4-1BB is required for a therapeutic response to anti-PD-L1
C57BL/6 or 4-1BB$^{-/-}$ mice were injected subcutaneously with 2x10^6 B16.SIY cells and treated with 100 μg anti-PD-L1 on days 7, 10, 13, and 16 after tumor implantation. WT No Treatment n = 9, WT anti-PD-L1 n = 10, 4-1BB$^{-/-}$ No Treatment n = 10, 4-1BB$^{-/-}$ n = 10. 2-Way ANOVA with a Bonferroni correction was used to compute statistical significance.

splenocytes from either WT or 4-1BB$^{-/-}$ mice to RAG2$^{-/-}$ mice and allowed for 6 weeks of rest. We then challenged the reconstituted RAG2$^{-/-}$ mice with subcutaneous B16.SIY and compared the outgrowth between untreated or anti-PD-L1 treated animals. Similar to the results in WT and 4-1BB$^{-/-}$ mice, RAG2$^{-/-}$ mice reconstituted with WT splenocytes had significantly enhanced tumor control in response to anti-PD-L1, but RAG2$^{-/-}$ mice receiving 4-1BB$^{-/-}$ splenocytes had a severely blunted effect of anti-PD-L1 (Figure 3.46). This result indicated that deficiency of 4-1BB on lymphocytes, and likely CD8^{+} T cells, explained the lack of therapeutic response of 4-1BB$^{-/-}$ animals to anti-PD-L1 antibodies.

3.20 CD103^{+} DCs express the most 4-1BBL in the tumor microenvironment

Because 4-1BB signaling on T cells appeared to be necessary for maintaining maximum numbers of CD8^{+} TIL and for efficacy of anti-PD-L1 immunotherapy, we wondered what the source was of 4-1BBL in the tumor microenvironment. As 4-1BBL is reported to be mostly expressed on antigen-presenting cells, we profiled different MHCII^{+} cell populations in the tumor microenvironment. Interestingly, the CD11c^{+}CD103^{+} cell population expressed the highest levels of 4-1BBL (Figure 3.47A, 3.47B, and 3.47C). This population of DCs is the most critical for priming T cells to generate responses to tumor-associated antigens, and also for recruiting effector T cells to the tumor site (Spranger, 2017). They have also been shown to be positively prognostic in human tumors (Broz, 2014). We therefore wanted to test the effects of deletion of DCs from tumors following the establishment of a T cell infiltrate, and whether agonist 4-1BB antibody could reverse the effects of DC deletion. To this end, we utilized mice that express the simian diphtheria toxin receptor under the control of the CD11c promoter (CD11c-DTR mice). Because long term administration of diphtheria toxin (DT) to these mice is fatal, we generated bone marrow chimeras in which we transplanted CD11c-DTR bone marrow into lethally irradiated CD45.1 congenic mice. After

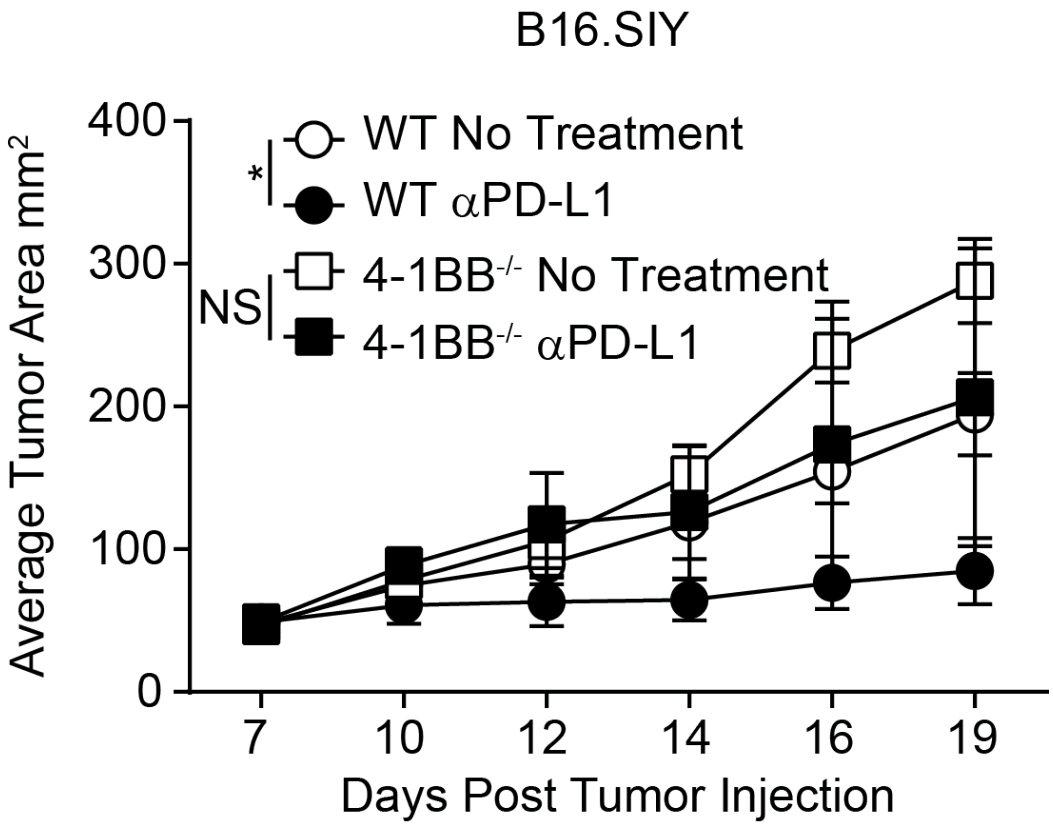

Figure 3.46: 4-1BB is required on lymphocytes for a therapeutic response to anti-PD-L1

RAG2$^{-/-}$ mice received either WT or 4-1BB$^{-/-}$ splenocytes and were allowed to reconstitute for 6 weeks. Mice were then injected subcutaneously with 2x10^6 B16.SIY cells and treated with 100 μg anti-PD-L1 on days 7, 10, 13, and 16 after tumor implantation. WT No Treatment n = 7, WT anti-PD-L1 n = 5, 4-1BB$^{-/-}$ No Treatment n = 8, 4-1BB$^{-/-}$ n = 5. 2-Way ANOVA with a Bonferroni correction was used to compute statistical significance.

reconstitution, chimeric mice were subcutaneously inoculated with B16.SIY cells. Mice were given DT on days 7 and 8, and daily FTY720 oral gavage was begun on day 7 to prevent additional T cell egress from lymph nodes. On day 9 we began immunotherapy of either anti-PD-L1 or anti-4-1BB. Mice that did not receive DT had significantly increased tumor control with either immunotherapy (Figure 3.48A and 3.48B). Intriguingly, mice that did receive DT had no increased tumor control from anti-PD-L1, but did have increased tumor control from anti-4-1BB (Figure 3.48A and 3.48B). These results indicate that DCs are required at the effector phase of anti-tumor T cell response for anti-PD-L1 efficacy, and that agonist anti-4-1BB antibody is sufficient to bypass the need for DCs in the tumor microenvironment.

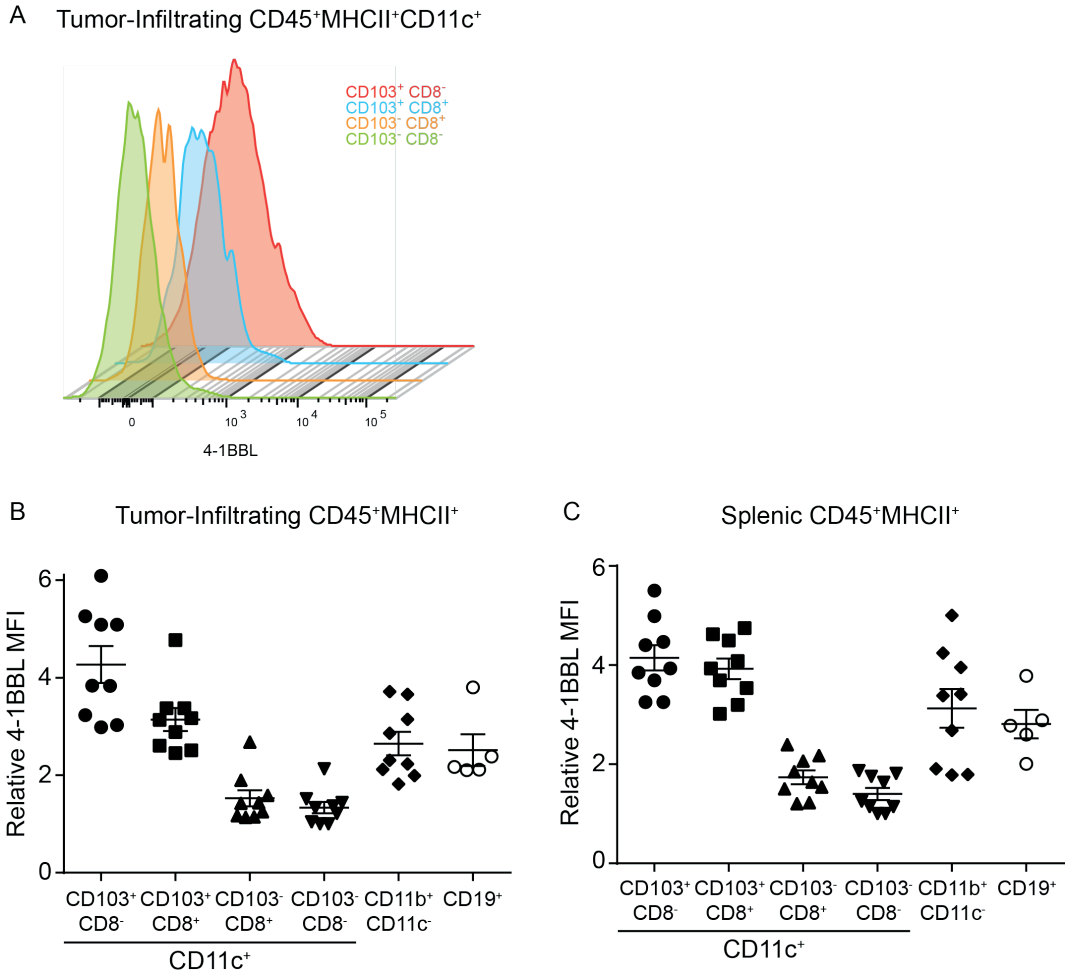

Figure 3.47: Tumor-infiltrating DCs that express CD103 also express the highest level of 4-1BBL

C57BL/6 mice were injected subcutaneously with $2x10^6$ B16.SIY cells. Tumors were allowed to form for 13 days, and then the tumor-infiltrating and splenic antigen presenting cells were analyzed via flow cytometry for 4-1BBL expression. (A) Representative histogram of 4-1BBL expression on $MHCII^+CD11c^+$ tumor infiltrating populations. (B) Quantification of the mean fluorescence intensity (MFI) of staining of a fluorescently labeled anti-4-1BBL antibody of tumor cell populations. (C) Quantification of the MFI of staining of a fluorescently labeled anti-4-1BBL antibody of spleen cell populations.

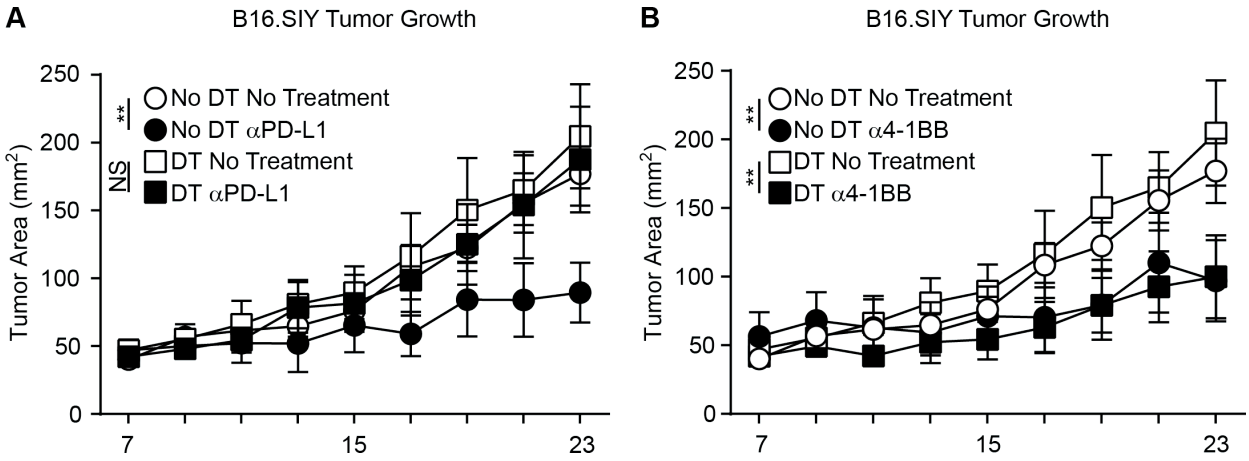

Figure 3.48: DCs are required for the therapeutic efficacy of anti-PD-L1 but not agonist anti-4-1BB antibody.

B6.SJL mice expressing the CD45.1 allele were lethally irradiated and reconstituted with CD11c-DTR bone marrow expressing the CD45.2 allele. After reconstitution, mice were injected subcutaneously with $2x10^6$ B16.SIY cells. Seven days post tumor injection, mice were treated with 500 ng DT. DT was administered on day 7, day 8, and then every other day for the duration of the experiment. FTY720 administration also began on day 7 and was given daily for the duration of the experiment. Antibodies were administered on days 9, 12, 15, and 18 post tumor injection. (A) The response to anti-PD-L1. (B) The response to anti-4-1BB. The No Treatment curves are the same between (A) and (B). No DT No Treatment n = 4, No DT anti-PD-L1 n = 4, No DT anti-4-1BB n = 4, DT No Treatment n = 5, DT anti-PD-L1 n = 5 DT anti-4-1BB n = 5.

CHAPTER 4

DISCUSSION

4.1 Overview

The results in this thesis increase our understanding of $CD8^+$ TIL dysfunction and why antigen-specific TIL are unable to reject progressing tumors. These results also provide new insight into how agonist 4-1BB antibodies reverse features of TIL dysfunction to mediate tumor regression. We found that TIL proliferate in the tumor microenvironment under steady state conditions, but do not accumulate as tumors progress. Proliferating TIL also underwent apoptosis, preventing TIL accumulation despite proliferation. Inhibiting TIL apoptosis increased TIL numbers and the efficacy of adoptive T cell transfer. Agonist 4-1BB antibodies directly engaged 4-1BB on $CD8^+$ TIL, which led to antigen-specific TIL accumulation. This accumulation was due to decreased TIL apoptosis and not increased TIL proliferation. TIL apoptosis therefore inhibits the anti-tumor T cell response, and reducing TIL cell apoptosis is an important mechanism of agonist 4-1BB immunotherapy (Figure 4.1). Our results indicate that $CD8^+$ TIL apoptosis contributes to the inability of TIL to reject the tumors , and could be an under-recognized feature of TIL dysfunction.

Additional experiments led to the discovery that TIL in the steady state receive signals through 4-1BB that help to maintain TIL numbers. Antibody blockade of 4-1BBL or genetic deletion of 4-1BB led to decreased TIL numbers and decreased tumor control, and mice that lacked 4-1BB had no therapeutic efficacy of anti-PD-L1. Interestingly, $CD103^+$ DCs in the tumor expressed the most 4-1BBL. Deletion of DCs after T cell priming and infiltration into the tumor microenvironment blunted the efficacy of an anti-PD-L1 antibody, but not an agonist anti-4-1BB antibody (Figure 4.2). These results indicated that DCs provide T cells with co-stimulatory signals in the tumor microenvironment, including 4-1BBL, that are critical for $CD8^+$ TIL during the anti-tumor immune response and necessary for the therapeutic response to anti-PD-L1.

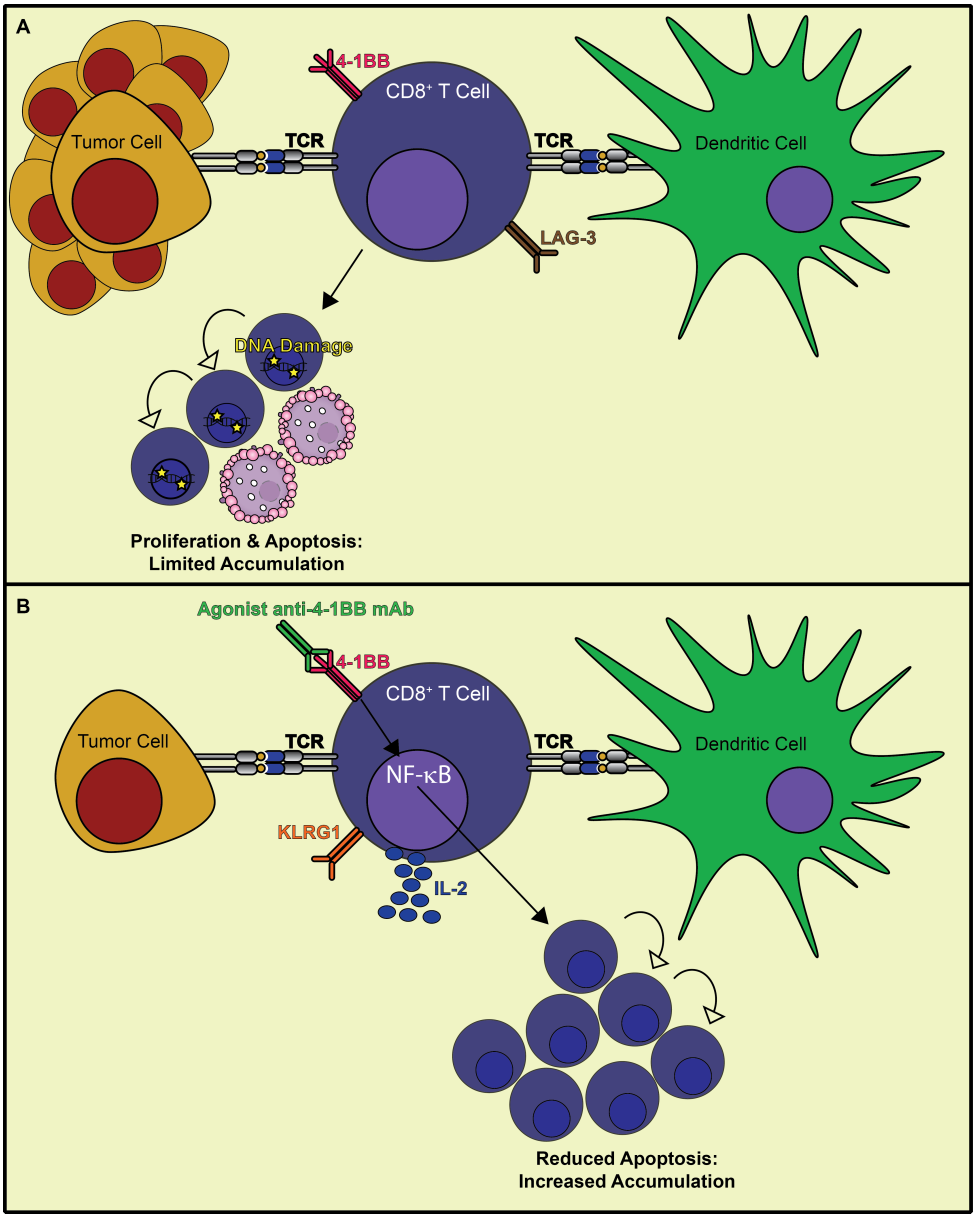

Figure 4.1: Agonist anti-4-1BB leads to CD8$^+$ TIL accumulation through decreased apoptosis

(A) In progressing tumors, CD8$^+$ TIL acquire the LAG-3$^+$4-1BB$^+$ phenotype, likely due to chronic exposure to tumor-derived antigens. It is possible that antigen presentation from both tumor cells and APCs contributes to this phenotype. CD8$^+$ TIL proliferate, but do not accumulate due to apoptosis. Expression of LAG-3 and 4-1BB correlates with proliferation and apoptosis of TIL, as well as accumulation of DNA double strand breaks as measured by the presence of γH2AX. It is currently unclear if there are causal relationships between proliferation, DNA damage and TIL apoptosis. (B) Agonist anti-4-1BB works in a CD8$^+$ TIL-intrinsic manner. Agonist anti-4-1BB correlates with decreased LAG-3 expression, and increased KLRG-1 and IL-2 expression. Agonist anti-4-1BB leads to the accumulation of CD8$^+$ TIL through decreased TIL apoptosis, resulting in increased tumor control.

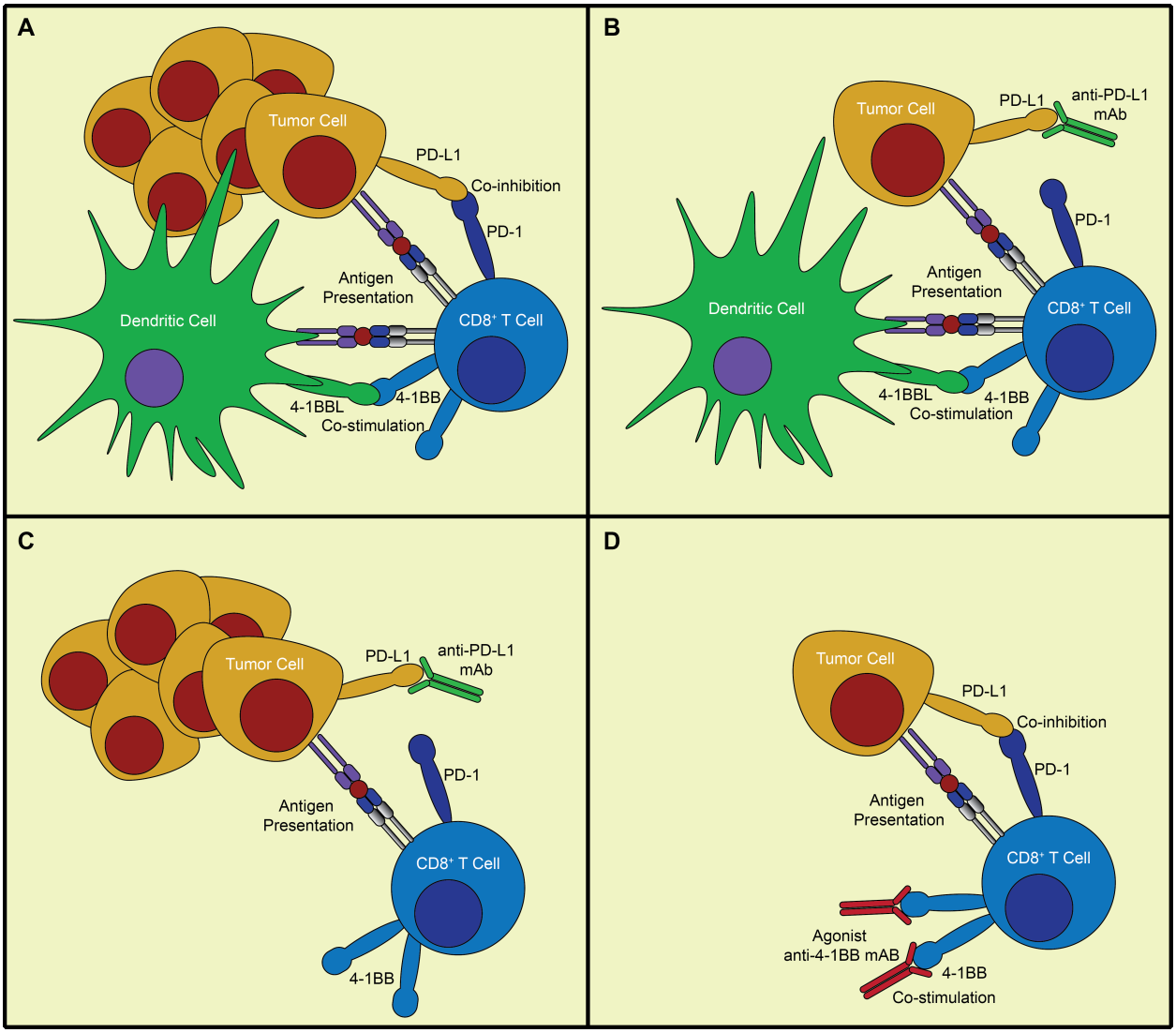

Figure 4.2: Signaling through 4-1BB is required for therapeutic efficacy of anti-PD-L1

(A) In progressing tumors, $CD8^+$ TIL receive co-stimulation through 4-1BBL – 4-1BB interactions. TIL also receive co-inhibitory signals through PD-L1 – PD-1 interactions. (B) Antibody blockade of PD-L1 leads to increased tumor control. (C) In the absence of either 4-1BB or DCs, blockade of PD-L1 yields no therapeutic benefit. Experiments with FTY720 suggest that DCs within the tumor microenvironment are critical during the effector phase of the anti-tumor T cell response for therapeutic efficacy of anti-PD-L1. (D) Provision of agonist anti-4-1BB leads to increased tumor control, even in the absence of DCs. 4-1BB signaling in the tumor microenvironment is therefore sufficient to replace co-stimulation from DCs.

4.2 Cell-intrinsic activation of 4-1BB on tumor-infiltrating CD8$^+$ T cells mediates antigen-specific T cell expansion and tumor regression after agonist 4-1BB antibody administration

4-1BB is a TNFR superfamily member that was identified as a gene that is upregulated after T cell activation (Kwon, 1989). After its discovery, it was realized that 4-1BB functions as a costimulatory molecule that promotes T cell activity (Shuford, 1997), and agonist 4-1BB antibodies were found to promote tumor regression in syngeneic mouse models of cancer (Melero, 1997). While early studies of 4-1BB focused mainly on its expression and role on T cells, many studies since then have suggested a role for 4-1BB in activating multiple immune cell types, including DCs, monocytes, B cells, and natural killer cells (Vinay, 2011). In addition, it has been reported that tumor endothelial cells can express 4-1BB, and that ligation of endothelial cell 4-1BB can mediate increased entry of T cells into tumors (Palazón, 2011). We therefore performed experiments to determine if agonist 4-1BB antibodies could exert effects on CD8$^+$ T cells in a non-cell autonomous manner. First, we used bone marrow chimeric mice where 4-1BB$^{-/-}$ bone marrow was used to reconstitute lethally irradiated WT hosts. These mice would express 4-1BB on all non-hematopoietic compartments, such as endothelial cells, but lack 4-1BB expression on hematopoietic cells. Mice reconstituted with 4-1BB$^{-/-}$ bone marrow had anti-tumor effects of agonist 4-1BB antibody, clearly demonstrating that 4-1BB expression in the hematopoietic compartment was required for anti-tumor efficacy.

Our experiments in 4-1BB$^{-/-}$ and WT mixed bone marrow chimeras revealed that in secondary lymphoid organs, as well as in the tumor itself, agonist 4-1BB antibodies expanded antigen-specific CD8$^+$ T cells in a completely cell-intrinsic fashion. Following agonist antibody administration to tumor bearing mice, there was no expansion of SIY-reactive cells in the 4-1BB$^{-/-}$ CD8$^+$ T cell compartment, compared to the marked expansion of WT SIY-reactive cells CD8$^+$ T cells. If there were non-cell autonomous effects of 4-1BB signaling in

expanding antigen-specific $CD8^+$ T cells, 4-1BB$^{-/-}$ $CD8^+$ T cells should have at least showed some partial effects of agonist 4-1BB antibodies.

These experiments did not, however, address if 4-1BB signaling on non-T cells was playing a contributory role in tumor regression. Many studies have recently suggested that combination immunotherapy using agonist 4-1BB antibodies combined with antibodies against receptors expressed on tumor cells elicit tumor killing by 4-1BB ligation on NK cells (Kohrt, 2011; Kohrt, 2012; Kohrt, 2014). These studies found that NK cells upregulated 4-1BB upon encountering antibody-bound tumor cells, and agonist 4-1BB antibodies enhanced NK killing of tumor cells via an Fc receptor-dependent mechanism. Our laboratory has demonstrated that B16 melanoma cells upregulate PD-L1 in vivo due to IFN-γ signaling (Spranger, 2013). Therefore it was plausible in our studies that the efficacy of anti-PD-L1 plus agonist 4-1BB antibody immunotherapy was at least partially dependent on NK cells killing tumor cells coated with anti-PD-L1 antibody. However, our experiments in RAG2$^{-/-}$ mice showed no efficacy of any immunotherapy, and depletion of NK cells resulted in no defect in tumor control compared to control mice during either agonist 4-1BB combination immunotherapy. Therefore, in the context of B16.SIY melanomas, NK cells were dispensable for tumor rejection in response to agonist 4-1BB antibody.

Additional T cell depletion experiments showed a clear role for $CD8^+$ T cells, but not $CD4^+$ T cells, in tumor control after agonist 4-1BB combination immunotherapy. Therefore, our next experiments were to determine if agonist 4-1BB immunotherapy was acting on 4-1BB expressed by $CD8^+$ TIL to mediate tumor regression. Due to the striking expansion of SIY-reactive $CD8^+$ T cells in both secondary lymphoid tissues and the tumor, we sought to determine if the efficacy of agonist 4-1BB combination immunotherapy was acting primarily through increased priming of antigen-specific $CD8^+$ T cells, or at the effector phase of the $CD8^+$ T cell response. To uncouple the effects on $CD8^+$ T cell priming and the $CD8^+$ T cell effector phase, we used the S1P1 agonist FTY720 to prevent T cell egress from lymphoid tissues during immunotherapy administration. With this approach, we found

no defect in tumor control after agonist 4-1BB combination immunotherapy, indicating that agonist 4-1BB antibody therapy primarily targeted 4-1BB expressed on $CD8^+$ T cells already residing in the tumor microenvironment. In our model systems, therefore, it appears that agonist activation of 4-1BB expressed on $CD8^+$ TIL directly revitalizes their functionality and phenotype to lead to increased tumor control. These results imply that increased co-stimulation in the tumor microenvironment could be sufficient to enhance T cell functionality and overcome the immune suppressive environment established by tumor cells and other regulatory immune cells. This interpretation is consistent with data demonstrating that forced expression of 4-1BBL on tumor cells is sufficient to lead to enhanced tumor control in vivo (Mogi, 2000).

4.3 4-1BB signaling in the tumor microenvironment is required for the accumulation of $CD8^+$ TIL

Another interesting observation from the 4-$1BB^{-/-}$ and WT mixed bone marrow chimeras was the dichotomy between the ratio of SIY-reactive 4-$1BB^{-/-}$:WT $CD8^+$ T cells in the spleen and tumor. The enhanced reconstitution of 4-$1BB^{-/-}$ $CD8^+$ T cells suggests that there may be a role for 4-1BB in regulating the development of some type of hematopoietic precursor cell, or that T cells that lack 4-1BB are more proliferative than 4-1BB-expressing T cells at early stages. Both may be true, as the interaction between 4-1BBL and 4-1BB on myeloid precursors appears to limit myelopoiesis and the differentiation of DCs (Lee, 2008). Additionally, 4-$1BB^{-/-}$ T cells have been shown to be hyper proliferative after anti-CD3 or mitogen activation (Kwon, 2002), potentially explaining the skewing in the periphery seen in mixed bone marrow chimeras. Despite the enhanced reconstitution of 4-$1BB^{-/-}$ $CD8^+$ T cells in spleens and lymph nodes, the ratio of 4-$1BB^{-/-}$: WT dropped significantly within the tumor, indicating that $CD8^+$ T cells are advantaged by 4-1BB expression once in the tumor microenvironment. Additionally, even though 4-$1BB^{-/-}$ and WT $CD8^+$ T cells were able to

generate the same percentage of SIY-reactive cells in lymph nodes and spleens, the percentage of 4-1BB$^{-/-}$ CD8^{+} TIL that were SIY-reactive again fell significantly below the percentage of WT CD8^{+} TIL, leading to numerically more WT SIY-reactive CD8^{+} TIL than 4-1BB$^{-/-}$ CD8^{+} TIL. These results suggest a critical role for 4-1BB signaling on CD8^{+} TIL during the endogenous anti-tumor immune response independent of agonist 4-1BB immunotherapy, and that co-stimulation through 4-1BB within the tumor microenvironment is a critical factor required for CD8^{+} TIL persistence.

Interestingly, as measured seven days post tumor implantation, 4-1BB$^{-/-}$ mice formed an initial immune response against B16.SIY that was similar to WT mice. However, by 14 days after tumor injection, WT mice had significantly higher numbers of CD8^{+} TIL and SIY-reactive CD8^{+} TIL than 4-1BB$^{-/-}$ mice, even though the numbers of SIY-reactive cells in the spleen were similar. This indicated that while 4-1BB$^{-/-}$ mice initially generate similar number of CD8^{+} TIL at earlier time points, 4-1BB signaling may be involved in maintaining CD8^{+} TIL over long periods of time in the tumor microenvironment. This mechanism potentially explains the poor survival or persistence of 4-1BB$^{-/-}$ CD8^{+} TIL.

To better determine if the lack of ability of 4-1BB$^{-/-}$ CD8^{+} TIL to persist in the tumor microenvironment was due to lack of active 4-1BBL signaling, we utilized a blocking antibody against 4-1BBL that would interrupt signals from 4-1BBL to 4-1BB. Blockade of 4-1BBL after initial priming of T cells resulted in faster tumor growth and diminished numbers of CD8^{+} TIL and SIY-reactive CD8^{+} TIL, suggesting that actively blocking 4-1BB signaling during the effector phase of the CD8^{+} T cell response prevented the accumulation of CD8^{+} TIL. Additionally, these results were confirmed while administering 4-1BBL blocking antibody concomitantly with FTY720 treatment, demonstrating that blockade of 4-1BBL 4-1BB interactions in the tumor microenvironment leads to reduced CD8^{+} TIL. 4-1BB signaling is therefore required to maintain maximal numbers of CD8^{+} TIL. This result highlights the importance of co-stimulation during the effector phase of the anti-tumor T cell response, after the initial priming of T cells in the tumor-draining lymph node. Co-

stimulation during the effector phase has not been well studied, and further investigation of this process is warranted. It was encouraging to find that in human melanoma samples, *4-1BBL* transcript levels correlated with *CD8A* transcript levels, suggesting that 4-1BBL–4-1BB interactions could be important for human $CD8^+$ TIL as well.

4.4 4-1BB expression on T cells is required for therapeutic efficacy of anti-PD-L1 immunotherapy

Factors that influence the response to checkpoint blockade immunotherapies such as blockade of the PD-1/PD-L1 pathway are largely unknown. It has been demonstrated in patients that a preexisting immune response with infiltration of $CD8^+$ T cells into the tumor or tumor margin correlates with responsiveness to anti-PD-1 therapy (Tumeh, 2014). Additionally, recent studies have suggested that the anti-tumor efficacy of PD-L1 blockade requires CD28 signaling, implying that co-stimulation is critical for the success of immunotherapy (Hui, 2017; Kamphorst, 2017). Based on our identified role of 4-1BB at the effector phase of the anti-tumor T cell response, we examined whether endogenous 4-1BB was necessary for tumor regression after anti-PD-L1 immunotherapy. We were intrigued to find that tumors in $4\text{-}1BB^{-/-}$ mice were unresponsive to PD-L1 blockade, similar to what was seen with concomitant blockade of CD28 and PD-L1 (Kamphorst, 2017). This appeared to be a T cell-intrinsic effect of 4-1BB, as $RAG2^{-/-}$ mice reconstituted with $4\text{-}1BB^{-/-}$ splenocytes also had a severely blunted response to PD-L1 blockade compared to $RAG2^{-/-}$ mice reconstituted with WT splenocytes. These results suggest that lack of co-stimulation in general, and not just CD28, could affect the efficacy of PD-L1 blockade in mediating tumor regression. Further studies testing how additional co-stimulatory pathways affect the response to PD-L1 blockade would clarify if co-stimulation is generally required for an anti-tumor response to immunotherapy. Additionally, biopsies of human tumors should be profiled to determine if expression of co-stimulatory ligands or receptors correlate with a response to blockade of

PD-1 or PD-L1. Differences in co-stimulation could explain why some patients with infiltrating T cells in their tumors respond to checkpoint blockade while others do not, despite T cell infiltration.

Because we found ample evidence that 4-1BB signaling was actively happening in the tumor microenvironment, we searched for the source of 4-1BBL that would mediate this co-stimulation. Profiling of different antigen-presenting cell populations in B16.SIY-bearing mice revealed that $CD103^+$ DCs expressed the highest levels of 4-1BBL, both in the tumor and spleen. This was an interesting result as $CD103^+$ DCs have been shown to be required for priming of tumor antigen-specific $CD8^+$ T cells, as well as mediating their recruitment to the tumor microenvironment through the expression of CXCL9 and CXCL10 (Spranger, 2015; Spranger, 2017). These DCs are also thought to be important for tumor regression after adoptive transfer of activated, antigen-specific $CD8^+$ T cells (Spranger, 2017), and correlated with improved survival in patients (Broz, 2014).

In order to test more directly the importance of DCs and 4-1BB co-stimulation in the setting of anti-PD-L1 immunotherapy, so we generated chimeric mice reconstituted with C11c-DTR bone marrow. We found that CD11c-expressing cells were required for increased tumor control after anti-PD-L1 immunotherapy. This result was interesting. It has recently been found that CD28 is required for anti-PD-L1 immunotherapy efficacy (Kamphorst, 2017), however, the anatomic location and cell types that might be responsible for providing CD28 signals to T cells at the necessary times for anti-PD-L1 efficacy were not known. Our data suggest that not just CD28, but potentially a broad range of co-stimulatory molecules, could be important for the efficacy of anti-PD-L1 immunotherapy. It is therefore possible that CD28 and other co-stimulatory signals expressed by DCs in the tumor microenvironment could be necessary for the efficacy of anti-PD-L1 immunotherapy.

4.5 4-1BB combination immunotherapy leads to immunologic memory that is dependent on CD4$^+$ T cells during the initial tumor rejection

That a number of mice completely rejected their B16.SIY tumors allowed us to study the effects of 4-1BB combination immunotherapy on the formation of memory against tumor antigens. We found that almost all (10/11) mice that completely rejected their tumors after either anti-4-1BB + anti-CTLA-4 or anti-4-1BB + anti-PD-L1 were protected from a secondary tumor challenge 8-plus weeks after the primary challenge. This corresponded with the presence of antigen-specific cells as measured by an IFN-γ ELISPOT performed on splenocytes after one or two challenges with B16.SIY.

Interestingly, depletion of CD4$^+$ T cells during the initial tumor regression mediated by combination immunotherapy led to a lack of protection against a second challenge with B16.SIY. CD4$^+$ T cells have been implicated in multiple ways in helping to generate and maintain a functional CD8$^+$ memory response (Laidlaw, 2016). However, other studies have shown that the administration of agonist 4-1BB antibodies lead to formation of memory that is not dependent on CD4$^+$ T cells (Willoughby, 2014). Our results indicate that in the tumor context, formation of immunological memory requires CD4$^+$ T cells to be present during the initial tumor rejection, even though they are not necessary for rejection itself. Our experiments did not clarify if a lack of CD8$^+$ or CD4$^+$ memory cells was the reason for failure to control a secondary challenge with B16.SIY. It could be the case that CD8$^+$ T cells in the tumor setting require CD4$^+$ T cells for either memory formation or the maintenance of memory CD8$^+$ T cells. It could also be that in this setting, CD8$^+$ memory T cells form independently of CD4$^+$ T cells, but CD4$^+$ T cells also form memory against tumor antigens, and that control of a second tumor requires both CD8$^+$ and CD4$^+$ memory T cells. Future experiments could clarify whether tumor antigen-specific memory CD8$^+$ T cells are generated and maintained after 4-1BB agonist antibody administration in a CD4-independent manner,

as has been found in vaccination studies (Laidlaw, 2016).

4.6 Proliferation and apoptosis of CD8$^+$ T cells in different anatomic locations

During our investigations we found that 4-1BB combination immunotherapy increased the number of SIY-reactive CD8$^+$ T cells in multiple anatomic locations, including the tumor-draining lymph node, spleen, and tumor. We wanted to assess what the mechanism of expansion was in these various organ sites, and began by investigating the rates of proliferation of CD8$^+$ T cells. BrdU incorporation measures cells that are actively replicating their DNA at the time of administration, and so provides a quantification of cells that are actively dividing. After agonist 4-1BB combination immunothearpy, we found large increases in the BrdU incorporation of CD8$^+$ T cells in the tumor-draining lymph nodes and spleens of mice, but not within the tumor, which was interesting as it suggested that the effects of immunotherapy could be different in different anatomic locations. Likely this is related to the differentiation state of CD8$^+$ T cells, as well as the levels of antigen in different anatomic sites. It is well documented that CD8$^+$ T cells residing within tumors assume unique phenotypic and functional characteristics, usually termed exhaustion or dysfunction (Crespo 2013). CD8$^+$ TIL were proliferating at much higher rates in the absence of immunotherapy than in the lymph nodes or spleens of tumor-bearing mice. Phenotypic analysis of proliferating cells was consistent with this notion, as we found that CD8$^+$ TIL that expressed LAG-3 as well as PD-1 were more proliferative than TIL that expressed PD-1 but not LAG-3, or TIL that expressed neither inhibitory receptor. Data from our laboratory has shown that these LAG-3$^+$ cells are likely tumor antigen-specific cells (Williams, 2017). It is therefore feasible that their proliferation is due to stimulation with their cognate antigens. However, other work has shown that T cell proliferation in the tumor microenvironment may depend on cytokines like IL-15 (Boldajipour, 2016). Regardless, proliferation of CD8$^+$ T cells in the

tumor microenvironment was not augmented by agonist 4-1BB combination immunotherapy.

Despite the consistent proliferation of $CD8^+$ TIL over several time points during the endogenous immune response, there was no significant accumulation of $CD8^+$ TIL over time, indicating that some process was counterbalancing the observed proliferation. Additionally, we knew from our FTY720 experiments that SIY-reactive $CD8^+$ TIL accumulation was not dependent on trafficking of $CD8^+$ T cells from lymphoid tissues into the tumor. Therefore, we investigated apoptosis of $CD8^+$ TIL as a potential counterbalance to proliferation that would result in the lack of accumulation we observed over time. Indeed, we found that $CD8^+$ TIL were undergoing apoptosis in steady state conditions, and that this apoptosis was specific to the tumor microenvironment. Like proliferation, apoptosis measured by active caspase-3 staining correlated with the phenotype of the $CD8^+$ TIL, with LAG-3- and 4-1BB-expressing $CD8^+$ TIL having the highest active caspase-3 staining. This could be similar to what has been observed in viral infection models, where T cell exhaustion during chronic viral infection has been associated with increased apoptosis of $CD8^+$ T cells (Blackburn, 2008). This observation indicated that cells in the proliferative T cell fraction may also be undergoing apoptosis. Co-staining of Ki-67 and active caspase-3 confirmed that a subset of the proliferating cells were indeed apoptotic. Thus $CD8^+$ TIL apoptosis is reminiscent of activation-induced cell death, in which activated cells both proliferate and die as a mechanism to cull overall T cell numbers (Green, 2003). The cause of this apoptosis has yet to be understood. It appears to be specific to the tumor microenvironment in our model, but not simply caused by residence within the tumor: $CD8^+$ TIL that did not express PD-1 did not proliferate or undergo apoptosis in situ, suggesting that these processes were not simply a product of residing within the tumor microenvironment.

Apoptosis of $CD8^+$ TIL appeared to be a functional barrier to anti-tumor immunity, as overexpression of Bcl-x_L decreased $CD8^+$ TIL apoptosis and led to an increased accumulation of $CD8^+$ TIL. This translated to increased tumor control on a per cell basis, as determined by the transfer of 2C cells that overexpressed Bcl-x_L into tumor-bearing mice.

The increased tumor control in this setting demonstrated that decrease of T cell apoptosis alone was sufficient for increased functionality of $CD8^+$ T cells. Therefore, apoptosis is at least in part responsible for what is known as dysfunction of $CD8^+$ T cells in the tumor microenvironment. Consistent with this, spontaneously rejected tumors showed contained an increased accumulation of SIY-reactive $CD8^+$ TIL with decreased apoptosis.

4.7 Agonist 4-1BB antibody decreases $CD8^+$ TIL apoptosis

Our findings that 4-1BB expression maintains $CD8^+$ TIL numbers, that agonist anti-4-1BB increases antigen-specific $CD8^+$ TIL numbers independent of T cell influx or increased proliferation in the tumor, in addition to our findings of decreased T cell apoptosis leading to increased anti-tumor immunity, led us to question if agonist 4-1BB antibody was countering $CD8^+$ TIL apoptosis. Indeed, we found that after administration of agonist 4-1BB combination immunotherapy, there was a decrease in the active caspase-3^+ fraction of $CD8^+$ TIL and especially SIY-reactive $CD8^+$ TIL. Single treatment studies revealed that most of the SIY-reactive TIL accumulation and anti-apoptotic effects were driven by the agonist 4-1BB antibody, with some apparent but not statistically significant contribution from anti-PD-L1 antibodies. This is in line with other findings of 4-1BB being a survival factor for $CD8^+$ T cells (Takahashi, 1999; Cooper, 2002; Weigelin, 2015), and with our own findings with 4-$1BB^{-/-}$ mice demonstrating that 4-1BB expression was required for maintaining the numbers of $CD8^+$ TIL. Co-stimulation through 4-1BB therefore appears to be a potent survival factor for $CD8^+$ TIL that is necessary for their maintenance and that can be manipulated through immunotherapy to improve $CD8^+$ TIL cell numbers and functionality. This is consistent with CAR T cell studies, where inclusion of an intracellular 4-1BB signaling domain enhances the persistence and efficacy of transferred engineered T cells (Long, 2015).

4.8 Increased NF-κB signaling in CD8$^+$ TIL resembles the phenotypic changes associated with agonist 4-1BB antibody administration

Phenotyping of CD8$^+$ TIL after immunotherapy revealed a decrease in the surface levels of multiple immune inhibitory receptors. Single treatment experiments revealed that these decreases were driven mostly by agonist anti-4-1BB. This observation indicates a unique ability of 4-1BB signaling to decrease the amount of inhibitory signals that CD8$^+$ TIL receive. Decreased inhibitory receptor expression was not seen with blockade of CTLA-4 or PD-L1, indicating that agonist anti-4-1BB altered CD8$^+$ TIL gene expression in different ways than removal of inhibitory signals alone.

Gene expression profiling revealed that agonist 4-1BB monotherapy resulted in very similar gene expression profiles to either combination therapy that involved agonist 4-1BB antibody. This suggested that agonist 4-1BB was driving most of these changes, similar to the inhibitory receptor downregulation. Using Ingenuity Pathway Analysis, we found that among the upregulated genes there were major hubs around IL-2 and NF-κB signaling. These were intriguing results, as multiple papers from our laboratory and others have implicated these pathways in both the spontaneous and post-immunotherapy immune response against tumors (Spranger, 2014; Williams, 2017; Barnes, 2015; Evaristo, 2016).

The IL-2 pathway was especially interesting. We previously found restored IL-2 production in CD8$^+$ TIL after combination immunotherapy (Spranger, 2014; Williams, 2017). We also found increased IL-2 transcript levels after 4-1BB combination immunotherapy, and found that CD25, the high affinity IL-2 receptor subunit, was expressed on CD8$^+$ TIL in the absence of immunotherapy. This result raised the possibility of a positive feedback loop where 4-1BB signaling drove IL-2 expression that bound to CD25 to stimulate CD8$^+$ TIL in an autocrine fashion. However, neither systemic nor intratumoral administration of multiple IL-2 neutralizing antibodies decreased the efficacy of anti-4-1BB + anti-PD-L1 immunother-

apy. Mixed bone marrow chimeras yielded consistent results. $CD25^{-/-}$ $CD8^{+}$ TIL had a lower percentage of SIY-reactive cells and lower KLRG1 expression without immunotherapy, indicating fewer and less effector-like tumor antigen-specific cells from this compartment. Despite these defects in spontaneous anti-tumor immunity, however, the expansion of SIY-reactive cells and the upregulation of KLRG1 was preserved in the $CD25^{-/-}$ $CD8^{+}$ TIL after agonist 4-1BB combination immunotherapy. Thus, while IL-2 signaling through CD25 may play a role in the spontaneous anti-tumor T cell response, an IL-2 – CD25 autocrine loop is not necessary for the response to agonist 4-1BB combination immunotherapy. IL-2 expression may still be a useful biomarker to indicate a productive anti-tumor response after immunotherapy. IL-2 expression could be studied in patients after immunotherapy to determine if IL-2 production correlates with the increase in $CD8^{+}$ TIL or tumor regression.

Experiments using IKKβ-CA mice revealed that activation of the NF-κB pathway in T cells resulted in a striking resemblance to agonist anti-4-1BB immunotherapy. Increased NF-κB signaling resulted in a larger fraction of SIY-reactive $CD8^{+}$ TIL, increased KLRG1 expression, and decreased LAG-3 expression. Additionally, it resulted in decreased active caspase-3 expression in $CD8^{+}$ TIL. It was previously shown that NF-κB activation in T cells was necessary and sufficient for tumor control (Barnes, 2015; Evaristo, 2016). Our data suggest that a part of the increased tumor control in the IKKβ-CA mice may be due to the increased survival of TIL. It also appears that in the IKKβ-CA mice, the $CD8^{+}$ TIL do not assume the dysfunctional phenotype, as they retain KLRG1 expression and do not upregulate LAG-3. Also interesting is the increased γH2AX in $CD8^{+}$ TIL from IKKβ-CA mice. This suggests that γH2AX is in fact upstream of T cell apoptosis, and that increased NF-κB signaling allows T cells to survive despite the presence of DNA damage. Supporting this idea is a previous study showing that NF-κB can protect T cells from DNA damage-induced cell death through activation of Mdm2 (Busuttil, 2010).

4.9 Future Directions

4.9.1 Determining the cause of CD8$^+$ TIL cell apoptosis

One important finding of this work was that endogenously primed, antigen-specific CD8$^+$ T cells are undergoing apoptosis in the tumor microenvironment. Importantly, blocking T cell apoptosis led to accumulation of TIL and improved tumor control. While the cause of TIL apoptosis is unknown, it appeared to be a product of T cell activation combined with residence in the tumor microenvironment. Determining the cause of spontaneous apoptosis of activated CD8$^+$ T cells in the tumor microenvironment will lead to a better understanding of factors that limit anti-tumor T cell responses. This may lead to specific therapies able to target causes of T cell apoptosis that could enhance the immune response against cancer. These therapies could potentially augment the endogenous immune response and synergize with checkpoint blockade, leading to enhanced responses to current immunotherapies. Future studies to determine the mechanism of CD8$^+$ TIL death could focus on the following processes:

Metabolism

Engagement of the TCR combined with co-stimulation greatly alter metabolism as T cells transition from nave to activated effector cells (Buck 2015). Effector T cells become highly glycolytic as they activate the mTOR pathway and upregulate glucose transporters (Buck, 2015). Proper activation of metabolic pathways as well as sufficient nutrient levels have been shown to be critical to achieve maximal T cell responses (Cham, 2005). Metabolic competition between tumor cells and T cells in the tumor microenvironment can limit the nutrients available to T cells and contribute to lack of T cell function that facilitates tumor progression (Chang, 2015; Ho, 2015). One consequence of metabolite deficiency can be increased T cell death, with evidence demonstrating that multiple metabolic pathways can have an effect on T cell apoptosis (Fallarino, 2002; Lee, 2014; Blagih, 2015; Geiger,

2016). Interestingly, both T cell and tumor metabolism can be targeted by immunotherapy, resulting in more favorable metabolic function in T cells (Chang, 2016). This suggests that $CD8^+$ TIL could be undergoing apoptosis in the tumor microenvironment because they lack the nutrients to properly respond to the antigenic stimuli they are receiving. We found up-regulation of glucose transporter transcripts by gene array and qPCR after agonist 4-1BB combination immunotherapy, suggesting that changes in TIL apoptosis could be linked to improved metabolic substrate uptake. This would be consistent with findings studying CAR T cells, where the inclusion of a 4-1BB signaling domain leads to increased persistence and a distinct metabolic signature (Kawalekar, 2016). Thus, changes in metabolism might explain the rescue from apoptosis induced by agonist anti-4-1BB combination immunotherapy.

DNA damage

Activated T cells have recently been shown to accumulate high levels of DNA damage, likely from their rapid proliferation (McNally, 2017). In our studies we found a high basal rate of proliferation specifically in the $CD8^+$ TIL compartment. The proliferating $CD8^+$ TIL also contained an apoptotic fraction, indicating that some of the proliferating cells were in fact undergoing apoptosis. In contrast, PD-1^- $CD8^+$ TIL did not proliferate, nor did they undergo apoptosis. Additionally, we found an accumulation of double-stranded DNA breaks, as measured by γH2AX staining, in proliferating $CD8^+$ TIL. This damage was specific to the proliferating TIL, and not proliferating $CD8^+$ cells in the spleens and lymph nodes of mice. Cellular stress, ROS, or other factors in the tumor microenvironment could potentially lead to this increased DNA damage.

One group recently showed that inhibition of Mdm2 in activated, proliferating T cells could lead to their selective depletion, which did not affect non-proliferating T cells (McNally, 2017). Interestingly, we found through gene array analysis that agonist 4-1BB immunotherapy upregulated Mdm2 transcript levels. Therefore agonist 4-1BB immunotherapy might be working to increase $CD8^+$ TIL accumulation by preventing the sensing of DNA damage that

would normally lead to $CD8^+$ TIL apoptosis.

Other studies have also found that the p53 pathway regulates immune responses. Activation of $CD4^+$ T cells leads to Mdm2 upregulation and p53 inhibition (Watanabe, 2014). Preventing p53 inhibition led to an inability of activated $CD4^+$ T cells to proliferate in response to TCR stimulus. Another study found that NF-κB signaling downstream of TCR signaling can lead to increased Mdm2 expression that inhibits cell death of activated T cells (Busuttil, 2010). Using pathway analysis of genes upregulated by immunotherapy, we found that agonist anti-4-1BB immunotherapy was potentially acting through the NF-κB pathway. This opens the possibility that 4-1BB induced NF-κB activation leads to Mdm2 upregulation and p53 inhibition, resulting in reduced $CD8^+$ TIL apoptosis.

Additionally, recent work from another group has demonstrated that transferred antigen-specific $p53^{-/-}$ T cells control tumors better than WT cells, indicating that DNA damage sensing might be important for inhibiting T cell responses to tumors (Banerjee, 2016). One proposed mechanism by which p53 induces apoptosis is by interacting with anti-apoptotic Bcl-2 family proteins like Bcl-x_L to inhibit their anti-apoptotic effects (Chipuk, 2006). A p53-dependent mechanism of $CD8^+$ TIL apoptosis is therefore consistent with our data showing that transgenic Bcl-x_L expression is sufficient to decrease $CD8^+$ TIL apoptosis and improve the control of B16.SIY tumors by adoptively transferred 2C T cells. Overall, agonist 4-1BB antibody could be decreasing $CD8^+$ TIL apoptosis through upregulation of the NF-κB pathway, which upregulates Mdm2. Mdm2 then suppresses p53, which decreases the amount of DNA damage-induced cell death that occurs in $CD8^+$ TIL in the tumor microenvironment. Additionally, suppression of p53 may also increase the functionality of T cells, resulting in more $CD8^+$ TIL that are better able to mediate tumor regression.

4.9.2 The role of co-stimulation in the tumor microenvironment

We have found that many co-stimulatory receptors, such as CD27, GITR and OX40 are expressed in addition to 4-1BB on $CD8^+$ TIL (Williams, 2017). These pathways are all

under investigation as potential targets for immunotherapy of cancer, and agonist antibodies against these proteins can lead to tumor regression in preclinical models (van de Ven, 2015; Aspeslagh, 2015; Knee, 2016). That TIL would express these receptors and benefit from their activation raises the question of whether there are corresponding ligands for these receptors present in the tumor microenvironment. It is appreciated that supplementing effector T cells with agonist antibodies that activate co-stimulatory pathways can enhance their function, proliferation, and survival. Less well understood is whether effector T cells utilize co-stimulation during endogenous immune responses, and if so, what the role of co-stimulation in the tumor microenvironment is.

It was recently found that $CD103^+$ DCs benefit many aspects of anti-tumor immunity by mediating the priming and recruitment of antigen-specific T cells to tumors (Spranger, 2015; Spranger, 2017). It was also found that T cells can interact with DCs in the tumor microenvironment, and that the presence of $CD103^+$ DCs positively influences ongoing anti-tumor immunity (Broz, 2014). Of the tumor-infiltrating APCs analyzed, we found that $CD103^+$ DCs had the highest expression of 4-1BBL, suggesting they provide $CD8^+$ TIL with co-stimulatory signals prior to immunotherapy. The effects of infiltrating DCs and other myeloid cells on $CD8^+$ TIL should be examined further, as well as what other co-stimulatory molecules different subsets of tumor-infiltrating APCs express. Our findings that 4-1BB$^{-/-}$ $CD8^+$ TIL accumulated poorly in the tumor compared to their WT counterparts, and that blockade of 4-1BBL decreased the infiltration of $CD8^+$ TIL, suggest that co-stimulation actively supports the maintenance of $CD8^+$ TIL numbers. It would be interesting to determine if other co-stimulatory molecules were also contributing to maintaining the number of $CD8^+$ TIL, and which cell types TIL must interact with to receive various co-stimulatory signals.

Another question is how co-stimulation helps to maintain $CD8^+$ TIL. 4-1BB signaling appears to increase TIL survival, as demonstrated with decreased active caspase-3 levels after agonist 4-1BB immunotherapy, and decreased numbers of $CD8^+$ TIL in 4-1BB$^{-/-}$ mice. It

would be interesting to determine if different co-stimulatory receptors have mostly redundant or unique functions in terms of how they affect $CD8^+$ TIL survival, proliferation, and functionality. Activation of multiple co-stimulatory molecules could be an immunotherapeutic approach to maximize the function of tumor infiltrating T cells.

Additionally, our results demonstrating that CD11c-expressing cells within the tumor site are necessary for the effects of anti-PD-L1 immunotherapy are striking. This implies that co-stimulation in the tumor microenvironment is essential for anti-PD-L1 immunotherapy efficacy, and that DCs likely provide the majority of co-stimulation to T cells within the tumor. Immunotherapy with only agonist anti-4-1BB still retained its efficacy in the absence of DCs, suggesting agonist anti-4-1BB can replace the function of DCs. These results support a model in which DCs provide co-stimulation through 4-1BBL to $CD8^+$ T cells, which can be replaced by agonist anti-4-1BB antibody.

4.9.3 What alterations in T cell function are necessary for tumor rejection after immunotherapy?

It remains unknown what functions of T cells are actually altered to mediate tumor regression after immunotherapy. Our laboratory has recently shown that $CD8^+$ TIL that express multiple inhibitory receptors still retain the ability to proliferate, produce IFN-γ, and lyse target cells ex vivo (Williams, 2017). We found in this thesis that apoptosis may be an important factor in limiting the anti-tumor immune response. We also found that anti-4-1BB immunotherapy correlated with a change in $CD8^+$ TIL phenotype. $CD8^+$ TIL expressed lower levels of inhibitory receptors and higher levels of KLRG1 after agonist anti-4-1BB immunotherapy. Additionally, $CD8^+$ TIL increased their ability to produce IL-2, but IL-2 signaling was not found to be necessary for tumor regression after immunotherapy. The question still remains whether increasing the number of TIL through decreased apoptosis is sufficient to carry out the effects of 4-1BB combination immunotherapy, or if some yet to be determined change in T cell function is also required. Our gene array analysis revealed

multiple granzyme genes that were upregulated after immunotherapy, insinuating that increased cytotoxicity could play a role in increased tumor cell killing after immunotherapy. Experiments could be conducted with perforin-and FasL-deficient animals to determine the necessity of either cytolysis pathway in tumor regression after agonist 4-1BB combination immunotherapy. If animals that are deficient for both perforin and FasL still have increased tumor control after immunotherapy, then there may be indirect mechanisms outside of tumor cell killing that mediate increased tumor control. Overall, the functions that mediate tumor control both in the endogenous tumor response and after immunotherapy will be critical to understand, as they may be directly targetable to further increase the efficacy of immunotherapy.

4.10 Conclusion

Taken together, our results imply that DCs provide co-stimulation through 4-1BBL that activates NF-κB signaling in effector CD8$^+$ T cells. Co-stimulation through 4-1BB signaling maintains numbers of CD8$^+$ TIL and is necessary for the efficacy of anti-PD-L1 immunotherapy. Agonist 4-1BB antibodies increase NF-κB pathway activity in CD8$^+$ TIL to promote their survival and accumulation. Increased 4-1BB signaling also maintains activated CD8$^+$ TIL in a short-lived effector cell-like differentiation status, where they express KLRG1 and IL-2. Although IL-2 signaling on CD8$^+$ TIL was not necessary for TIL expansion after agonist 4-1BB immunotherapy, IL-2 expression may indicate that CD8$^+$ TIL remain highly functional, as IL-2 expression correlated with tumor regression after agonist 4-1BB immunotherapy. Thus, increased co-stimulation of effector CD8$^+$ T cells prevents their death and dysfunction, leading to enhanced CD8$^+$ T cell responses and control of tumors. It should be explored whether increased co-stimulation of CD8$^+$ effector T cells outside of the tumor context can prevent their dysfunction or exhaustion, and which APCs and co-stimulatory signals are important for maintaining CD8$^+$ T cell function during chronic immune responses.

REFERENCES

Acuto, O. and Michel, F. (2003). Cd28-mediated co-stimulation: a quantitative support for TCR signaling. *Nature Reviews Immunology*, 3(12):939–51.

Banerjee, A., Thyagarajan, K., Chatterjee, S., Chakraborty, P., Kesarwani, P., Soloshchenko, M., Al-Hommrani, M., Andrijauskaite, K., Moxley, K., Janakiraman, H., Scheffel, M. J., Helke, K., Armenson, K., Palanisamy, V., Rubinstein, M. P., Mayer, E. G., Cole, D. J., Paulos, C. M., Voelkel-Johnson, C., Nishimura, M. I., and Mehrotra, S. (2016). Lack of p53 augments antitumor functions in cytolytic T cells. *Cancer Research*, 76(18):5229–40.

Barnes, S. E., Wang, Y., Chen, L., Molinero, L. L., Gajewski, T. F., Evaristo, C., and Alegre, M. L. (2015). T cell-NF-κB activation is required for tumor control in vivo. *Journal for Immunotherapy of Cancer*, 3(1).

Bertram, E. M., Dawicki, W., Sedgmen, B., Bramson, J. L., Lynch, D. H., and Watts, T. H. (2004). A switch in costimulation from CD28 to 4-1BB during primary versus secondary CD8 T cell response to influenza in vivo. *The Journal of Immunology*, 172(2):981–8.

Bister, K. (2015). Discovery of oncogenes: The advent of molecular cancer research. *Proceedings of the National Academy of Sciences*, 112(50):15259–15260.

Blackburn, S. D., Shin, H., Freeman, G. J., and Wherry, E. J. (2008). Selective expansion of a subset of exhausted CD8 T cells by αPD-L1 blockade. *Proceedings of the National Academy of Sciences*, 105(39):15016–21.

Blagih, J., Coulombe, F., Vincent, E. E., Dupuy, F., Galicia-Vzquez, G., Yurchenko, E., Raissi, T. C., van der Windt, G. J., Viollet, B., Pearce, E. L., Pelletier, J., Piccirillo, C. A., Krawczyk, C. M., Divangahi, M., and G, J. R. (2015). The energy sensor AMPK regulates T cell metabolic adaptation and effector responses in vivo. *Immunity*, 42(1):41–54.

Blank, A. E., Baumgarten, P., Zeiner, P., Zachskorn, C., Lffler, C., Schittenhelm, J., Czupalla, C. J., Capper, D., Plate, K. H., Harter, P. N., and Mittelbronn, M. (2015). Tumour necrosis factor receptor superfamily member 9 (TNFRSF9) is up-regulated in reactive astrocytes in human gliomas. *Neuropathology and Applied Neurobiology*, 41(2):e56–67.

Boczkowski, D., Lee, J., Pruitt, S., and Nair, S. (2009). DCs engineered to secrete anti-GITR antibodies are effective adjuvants to DCs-based immunotherapy. *Cancer Gene Therapy*, 16(12):900–11.

Boldajipour, B., Nelson, A., and Krummel, M. F. (2016). Tumor-infiltrating lymphocytes are dynamically desensitized to antigen but are maintained by homeostatic cytokine. *JCI Insight*, 1(20):e89289.

Bos, P. D., Plitas, G., Rudra, D., Lee, S. Y., and Rudensky, A. Y. (2013). Transient regulatory T cell ablation deters oncogene-driven breast cancer and enhances radiotherapy. *The Journal of Experimental Medicine*, 210(11):2435–66.

Bosenberg, M., Muthusamy, V., Curley, D. P., Wang, Z., Hobbs, C., Nelson, B., Nogueira, C., Horner, J., Depinho, R., and Chin, L. (2006). Characterization of melanocyte-specific inducible cre recombinase transgenic mice. *Genesis*, 44:262–267.

Boveri, T. (1914). *Zur Frage der Entstehung maligner Tumoren*. Fischer.

Boyman, O. and Sprent, J. (2012). The role of interleukin-2 during homeostasis and activation of the immune system. *Nature Reviews Immmunology*, 12(3):180–190.

Brahmer, J. R., Tykodi, S. S., Chow, L. Q., Hwu, W. J., Topalian, S. L., Hwu, P., Drake, C. G., Camacho, L. H., Kauh, J., Odunsi, K., Pitot, H. C., Hamid, O., Bhatia, S., Martins, R., Eaton, K., Chen, S., Salay, T. M., Alaparthy, S., Grosso, J. F., Korman, A. J., Parker, S. M., Agrawal, S., Goldberg, S. M., Pardoll, D. M., Gupta, A., and Wigginton, J. M. (2012). Safety and activity of anti-PD-L1 antibody in patients with advanced cancer. *The New England Journal of Medicine*, 366(26):2455–65.

Brinkmann, V., Davis, M. D., Heise, C. E., Albert, R., Cottens, S., Hof, R., Bruns, C., Prieschl, E., Baumruker, T., and Hiestand, P. (2002). The immune modulator FTY720 targets sphingosine 1-phosphate receptors. *The Journal of Biological Chemistry*, 277(24):21453–7.

Broz, M. L., Binnewies, M., Boldajipour, B., Nelson, A. E., Pollack, J. L., Erle, D. J., Barczak, A., Rosenblum, M. D., Daud, A., Barber, D. L., Amigorena, S., Van't Veer, L. J., Sperling, A. I., Wolf, D. M., and Krummel, M. F. (2014). Dissecting the tumor myeloid compartment reveals rare activating antigen-presenting cells critical for T cell immunity. *Cancer Cell*, 26(5):638–52.

Buck, M. D., O'Sullivan, D., and Pearce, E. L. (2015). T cell metabolism drives immunity. *The Journal of Experimental Medicine*, 212(9):1345–60.

Busuttil, V., Droin, N., McCormick, L., Bernassola, F., Candi, E., Melino, G., and Green, D. R. (2010). NF-κB inhibits T-cell activation-induced and p73-dependent cell death by induction of MDM2. *Proceedings of the National Academy of Sciences*, 107(42):18061–6.

Casey, S. C., Tong, L., Li, Y., Do, R., Walz, S., Fitzgerald, K., Gouw, A., Baylot, V., Gtgemann, I., Eilers, M., and Felsher, D. W. (2016). MYC regulates the antitumor immune response through CD47 and PD-L1. *Science*, 352(6282):227–31.

Cham, C. M. and Gajewski, T. F. (2005). Glucose availability regulates IFN-γ production and p70S6 kinase activation in $CD8^+$ effector T cells. *The Journal of Immunology*, 174(8):4670–7.

Chang, C. H. and Pearce, E. L. (2016). Emerging concepts of T cell metabolism as a target of immunotherapy. *Nature Immunology*, 17(4):364–8.

Chang, C. H., Qiu, J., O'Sullivan, D., Buck, M. D., Noguchi, T., Curtis, J. D., Chen, Q., Gindin, M., Gubin, M. M., van der Windt, G. J., Tonc, E., Schreiber, R. D., Pearce, E. J., and Pearce, E. L. (2015). Metabolic competition in the tumor microenvironment is a driver of cancer progression. *Cell*, 162(6):1229–41.

Charo, J., Finkelstein, S. E., Grewal, N., Restifo, N. P., Robbins, P. F., and Rosenberg, S. A. (2005). Bcl-2 overexpression enhances tumor-specific T-cell survival. *Cancer Research*, 65(5):2001–8.

Chen, G. Y. and Nuez, G. (2010). Sterile inflammation: sensing and reacting to damage. *Nature Reviews Immunology*, 10(12):826–37.

Chen, L., Ashe, S., Brady, W. A., Hellstrm, I., Hellstrm, K. E., Ledbetter, J. A., McGowan, P., and Linsley, P. S. (1992). Costimulation of antitumor immunity by the B7 counterreceptor for the T lymphocyte molecules CD28 and CTLA-4. *Cell*, 71(7):1093–102.

Chen, L. and Flies, D. B. (2013). Molecular mechanisms of T cell co-stimulation and co-inhibition. *Nature Reviews Immunology*, 13(4):227–42.

Cheung, A. F., Dupage, M. J., Dong, H., Chen, J., and Jacks, T. (2008). Regulated expression of a tumor-associated antigen reveals multiple levels of T-cell tolerance in a mouse model of lung cancer. *Cancer Research*, 68:9459–9468.

Chipuk, J. E. and Green, D. R. (2006). Dissecting p53-dependent apoptosis. *Cell Death and Differentiation*, 13(6):994–1002.

Cohen, C. J., Gartner, J. J., Horovitz-Fried, M., Shamalov, K., Trebska-McGowan, K., Bliskovsky, V. V., Parkhurst, M. R., Ankri, C., Prickett, T. D., Crystal, J. S., Li, Y. F., El-Gamil, M., Rosenberg, S. A., and Robbins, P. F. (2015). Isolation of neoantigen-specific T cells from tumor and peripheral lymphocytes. *The Journal of Clinical Investigation*, 125(10):3981–91.

Coombs, C. C., Tavakkoli, M., and Tallman, M. S. (2015). Acute promyelocytic leukemia: where did we start and where are we now and and the future. *Blood Cancer Journal*, 5:e304.

Cooper, D., Bansal-Pakala, P., and Croft, M. (2002). 4-1BB (CD137) controls the clonal expansion and survival of CD8 T cells in vivo but does not contribute to the development of cytotoxicity. *European Journal of Immunology*, 32(2):521–9.

Coulie, P. G., Van den Eynde, B. J., van der Bruggen, P., and Boon, T. (2014). Tumour antigens recognized by T lymphocytes: at the core of cancer immunotherapy. *Nature Reviews Cancer*, 14(2):135–46.

Cox, A. D. and Der, C. J. (2010). Ras history: The saga continues. *Small GTPases*, 1(1):2–27.

Crespo, J., Sun, H., Welling, T. H., Tian, Z., and Zou, W. (2013). T cell anergy and exhaustion and senescence and and stemness in the tumor microenvironment. *Current Opinion in Immunology*, 25(2):213–21.

Curran, M. A., Kim, M., Montalvo, W., Al-Shamkhani, A., and Allison, J. P. (2011). Combination CTLA-4 blockade and 4-1BB activation enhances tumor rejection by increasing T-cell infiltration, proliferation and cytokine production. *PLos One*, 6(4):e19499.

Curtsinger, J. M. and Mescher, M. F. (2010). Inflammatory cytokines as a third signal for T cell activation. *Current Opinion in Immunology*, 22(3):333–40.

Daley, S. R., Hu, D. Y., and Goodnow, C. C. (2013). Helios marks strongly autoreactive $CD4^+$ T cells in two major waves of thymic deletion distinguished by induction of PD-1 or NF-κB. *The Journal of Experimental Medicine*, 210(2):269–85.

Dankort, D., Filenova, E., Collado, M., Serrano, M., Jones, K., and McMahon, M. (2007). A new mouse model to explore the initiation and progression and and therapy of BRAFV600E-induced lung tumors. *Genes and Development*, 21:379–84.

Daud, A. I., Loo, K., Pauli, M. L., Sanchez-Rodriguez, R., Sandoval, P. M., Taravati, K., Tsai, K., Nosrati, A., Nardo, L., Alvarado, M. D., Algazi, A. P., Pampaloni, M. H., Lobach, I. V., Hwang, J., Pierce, R. H., Gratz, I. K., Krummel, M. F., and Rosenblum, M. D. (2016). Tumor immune profiling predicts response to anti-PD-1 therapy in human melanoma. *The Journal of Clinical Investigation*, 126(9):3447–52.

de Villartay, J. P., Fischer, A., and Durandy, A. (2003). The mechanisms of immune diversification and their disorders. *Nature Reviews Immunology*, 3(12):962–72.

Der, C. J., Krontiris, T. G., and Cooper, G. M. (1982). Transforming genes of human bladder and lung carcinoma cell lines are homologous to the ras genes of Harvey and Kirsten sarcoma viruses. *Proceedings of the National Academy of Sciences*, 79:3637–3650.

Diamond, M. S., Kinder, M., Matsushita, H., Mashayekhi, M., Dunn, G. P., Archambault, J. M., Lee, H., Arthur, C. D., White, J. M., Kalinke, U., Murphy, K. M., and Schreiber, R. D. (2011). Type I interferon is selectively required by DCs for immune rejection of tumors. *Nature Reviews Immunology*, 208(10):1989–2003.

Doering, T. A., Crawford, A., Angelosanto, J. M., Paley, M. A., Ziegler, C. G., and Wherry, E. J. (2012). Network analysis reveals centrally connected genes and pathways involved in $CD8^+$ T cell exhaustion versus memory. *Immunity*, 37(6):1130–44.

Druker, B. J. (2014). Janet Rowley. *Nature*, 505(7487):484.

Duesberg, P. H. and Vogt, P. K. (1970). Differences between the ribonucleic acids of transforming and nontransforming avian tumor viruses. *Proceedings of the National Academy of Sciences*, 67(4):1673–1680.

Ehrlich, P. (1909). Ueber den jetzigen Stand der Karzinomforschung. *Nederlands Tijdschrift voor Geneeskunde*, 5:273–290.

Evaristo, C., Spranger, S., Barnes, S. E., Miller, M. L., Molinero, L. L., Locke, F. L., Gajewski, T. F., and Alegre, M. L. (2016). Cutting Edge: Engineering Active IKKβ in T Cells Drives Tumor Rejection. *The Journal of Immmunology*, 196(7):2933–8.

Fallarino, F., Grohmann, U., Vacca, C., Bianchi, R., Orabona, C., Spreca, A., Fioretti, M. C., and Puccetti, P. (20002). T cell apoptosis by tryptophan catabolism. *Cell Death and Differentiation*, 9(10):1069–77.

Flynn, K. and Mullbacher, A. (1996). Memory alloreactive cytotoxic T cells do not require costimulation for activation in vitro. *Immunology and Cell Biology*, 74:413–20.

French, R., Taraban, V., Crowther, G., Rowley, T., Gray, J., Johnson, P., Tutt, A., Al-Shamkhani, A., and Glennie, M. (2007). Eradication of lymphoma by CD8 T cells following anti-CD40 monoclonal antibody therapy is critically dependent on CD27 costimulation. *Blood*, 109(11):4810–4815.

Fuertes, M. B., Kacha, A. K., Kline, J., Woo, S. R., Kranz, D. M., Murphy, K. M., and Gajewski, T. F. (2011). Host type I IFN signals are required for antitumor $CD8^+$ T cell responses through $CD8\alpha^+$ DCs. *The Journal of Experimental Medicine*, 208(10):2005–16.

Fuertes Marraco, S. A., Neubert, N. J., Verdeil, G., and Speiser, D. E. (2015). Inhibitory Receptors Beyond T Cell Exhaustion. *Frontiers in Immunology*, 6(310).

Furtado, G. C., Curotto de Lafaille, M. A., Kutchukhidze, N., and Lafaille, J. J. (2002). Interleukin 2 signaling is required for $CD4^+$ regulatory T cell function. *The Journal of Experimental Medicine*, 196(6):851–7.

Gajewski, T. F., Schreiber, H., and Fu, Y. X. (2013). Innate and adaptive immune cells in the tumor microenvironment. *Nature Immmunology*, 14(10):1014–22.

Garrido, F., Aptsiauri, N., Doorduijn, E. M., Garcia Lora, A. M., and van Hall, T. (2016). The urgent need to recover MHC class I in cancers for effective immunotherapy. *Current Opinion in Immunology*, 39:44–51.

Garrod, K. R., Moreau, H. D., Garcia, Z., Lematre, F., Bouvier, I., Albert, M. L., and Bousso, P. (2012). Dissecting T cell contraction in vivo using a genetically encoded reporter of apoptosis. *Cell Reports*, 2(5):1438–47.

Geiger, R., Rieckmann, J. C., Wolf, T., Basso, C., Feng, Y., Fuhrer, T., Kogadeeva, M., Picotti, P., Meissner, F., Mann, M., Zamboni, N., Sallusto, F., and Lanzavecchia, A. (2016). L-arginine modulates T cell metabolism and enhances survival and anti-tumor activity. *Cell*, 167(3):829–842.

Gough, M. J., Ruby, C., Redmond, W. L., Dhungel, B., Brown, A., and Weinberg, A. D. (2008). OX40 agonist therapy enhances CD8 infiltration and decreases immune suppression in the tumor. *Cancer Research*, 68(13):5206–15.

Green, D. R., Droin, N., and Pinkoski, M. (2003). Activation-induced cell death in T cells. *Immunological Reviews*, 193:70–81.

Gros, A., Parkhurst, M. R., Tran, E., Pasetto, A., Robbins, P. F., Ilyas, S., Prickett, T. D., Gartner, J. J., Crystal, J. S., Roberts, I. M., Trebska-McGowan, K., Wunderlich, J. R., Yang, J. C., and Rosenberg, S. A. (2016). Prospective identification of neoantigen-specific lymphocytes in the peripheral blood of melanoma patients. *Nature Medicine*, 22(4):433–8.

Gubin, M. M., Artyomov, M. N., Mardis, E. R., and Schreiber, R. D. (2015). Tumor neoantigens: building a framework for personalized cancer immunotherapy. *The Journal of Clinical Investigation*, 125(9):3413–21.

Habib-Agahi, M., Phan, T. T., and Searle, P. F. (2007). Co-stimulation with 4-1BB ligand allows extended T-cell proliferation and synergizes with CD80/CD86 and can reactivate anergic T cells. *International Immunology*, 19(12):1383–94.

Hanahan, D. and Weinberg, R. A. (2000). The hallmarks of cancer. *Cell*, 100(1):57–70.

Harlin, H., Meng, Y., Peterson, A. C., Zha, Y., Tretiakova, M., Slingluff, C., McKee, M., and Gajewski, T. F. (2009). Chemokine expression in melanoma metastases associated with $CD8^+$ T-cell recruitment. *Cancer Research*, 69(7):3077–85.

Hawiger, D., Inaba, K., Dorsett, Y., Guo, M., Mahnke, K., Rivera, M., Ravetch, J. V., Steinman, R. M., and Nussenzweig, M. C. (2001). DCs induce peripheral T cell unresponsiveness under steady state conditions in vivo. *The Journal of Experimental Medicine*, 194:769–779.

Hildner, K., Edelson, B. T., Purtha, W. E., Diamond, M., Matsushita, H., Kohyama, M., Calderon, B., Schraml, B. U., Unanue, E. R., Diamond, M. S., Schreiber, R. D., Murphy, T. L., and Murphy, K. M. (2008). Batf3 deficiency reveals a critical role for $CD8\alpha^+$ DCs in cytotoxic T cell immunity. *Science*, 322(5904):1097–100.

Ho, P. C., Bihuniak, J. D., Macintyre, A. N., Staron, M., Liu, X., Amezquita, R., Tsui, Y. C., Cui, G., Micevic, G., Perales, J. C., Kleinstein, S. H., Abel, E. D., Insogna, K. L., Feske, S., Locasale, J. W., Bosenberg, M. W., Rathmell, J. C., and Kaech, S. M. (2015). Phosphoenolpyruvate is a metabolic checkpoint of anti-tumor T cell responses. *Cell*, 162(6):1217–28.

Hodi, F. S., O'Day, S. J., McDermott, D. F., Weber, R. W., Sosman, J. A., Haanen, J. B., Gonzalez, R., Robert, C., Schadendorf, D., Hassel, J. C., Akerley, W., van den Eertwegh, A. J., Lutzky, J., Lorigan, P., Vaubel, J. M., Linette, G. P., Hogg, D., Ottensmeier, C. H., Lebbe, C., Peschel, C., Quirt, I., Clark, J. I., Wolchok, J. D., Weber, J. S., Tian, J., Yellin, M. J., Nichol, G. M., Hoos, A., and Urba, W. J. (2010). Improved survival with ipilimumab in patients with metastatic melanoma. *The New England Journal of Medicine*, 363(8):711–23.

Honda, T., Egen, J. G., Lmmermann, T., Kastenmller, W., Torabi-Parizi, P., and Germain, R. N. (2014). Tuning of antigen sensitivity by t cell receptor-dependent negative feedback controls t cell effector function in inflamed tissues. *Immunity*, 40(2):235–247.

Hui, E., Cheung, J., Zhu, J., Su, X., Taylor, M. J., Wallweber, H. A., Sasmal, D. K., Huang, J., Kim, J. M., Mellman, I., and Vale, R. D. (2017). T cell costimulatory receptor CD28 is a primary target for PD-1-mediated inhibition. *Science*, 355(6332):1428–1433.

Huppa, J. B. and Davis, M. M. (2003). T-cell-antigen recognition and the immunological synapse. *Nature Reviews Immunology*, 3(12):973–83.

Hutloff, A., Dittrich, A. M., Beier, K. C., Eljaschewitsch, B., Kraft, R., Anagnostopoulos, I., and Kroczek, R. A. (1999). ICOS is an inducible T-cell co-stimulator structurally and functionally related to CD28. *Nature*, 397(6716):263–6.

Igney, F. H. and Krammer, P. H. (2005). Tumor counterattack: fact or fiction? *Cancer Immunology, Immunotherapy*, 54(11):1127–36.

Janeway, C. A. and Medzhitov, R. (2002). Innate immune recognition. *Annual Review of Immunology*, 20:197–216.

Jass, J. R., Love, S. B., and Northover, J. M. (1987). A new prognostic classification of rectal cancer. *Lancet*, 1:1303–1306.

Ji, R. R., Chasalow, S. D., Wang, L., Hamid, O., Schmidt, H., Cogswell, J., Alaparthy, S., Berman, D., Jure-Kunkel, M., Siemers, N. O., Jackson, J. R., and Shahabi, V. (2012). An immune-active tumor microenvironment favors clinical response to ipilimumab. *Cancer Immunology, Immunotherapy*, 61(7):1019–31.

June, C. H., Bluestone, J. A., Nadler, L. M., and Thompson, C. B. (1994). The B7 and CD28 receptor families. *Immunology Today*, 15(7):321–31.

Kahan, S. M., Wherry, E. J., and Zajac, A. J. (2015). T cell exhaustion during persistent viral infections. *Virology*, 479-480:180–93.

Kamphorst, A. O., Wieland, A., Nasti, T., Yang, S., Zhang, R., Barber, D. L., Konieczny, B. T., Daugherty, C. Z., Koenig, L., Yu, K., Sica, G. L., Sharpe, A. H., Freeman, G. J., Blazar, B. R., Turka, L. A., Owonikoko, T. K., Pillai, R. N., Ramalingam, S. S., Araki, K., and Ahmed, R. (2017). Rescue of exhausted CD8 T cells by PD-1-targeted therapies is CD28-dependent. *Science*, 355(6332):1423–1427.

Kawalekar, O. U., O'Connor, R. S., Fraietta, J. A., Guo, L., McGettigan, S. E., Posey, A. D., Patel, P. R., Guedan, S., Scholler, J., Keith, B., Snyder, N. W., Blair, I. A., Milone, M. C., and June, C. H. (2016). Distinct signaling of coreceptors regulates specific metabolism pathways and impacts memory development in CAR T cells. *Immunity*, 44(2):380–90.

Kim, S. K., Schluns, K. S., and Lefrancois, L. (1999). Induction and visualization of mucosal memory CD8 t cells following systemic virus infection. *The Journal of Immunology*, 163:4125–32.

Kline, J., Zhang, L., Battaglia, L., Cohen, K. S., and Gajewski, T. F. (2012). Cellular and molecular requirements for rejection of B16 melanoma in the setting of regulatory T cell depletion and homeostatic proliferation. *The Journal of Immunology*, 188(6):2630–42.

Kohrt, H. E., Colevas, A. D., Houot, R., Weiskopf, K., Goldstein, M. J., Lund, P., Mueller, A., Sagiv-Barfi, I., Marabelle, A., Lira, R., Troutner, E., Richards, L., Rajapaska, A., Hebb, J., Chester, C., Waller, E., Ostashko, A., Weng, W. K., Chen, L., Czerwinski, D., Fu, Y. X., Sunwoo, J., and Levy, R. (2014). Targeting CD137 enhances the efficacy of cetuximab. *The Journal of Clinical Investigation*, 124(6):2668–82.

Kohrt, H. E., Houot, R., Goldstein, M. J., Weiskopf, K., Alizadeh, A. A., Brody, J., Muller, A., Pachynski, R., Czerwinski, D., Coutre, S., Chao, M. P., Chen, L., Tedder, T. F., and Levy, R. (2011). CD137 stimulation enhances the antilymphoma activity of anti-CD20 antibodies. *Blood*, 117(8):2423–32.

Kohrt, H. E., Houot, R., Weiskopf, K., Goldstein, M. J., Scheeren, F., Czerwinski, D., Colevas, A. D., Weng, W. K., Clarke, M. F., Carlson, R. W., Stockdale, F. E., Mollick, J. A., Chen, L., and Levy, R. (2012). Stimulation of natural killer cells with a CD137-specific antibody enhances trastuzumab efficacy in xenotransplant models of breast cancer. *The Journal of Clinical Investigation*, 122(2):1066–75.

Kono, H. and Rock, K. L. (2008). How dying cells alert the immune system to danger. *Nature Reviews Immunology*, 8(4):279–89.

Kwon, B. S., Hurtado, J. C., Lee, Z. H., Kwack, K. B., Seo, S. K., Choi, B. K., Koller, B. H., Wolisi, G., Broxmeyer, H. E., and Vinay, D. S. (2002). Immune responses in 4-1BB (CD137)-deficient mice. *The Journal of Immunology*, 168:5483–5490.

Kwon, B. S. and Weissman, S. M. (1989). cDNA sequences of two inducible T-cell genes. *Proceedings of the National Academy of Sciences*, 86:1963–1967.

Laidlaw, B. J., Craft, J. E., and Kaech, S. M. (2016). The multifaceted role of $CD4^+$ T cells in $CD8^+$ T cell memory. *Nature Reviews Immunology*, 16(2):102–11.

Larkin, J., Chiarion-Sileni, V., Gonzalez, R., Grob, J. J., Cowey, C. L., Lao, C. D., Schadendorf, D., Dummer, R., Smylie, M., Rutkowski, P., Ferrucci, P. F., Hill, A., Wagstaff, J., Carlino, M. S., Haanen, J. B., Maio, M., Marquez-Rodas, I., McArthur, G. A., Ascierto, P. A., Long, G. V., Callahan, M. K., Postow, M. A., Grossmann, K., Sznol, M., Dreno, B., Bastholt, L., Yang, A., Rollin, L. M., Horak, C., Hodi, F. S., and Wolchok, J. D. (2016). The multifaceted role of $CD4^+$ T cells in $CD8^+$ T cell memory. *Nature Reviews Immunology*, 16(2):102–11.

Latchman, Y. E., Liang, S. C., Wu, Y., Chernova, T., Sobel, R. A., Klemm, M., Kuchroo, V. K., Freeman, G. J., and Sharpe, A. H. (2004). PD-L1-deficient mice show that PD-L1 on T cells, antigen-presenting cells, and host tissues negatively regulates T cells. *Proceedings of the National Academy of Sciences*, 101(29):10691–6.

Le, D. T., Uram, J. N., Wang, H., Bartlett, B. R., Kemberling, H., Eyring, A. D., Skora, A. D., Luber, B. S., Azad, N. S., Laheru, D., Biedrzycki, B., Donehower, R. C., Zaheer, A., Fisher, G. A., Crocenzi, T. S., Lee, J. J., Duffy, S. M., Goldberg, R. M., de la Chapelle, A., Koshiji, M., Bhaijee, F., Huebner, T., Hruban, R. H., Wood, L. D., Cuka, N., Pardoll, D. M., Papadopoulos, N., Kinzler, K. W., Zhou, S., Cornish, T. C., Taube, J. M., Anders, R. A., Eshleman, J. R., Vogelstein, B., and Diaz, L. A. J. (2015). PD-1 Blockade in Tumors with Mismatch-Repair Deficiency. *The New England Journal of Medicine*, 372(26):2509–20.

Lee, H. W., Park, S. J., Choi, B. K., Kim, H. H., Nam, K. O., and Kwon, B. S. (2004). 4-1BB promotes the survival of $CD8^+$ T lymphocytes by increasing expression of Bcl-x^L and Bfl-1. *Proceedings of the National Academy of Sciences*, 101(29):10691–6.

Lee, J., Walsh, M. C., Hoehn, K. L., James, D. E., Wherry, E. J., and Choi, Y. (2014). Regulator of fatty acid metabolism and acetyl coenzyme a carboxylase 1 and controls T cell immunity. *The Journal of Immunology*, 192(7):3190–9.

Lee, S. W., Park, Y., So, T., Kwon, B. S., Cheroutre, H., Mittler, R. S., and Croft, M. (2008). Identification of regulatory functions for 4-1BB and 4-1BBL in myelopoiesis and the development of DCs. *Nature Immmunology*, 9(8):917–26.

Lee, S. W., Park, Y., Song, A., Cheroutre, H., Kwon, B. S., and Croft, M. (2006). Functional Dichotomy between OX40 and 4-1BB in Modulating Effector CD8 T Cell Responses. *The Journal of Immmunology*, 177(7):4464–4472.

Long, A. H., Haso, W. M., Shern, J. F., Wanhainen, K. M., Murgai, M., Ingaramo, M., Smith, J. P., Walker, A. J., Kohler, M. E., Venkateshwara, V. R., Kaplan, R. N., Patterson, G. H., Fry, T. J., Orentas, R. J., and Mackall, C. L. (2015). 4-1BB costimulation ameliorates T cell exhaustion induced by tonic signaling of chimeric antigen receptors. *Nature Medicine*, 21(6):581–90.

Lu, Y. C., Yao, X., Crystal, J. S., Li, Y. F., El-Gamil, M., Gross, C., Davis, L., Dudley, M. E., Yang, J. C., Samuels, Y., Rosenberg, S. A., and Robbins, P. F. (2014). Efficient identification of mutated cancer antigens recognized by T cells associated with durable tumor regressions. *Clinical Cancer Research*, 20(13):3401–10.

Maceyka, M. and Spiegel, S. (2014). Sphingolipid metabolites in inflammatory disease. *Nature*, 510(7503):58–67.

Malchow, S., Leventhal, D. S., Lee, V., Nishi, S., Socci, N. D., and Savage, P. A. (2016). Aire Enforces Immune Tolerance by Directing Autoreactive T Cells into the Regulatory T Cell Lineage. *Immunity*, 44(5):1102–13.

Mandala, S., Hajdu, R., Bergstrom, J., Quackenbush, E., Xie, J., Milligan, J., Thornton, R., Shei, G. J., Card, D., Keohane, C., Rosenbach, M., Hale, J., Lynch, C. L., Rupprecht, K., Parsons, W., and Rosen, H. (2002). Alteration of lymphocyte trafficking by sphingosine-1-phosphate receptor agonists. *Science*, 296(5566):346–9.

Martin, S. J., Amarante-Mendes, G. P., Shi, L., Chuang, T. H., Casiano, C. A., O'Brien, G. A., Fitzgerald, P., Tan, E. M., Bokoch, G. M., Greenberg, A. H., and Green, D. R. (1996). The cytotoxic cell protease granzyme B initiates apoptosis in a cell-free system by proteolytic processing and activation of the ICE/CED-3 family protease and CPP32 and via a novel two-step mechanism. *The EMBO Journal*, 5:2407–2416.

Matloubian, M., Lo, C. G., Cinamon, G., Lesneski, M. J., Xu, Y., Brinkmann, V., Allende, M. L., Proia, R. L., and Cyster, J. G. (2004). Lymphocyte egress from thymus and peripheral lymphoid organs is dependent on S1P receptor 1. *Nature*, 427(6972):355–60.

McDonald, B. D., Bunker, J. J., Erickson, S. A., Oh-Hora, M., and Bendelac, A. (2015). Crossreactive $\alpha\beta$ T cell receptors are the predominant targets of thymocyte negative selection. *Immunity*, 43(5):859–69.

McDonald, B. D., Bunker, J. J., Ishizuka, I. E., Jabri, B., and Bendelac, A. (2014). Elevated T cell receptor signaling identifies a thymic precursor to the TCR$\alpha\beta^{+}$CD4^{-}CD8β^{-} intraepithelial lymphocyte lineage. *Immunity*, 41(2):219–29.

McGranahan, N., Furness, A., Rosenthal, R., Ramskov, S., Lyngaa, R., Saini, S., Jamal-Hanjani, M., Wilson, G. A., Birkbak, N. J., Hiley, C. T., Watkins, T. B., Shafi, S., Murugaesu, N., Mitter, R., Akarca, A. U., Linares, J., Marafioti, T., Henry, J. Y., Van Allen, E. M., Miao, D., Schilling, B., Schadendorf, D., Garraway, L. A., Makarov, V., Rizvi, N. A., Snyder, A., Hellmann, M. D., Merghoub, T., Wolchok, J. D., Shukla, S. A., Wu, C. J., Peggs, K. S., Chan, T. A., Hadrup, S. R., Quezada, S. A., and Swanton, C. (2016). Clonal neoantigens elicit T cell immunoreactivity and sensitivity to immune checkpoint blockade. *Science*, 351(6280):1463–9.

McNally, J. P., Millen, S. H., Chaturvedi, V., Lakes, N., Terrell, C. E., Elfers, E. E., Carroll, K. R., Hogan, S. P., Andreassen, P. R., Kanter, J., Allen, C. E., Henry, M. M., Greenberg, J. N., Ladisch, S., Hermiston, M. L., Joyce, M., Hildeman, D. A., Katz, J. D., and Jordan, M. B. (2017). Manipulating DNA damage-response signaling for the treatment of immune-mediated diseases. *Proceedings of the National Academy of Sciences*, 114(24):E4782–E4791.

Melero, I., Johnston, J. V., Shufford, W. W., Mittler, R. S., , and Chen, L. (1998). NK1.1 cells express 4-1BB (CDw137) costimulatory molecule and are required for tumor immunity elicited by anti-4-1BB monoclonal antibodies. *Cellular Immunology*, 190(2):167–72.

Melero, I., Shuford, W. W., Newby, S. A., Aruffo, A., Ledbetter, J. A., Hellstrom, K. E., Mittler, R. S., and Chen, L. (1997). Monoclonal antibodies against the 4-1BB T-cell activation molecule eradicate established tumors. *Nature Medicine*, 3(6):682–5.

Mogi, S., Sakurai, J., Kohsaka, T., Enomoto, S., Yagita, H., Okumura, K., and Azuma, M. (2000). Tumour rejection by gene transfer of 4-1BB ligand into a $CD80^+$ murine squamous cell carcinoma and the requirements of co-stimulatory molecules on tumour and host cells. *Immunology*, 101(4):541–7.

Mueller, D. L. (2000). T cells: A proliferation of costimulatory molecules. *Current Biology*, 10(6):R227–30.

Nishimura, H., Nose, M., Hiai, H., Minato, N., and Honjo, T. (1999). Development of lupus-like autoimmune diseases by disruption of the PD-1 gene encoding an ITIM motif-carrying immunoreceptor. *Immunity*, 11(2):141–51.

Odorizzi, P. M., Pauken, K. E., Paley, M. A., Sharpe, A., and Wherry, E. J. (2015). Genetic absence of PD-1 promotes accumulation of terminally differentiated exhausted $CD8^+$ T cells. *The Journal of Experimental Medicine*, 212(7):1125–37.

Oh, H. S., Choi, B. K., Kim, Y. H., Lee, D. G., Hwang, S., Lee, M. J., Park, S. H., Bae, Y. S., and Kwon, B. S. (2015). 4-1BB signaling enhances primary and secondary population expansion of $CD8^+$ T cells by maximizing autocrine IL-2/IL-2 receptor signaling. *PLoS One*, 10(5):e0126765.

Pages, F., Berger, A., Camus, M., Sanchez-Cabo, F., Costes, A., Molidor, R., Mlecnik, B., Kirilovsky, A., Nilsson, M., Damotte, D., Meatchi, T., Bruneval, P., Cugnenc, P. H., Trajanoski, Z., Fridman, W. H., and Galon, J. (2005). Effector memory T cells and early

metastasis and and survival in colorectal cancer. *The New England Journal of Medicine*, 353:2654–2666.

Palazn, A., Teijeira, A., Martnez-Forero, I., Hervs-Stubbs, S., Roncal, C., Peuelas, I., Dubrot, J., Morales-Kastresana, A., Prez-Gracia, J. L., Ochoa, M. C., Ochoa-Callejero, L., Martnez, A., Luque, A., Dinchuk, J., Rouzaut, A., Jure-Kunkel, M., and Melero, I. (2011). Agonist anti-CD137 mAb act on tumor endothelial cells to enhance recruitment of activated T lymphocytes. *Cancer Research*, 71(3):801–11.

Paley, M. A., Kroy, D. C., Odorizzi, P. M., Johnnidis, J. B., Dolfi, D. V., Barnett, B. E., Bikoff, E. K., Robertson, E. J., Lauer, G. M., Reiner, S. L., and Wherry, E. J. (2012). Progenitor and terminal subsets of $CD8^+$ T cells cooperate to contain chronic viral infection. *Science*, 338(6111):1220–5.

Parada, L. F., Tabin, C. J., Shih, C., and Weinberg, R. A. (1982). Human EJ bladder carcinoma oncogene is homologue of Harvey sarcoma virus ras gene. *Nature*, 297:474–478.

Parry, R. V., Chemnitz, J. M., Frauwirth, K. A., Lanfranco, A. R., Braunstein, I., Kobayashi, S. V., Linsley, P. S., Thompson, C. B., and Riley, J. L. (2005). CTLA-4 and PD-1 receptors inhibit T-cell activation by distinct mechanisms. *Molecular Cell Biology*, 25(21):9543–53.

Pauken, K. E., Sammons, M. A., Odorizzi, P. M., Manne, S., Godec, J., Khan, O., Drake, A. M., Chen, Z., Sen, D. R., Kurachi, M., Barnitz, R. A., Bartman, C., Bengsch, B., Huang, A. C., Schenkel, J. M., Vahedi, G., Haining, W. N., Berger, S. L., and Wherry, E. J. (2016). Epigenetic stability of exhausted T cells limits durability of reinvigoration by PD-1 blockade. *Science*, 54(6316):1160–1165.

Peng, W., Chen, J. Q., Liu, C., Malu, S., Creasy, C., Tetzlaff, M. T., Xu, C., McKenzie, J. A., Zhang, C., Liang, X., Williams, L. J., Deng, W., Chen, G., Mbofung, R., Lazar, A. J., Torres-Cabala, C. A., Cooper, Z. A., Chen, P. L., Tieu, T. N., Spranger, S., Yu, X., Bernatchez, C., Forget, M. A., Haymaker, C., Amaria, R., McQuade, J. L., Glitza, I. C., Cascone, T., Li, H. S., Kwong, L. N., Heffernan, T. P., Hu, J., Bassett, Jr., R. L., Bosenberg, M. W., Woodman, S. E., Overwijk, W. W., Lizée, G., Roszik, J., Gajewski, T. F., Wargo, J. A., Gershenwald, J. E., Radvanyi, L., Davies, M. A., and Hwu, P. (2016). Loss of PTEN Promotes Resistance to T Cell-Mediated Immunotherapy. *Cancer Discovery*, 6(2):202–16.

Pinschewer, D. D., Ochsenbein, A. F., Odermatt, B., Brinkmann, V., Hengartner, H., , and Zinkernagel, R. M. (2016). FTY720 immunosuppression impairs effector T cell peripheral homing without affecting induction and expansion and and memory. *The Journal of Immunology*, 6(2):202–16.

Poltorak, A., He, X., Smirnova, I., Liu, M. Y., Van Huffel, C., Du, X., Birdwell, D., Alejos, E., Silva, M., Galanos, C., Freudenberg, M., Ricciardi-Castagnoli, P., Layton, B., and Beutler, B. (1998). Defective LPS signaling in C3H/HeJ and C57BL/10ScCr mice: mutations in Tlr4 gene. *Science*, 282(5396):2085–8.

Pulle, G., Vidric, M., and Watts, T. H. (2006). IL-15-dependent induction of 4-1BB promotes antigen-independent CD8 memory T cell survival. *The Journal of Immunology*, 176:2739–2748.

Rathmell, J. C. and Kaech, S. M. (2015). Phosphoenolpyruvate is a metabolic checkpoint of anti-tumor T cell responses. *Cell*, 162(6):1217–28.

Reis e Sousa, C. (2004). Activation of DCs: translating innate into adaptive immunity. *Current Opinion in Immunology*, 16(1):21–5.

Reis e Sousa, C. (2006). DCs in a mature age. *Nature Reviews Immunology*, 6:476–483.

Rizvi, N. A., Hellmann, M. D., Snyder, A., Kvistborg, P., Makarov, V., Havel, J. J., Lee, W., Yuan, J., Wong, P., Ho, T. S., Miller, M. L., Rekhtman, N., Moreira, A. L., Ibrahim, F., Bruggeman, C., Gasmi, B., Zappasodi, R., Maeda, Y., Sander, C., Garon, E. B., Merghoub, T., Wolchok, J. D., Schumacher, T. N., and Chan, T. A. (2015). Mutational landscape determines sensitivity to PD-1 blockade in non-small cell lung cancer. *Science*, 348(6230):124–8.

Roberts, E. W., Broz, M. L., Binnewies, M., Headley, M. B., Nelson, A. E., Wolf, D. M., Kaisho, T., Bogunovic, D., Bhardwaj, N., and Krummel, M. F. (2016). Critical role for $CD103^+/CD141^+$ DCs bearing CCR7 for tumor antigen trafficking and priming of T cell immunity in melanoma. *Cancer Cell*, 30(2):324–36.

Roche, P. A. and Furuta, K. (2015). The ins and outs of MHC class II-mediated antigen processing and presentation. *Nature Reviews Immunology*, 15(4):203–16.

Rous, P. (1917). A sarcoma of the fowl transmissible by an agent separable from the tumor cells. *The Journal of Experimental Medicine*, 13(4):397–411.

Rowley, J. D. (1973a). Identificaton of a translocation with quinacrine fluorescence in a patient with acute leukemia. *Annales de Génétique*, 16(2):109–12.

Rowley, J. D. (1973b). Letter: A new consistent chromosomal abnormality in chronic myelogenous leukaemia identified by quinacrine fluorescence and Giemsa staining. *Nature*, 243(5405):290–3.

Sacha, T. (2014). Imatinib in chronic myeloid leukemia: an overview. *Mediterranean Journal of Hematology and Infectious Diseases*, 6(1):e2014007.

Santos, E., Tronick, S. R., Aaronson, S. A., Pulciani, S., and Barbacid, M. (1982). T24 human bladder carcinoma oncogene is an activated form of the normal human homologue of BALB- and Harvey-MSV transforming genes. *Nature*, 298:343–347.

Saoulli, K., Lee, S. Y., Cannons, J. L., Yeh, W. C., Santana, A., Goldstein, M. D., Bangia, N., DeBenedette, M. A., Mak, T. W., Choi, Y., and Watts, T. H. (1998). CD28-independent and TRAF2-dependent costimulation of resting T cells by 4-1BB ligand. *The Journal of Experimental Medicine*, 187(11):1849–1862.

Schietinger, A., Delrow, J. J., Basom, R. S., Blattman, J. N., and Greenberg, P. D. (2012). Rescued tolerant CD8 T cells are preprogrammed to reestablish the tolerant stated. *Science*, 335(6069):723–7.

Schietinger, A. and Greenberg, P. D. (2014). Tolerance and exhaustion: defining mechanisms of T cell dysfunction. *Trends in Immunology*, 35(2):51–60.

Schietinger, A., Philip, M., Krisnawan, V. E., Chiu, E. Y., Delrow, J. J., Basom, R. S., Lauer, P., Brockstedt, D. G., Knoblaugh, S. E., Hämmerling, G. J., Schell, T. D., Garbi, N., and Greenberg, P. D. (2016). Tumor-specific T cell dysfunction is a dynamic antigen-driven differentiation program initiated early during tumorigenesis. *Immunity*, 45(2):389–401.

Schwartz, R. H. (1990). A cell culture model for T lymphocyte clonal anergy. *Science*, 248:1349–1356.

Scolnick, E. M. and Parks, W. P. (1974). Harvey sarcoma virus: a second murine type C sarcoma virus with rat genetic information. *Journal of Virology*, 13(6):1211–9.

Sen, D. R., Kaminski, J., Barnitz, R. A., Kurachi, M., Gerdemann, U., Yates, K. B., Tsao, H. W., Godec, J., LaFleur, M. W., Brown, F. D., Tonnerre, P., Chung, R. T., Tully, D. C., Allen, T. M., Frahm, N., Lauer, G. M., Wherry, E. J., Yosef, N., and Haining, W. N. (2016). The epigenetic landscape of T cell exhaustion. *Science*, 354(6316):1165–1169.

Shih, C., Shilo, B. Z., Goldfarb, M. P., Dannenberg, A., and Weinberg, R. A. (1979). Passage of phenotypes of chemically transformed cells via transfection of DNA and chromatin. *Proceedings of the National Academy of Sciences*, 76(11):5714–8.

Shiow, L. R., Rosen, D. B., Brdicková, N., Xu, Y., An, J., Lanier, L. L., Cyster, J. G., and Matloubian, M. (2006). CD69 acts downstream of interferon-α/β to inhibit S1P1 and lymphocyte egress from lymphoid organs. *Nature*, 440(7083):540–4.

Shuford, W. W., Klussman, K., Tritchler, D. D., Loo, D. T., Chalupny, J., Siadak, A. W., Brown, T. J., Emswiler, J., Raecho, H., Larsen, C. P., Pearson, T. C., Ledbetter, J. A., Aruffo, A., and Mittler, R. S. (1997). 4-1BB costimulatory signals preferentially induce $CD8^+$ T cell proliferation and lead to the amplification of in vivo cytotoxic T cell response. *The Journal of Experimental Medicine*, 186:47–55.

Sivan, A., Corrales, L., Hubert, N., Williams, J. B., Aquino-Michaels, K., Earley, Z. M., Benyamin, F. W., Lei, Y. M., Jabri, B., Alegre, M. L., Chang, E. B., and Gajewski, T. F. (2015). Commensal bifidobacterium promotes antitumor immunity and facilitates anti-PD-L1 efficacy. *Science*, 350(6264):1084–9.

Snyder, A., Makarov, V., Merghoub, T., Yuan, J., Zaretsky, J. M., Desrichard, A., Walsh, L. A., Postow, M. A., Wong, P., Ho, T. S., Hollmann, T. J., Bruggeman, C., Kannan, K., Li, Y., Elipenahli, C., Liu, C., Harbison, C. T., Wang, L., Ribas, A., Wolchok, J. D., and Chan, T. A. (2014). Genetic basis for clinical response to CTLA-4 blockade in melanoma. *The New England Journal of Medicine*, 373(23):2189–2199.

Speiser, D. E., Ho, P. C., and Verdeil, G. (2016). Regulatory circuits of T cell function in cancer. *Nature Reviews Immunology*, 16(10):599–611.

Spranger, S., Bao, R., and Gajewski, T. F. (2015). Melanoma-intrinsic β-catenin signalling prevents anti-tumour immunity. *Nature*, 523(7559):231–5.

Spranger, S., Dai, D., Horton, B., and Gajewski, T. F. (2017). Tumor-residing Batf3 DCs are required for effector T cell trafficking and adoptive T cell therapy. *Cancer Cell*, 31(5):711–723.

Spranger, S., Koblish, H. K., Horton, B., Scherle, P. A., Newton, R., , and Gajewski, T. F. (2014). Mechanism of tumor rejection with doublets of CTLA-4 and PD-1/PD-L1 and or IDO blockade involves restored IL-2 production and proliferation of $CD8^+$ T cells directly within the tumor microenvironment. *Journal for Immunotherapy of Cancer*, 2(3).

Spranger, S., Luke, J. J., Bao, R., Zha, Y., Hernandez, K. M., Li, Y., Gajewski, A. P., Andrade, J., and Gajewski, T. F. (2016). Density of immunogenic antigens does not explain the presence or absence of the T-cell-inflamed tumor microenvironment in melanoma. *Proceedings of the National Academy of Sciences*, 113(48):E7759–E7768.

Spranger, S., Spaapen, R. M., Zha, Y., Williams, J., Meng, Y., Ha, T. T., and Gajewski, T. F. (2013). Up-regulation of PD-L1 and IDO and T(regs) in the melanoma tumor microenvironment is driven by $CD8^+$ T cells. *Science Translational Medicine*, 5(200):200ra116.

Sprent, J. (1995). Antigen-presenting cells. Professionals and amateurs. *Current Biology*, 5(10):1095–7.

Stehelin, D., Varmus, H. E., Bishop, J. M., and Vogt, P. K. (1976). DNA related to the transforming gene(s) of avian sarcoma viruses is present in normal avian DNA. *Nature*, 260(5547):170–173.

Steinman, R. M. and Witmer, M. D. (1978). Lymphoid DCs are potent stimulators of the primary mixed leukocyte reaction in mice. *Proceedings of the National Academy of Sciences*, 75(10):5132–6.

Stritesky, G. L., Xing, Y., Erickson, J. R., Kalekar, L. A., Wang, X., Mueller, D. L., Jameson, S. C., and Hogquist, K. A. (2013). Murine thymic selection quantified using a unique method to capture deleted t cells. *Proceedings of the National Academy of Sciences*, 110(12):4679–84.

Suzuki, A., de la Pompa, J. L., Stambolic, V., Elia, A. J., Sasaki, T., del Barco Barrantes, I., Ho, A., Wakeham, A., Itie, A., Khoo, W., Fukumoto, M., and Mak, T. W. (2013). High cancer susceptibility and embryonic lethality associated with mutation of the PTEN tumor suppressor gene in mice. *Current Biology*, 8(21):1169–78.

Takahashi, C., Mittler, R. S., and Vella, A. T. (1999). Cutting edge: 4-1BB is a bona fide CD8 T cell survival signal. *The Journal of Immunology*, 162(9):5037–40.

Takeuchi, O. and Akira, S. (2010). Pattern recognition receptors and inflammation. *Cell*, 140(6):805–20.

Tivol, E. A., Borriello, F., Schweitzer, A. N., Lynch, W. P., Bluestone, J. A., and Sharpe, A. H. (1995). Loss of CTLA-4 leads to massive lymphoproliferation and fatal multiorgan tissue destruction and revealing a critical negative regulatory role of CTLA-4. *Immunity*, 3(5):541–7.

Topalian, S. L., Hodi, F. S., Brahmer, J. R., Gettinger, S. N., Smith, D. C., McDermott, D. F., Powderly, J. D., Carvajal, R. D., Sosman, J. A., Atkins, M. B., Leming, P. D., Spigel, D. R., Antonia, S. J., Horn, L., Drake, C. G., Pardoll, D. M., Chen, L., Sharfman, W. H., Anders, R. A., Taube, J. M., McMiller, T. L., Xu, H., Korman, A. J., Jure-Kunkel, M., Agrawal, S., McDonald, D., Kollia, G. D., Gupta, A., Wigginton, J. M., and Sznol, M. (2012). Safety and activity and and immune correlates of anti-PD-1 antibody in cancer. *The New England Journal of Medicine*, 366(26):2443–54.

Townsend, S. E. and Allison, J. P. (1993). Tumor rejection after direct costimulation of $CD8^+$ T cells by B7-transfected melanoma cells. *Science*, 259(5093):368–70.

Tumeh, P. C., Harview, C. L., Yearley, J. H., Shintaku, I. P., Taylor, E. J., Robert, L., Chmielowski, B., Spasic, M., Henry, G., Ciobanu, V., West, A. N., Carmona, M., Kivork, C., Seja, E., Cherry, G., Gutierrez, A. J., Grogan, T. R., Mateus, C., Tomasic, G., Glaspy, J. A., Emerson, R. O., Robins, H., Pierce, R. H., Elashoff, D. A., Robert, C., and Ribas, A. (2014). PD-1 blockade induces responses by inhibiting adaptive immune resistance. *Nature*, 515(7528):568–71.

Udaka, K., Wiesmuller, K. H., Kienle, S., Jung, G., and Walden, P. (1996). Self-MHC-restricted peptides recognized by an alloreactive T lymphocyte clone. *The Journal of Immunology*, 157(2):670–8.

Vinay, D. S. and Kwon, B. S. (2011). 4-1BB signaling beyond T cells. *Cellular and Molecular Immunology*, 8(4):281–4.

Ward-Kavanagh, L. K., Lin, W. W., Sedy, J. R., and Ware, C. F. (2016). The TNF receptor superfamily in co-stimulating and co-inhibitory responses. *Immunity*, 44(5):1005–19.

Watanabe, M., Moon, K. D., Vacchio, M. S., Hathcock, K. S., and Hodes, R. J. (2014). Downmodulation of tumor suppressor p53 by T cell receptor signaling is critical for antigen-specific $cd4^+$ T cell responses. *Immunity*, 40(5):681–91.

Wei, F., Zhong, S., Ma, Z., Kong, H., Medvec, A., Ahmed, R., Freeman, G. J., Krogsgaard, M., and Riley, J. L. (2013). Strength of PD-1 signaling differentially affects T-cell effector functions. *Proceedings of the National Academy of Sciences*, 110(27):E2480–9.

Weigelin, B., Bolaños, E., Teijeira, A., Martinez-Forero, I., Labiano, S., Azpilikueta, A., Morales-Kastresana, A., Quetglas, J. I., Wagena, E., Sánchez-Paulete, A. R., Chen, L., Friedl, P., and Melero, I. (2015). Focusing and sustaining the antitumor CTL effector killer response by agonist anti-CD137 mAb. *Proceedings of the National Academy of Sciences*, 112(24):7551–6.

Weinberg, R. A. (2008). In retrospect: The chromosome trail. *Nature*, 453(7169):725.

Westphal, E. (1891). Über Mastzellen. In Ehrlich, P., editor, *Farbenanalytische Untersuchungen*, pages 17–41. Hirschwald, Berlin.

Wherry, E. J. (2011). T cell exhaustion. *Nature Immunology*, 12(6):492–9.

Wilcox, R. A., Tamada, K., Strome, S. E., and Chen, L. (2002). Signaling through NK cell-associated CD137 promotes both helper function for $CD8^+$ cytolytic T cells and responsiveness to IL-2 but not cytolytic activity. *The Journal of Immunology*, 169(8):4230–6.

Willerford, D. M., Chen, J., Ferry, J. A., Davidson, L., Ma, A., and Alt, F. W. (1995). Interleukin-2 receptor alpha chain regulates the size and content of the peripheral lymphoid compartment. *Immunity*, 3(4):521–30.

Williams, J. B., Horton, B. L., Zheng, Y., Duan, Y., Powell, J. D., and Gajewski, T. F. (2017). The EGR2 targets LAG-3 and 4-1BB describe and regulate dysfunctional antigen-specific $CD8^+$ T cells in the tumor microenvironment. *The Journal of Experimental Medicine*, 214(2):381–400.

Willoughby, J. E., Kerr, J. P., Rogel, A., Taraban, V. Y., Buchan, S. L., Johnson, P. W., and Al-Shamkhani, A. (2014). Differential impact of CD27 and 4-1BB costimulation on effector and memory CD8 T cell generation following peptide immunization. *The Journal of Immunology*, 193(1):244–51.

Woo, S. R., Corrales, L., and Gajewski, T. F. (2014). Innate immune recognition of cancer. *Immunity*, 41(5):830–42.

Woondong, J., Doroshow, J. H., and Kummar, S. (2013). US FDA approved oral kinase inhibitors for the treatment of malignancies. *Current Problems in Cancer*, 37(3):110–114.

Wu, J. and Chen, Z. J. (2014). Innate immune sensing and signaling of cytosolic nucleic acids. *Annual Review of Immunology*, 32:461–88.

Yanagihara, S., Komura, E., Nagafune, J., Watarai, H., and Yamaguchi, Y. (1998). EBI1/CCR7 is a new member of DCs chemokine receptor that is up-regulated upon maturation. *The Journal of Immunology*, 161:3096–3102.

Yang, G., Hellström, K. E., Hellström, I., and Chen, L. (1995). Antitumor immunity elicited by tumor cells transfected with B7-2 and a second ligand for CD28/CTLA-4 costimulatory molecules. *The Journal of Immunology*, 154(6):2794–800.

Zhou, P., Balin, S. J., Mashayekhi, M., Hwang, K. W., Palucki, D. A., and Alegre, M. L. (2005). Transplantation tolerance in NF-κB-impaired mice is not due to regulation but is prevented by transgenic expression of Bcl-x_L. *The Journal of Immunology*, 174(6):3447–53.